EFFECTS OF DYNAMIC SHEAR STRESS ON ENDOTHELIAL CELLS, PLATELETS, AND THEIR INTERACTIONS

By

SARAVAN KUMAR SHANMUGAVELAYUDAM

Bachelor of Engineering in Mechanical Engineering
Anna University
Chennai, India
2007

Master of Science in Mechanical Engineering
Oklahoma State University
Stillwater, OK
2009

Submitted to the Faculty of the
Graduate College of the
Oklahoma State University
in partial fulfillment of
the requirements for
the Degree of
DOCTOR OF PHILOSOPHY
May, 2013

EFFECTS OF DYNAMIC SHEAR STRESS ON

ENDOTHELIAL CELLS, PLATELETS, AND

THEIR INTERACTIONS

Dissertation Approved:

Dr. Wei Yin

Dissertation Adviser

Dr. David A. Rubenstein

Dr. Heather Dawn Nicole Fahlenkamp

Dr. Pamela G. Lloyd

If I have seen further it is by standing on the shoulders of giants.

--- Sir Isaac Newton

To all my past and present mentors

ACKNOWLEDGEMENTS

I would first like to acknowledge my advisor Dr. Wei Yin for her guidance and support throughout my graduate school. This dissertation research wouldn't have been possible without her constant guidance. I would like to thank her for being available to discuss my research work. I want to thank her for giving me the freedom to pursue different things in the lab. I learnt the most from the time I spent in the lab, from designing experiments to mentoring colleagues, and I hope to put them to good use in the future. I would like to acknowledge Dr. David Rubenstein for his guidance and recommendations. He was my second advisor, and never hesitated to clarify my doubts. I would like to thank him for all his patience, and his time in teaching me in many occasions. I would also like to thank him for serving on my committee. I would like to thank Dr. Pamela Lloyd and Dr. Heather Fahlenkamp for serving on my committee and for their valuable feedback.

I would like to thank my parents Saradha and Shanmugavelayudam and my brother Karthik Kumar for all their sacrifices and unwavering support. Their love and faith kept me motivated throughout my graduate studies. I am grateful to all the members of BELOS lab who made the time I spent in this lab most enjoyable, memorable and a great experience. I am grateful to my friends for their help and their confidence in me. At last, I would like to acknowledge every single teacher from my past, for inspiring me, equipping me with the right attitude and for seeding the passion in me to pursue the wildest of my dreams.

Name: SARAVAN KUMAR SHANMUGAVELAYUDAM

Date of Degree: MAY, 2013

Title of Study: EFFECTS OF DYNAMIC SHEAR STRESS ON ENDOTHELIAL CELLS, PLATELETS AND THEIR INTERACTION

Major Field: MECHANICAL ENGINEERING

Abstract:

Coronary heart disease (CHD), characterized by degenerative changes in coronary circulation, is the leading cause of death in the US. Vascular wall endothelial cells (EC) and circulating blood platelets play a major role in pathogenesis of CHD. The normal functions and activities of EC and platelets can be significantly affected by blood flow induced shear stress. The major goal of this study was to estimate shear stress environment in the human left coronary artery using a computational fluid dynamics model, and to examine the effect of physiologically relevant dynamic shear stress on endothelial cells, platelets and their interaction. In this study, numerical simulations were conducted using a physiologically realistic left coronary artery 3D model under normal and disease (stenosis) conditions. The results indicated highly disturbed flow patterns under stenosis conditions. The dynamic shear stress waveforms (physiological and pathological) from numerical studies were applied to EC and platelets using a cone and plate shearing device, or a parallel plate flow chamber. Pathological shear stress (low and high) could significantly affect EC activation. For platelets, pathological shear stress induced significant changes in platelet proteome profiles, and caused complement activation. However, when platelets and EC were exposed to the same dynamic shear stress simultaneously, both EC and platelet response to shear stress changed. Pathological shear stress failed to activate EC, or lead to platelet complement activation. Further, when EC and platelets were sheared simultaneously, platelet adhesion to EC monolayer was observed, especially under low pulsatile shear stress. Together, the results suggest that platelet-EC interaction could protect EC and platelets from dynamic pathological shear stress, and it is potentially through physical contact between platelets and EC, i.e., platelet adhesion to EC. Further investigation is needed to identify mediators in this protective mechanism, which may lead to new therapeutic solutions to atherosclerosis and coronary artery disease.

TABLE OF CONTENTS

Chapter Page

LIST OF TABLES

LIST OF FIGURES

Figure Page

Figure Page

Figure Page

LIST OF ABBREVIATIONS

ADP	Adenosine diphosphate
APC	Activated protein C
ATP	Adenosine triphosphate
BAEC	Bovine aortic endothelial cells
BSA	Bovine serum albumin
C1-INH	C1 – inhibitor
CR1	Complement receptor - 1
CAD	Computer aided design
CFD	Computational fluid dynamics
CHD	Coronary heart disease
CVD	Cardiovascular disease
DAPI	4’-6-Diamidino-2-phenylindole
DPM	Discrete phase modeling
EC	Endothelial cells
ELISA	Enzyme linked immunosorbent assay
FITC	Fluorescein isothiocyanate
GPIbα	Glycoprotein Ibα
GPIIb/IIIa	Glycoprotein IIb/IIIa

HBMT	Hepes buffered modified Tyrode's solution
HCAEC	Human coronary artery endothelial cells
HUVEC	Human umbilical vein endothelial cells
ICAM-1	Intercellular adhesion molecule – 1
IL-1	Interleukin – 1
LAD	Left anterior descending artery
LCA	Left coronary artery
LCX	Left circumflex artery
LM	Left main artery
MALDI	Matrix assisted laser desorption ionization technique
mRNA	Messenger RNA
PAS	Platelet activated state
PECAM-1	Platelet endothelial cell adhesion molecule – 1
PMSF	Phenylmethylsulfonyl fluoride
PNPP	p-Nitrophenyl phosphate
PRP	Platelet rich plasma
PPP	Platelet poor plasma
PS	Phosphatidylserine
SELDI	Surface enhanced laser desorption ionization technique
TF	Tissue factor
TFPI	Tissue factor pathway inhibitor
TM	Thrombomodulin
TNF-α	Tumor necrosis factor - α
TRAP	Thrombin receptor activating peptide

TRITC	Tetramethylrhodamine-5-(and 6)-isothiocyanate
vWF	von Willebrand factor
WSS	Wall shear stress
WPB	Weibel Palade bodies

CHAPTER I

INTRODUCTION

Coronary arteries supply blood and oxygen to the heart muscles. Degenerative changes in the coronary circulation affect blood supply to the heart muscles and result in coronary heart disease (CHD). CHD is the leading fatal disease in the US (17.6 million deaths in 2008), accounting for nearly 50% of all cardiovascular disease (CVD) deaths (shown in Figure 1)[1]. Atherosclerosis is the single most common reason behind CHD, and most other CVDs. A characteristic feature of this vascular inflammatory disease is the localization and growth of atheroma/plaque, which reduces the lumen size of a blood vessel. The changes in endothelium (innermost layer of blood vessel) may result in an increased adhesion and trans-endothelial migration of lipids and leukocytes. The continuous deposition at the sub-endothelial layer induces inflammatory responses and results in plaque formation. Atherosclerosis in the coronary circulation alters the blood flow to the downstream region, which may result in an acute condition referred to as myocardial infarction.

In general, regions of complex blood flow are usually predisposed locations for anchoring of atherosclerotic lesions. The complex vascular geometry (such as bifurcation, curvature of heart, twists, and bends) along with the pulsatile nature of blood flow could result in disturbed blood flow patterns such as flow separation, skewing and recirculation.

Disturbed flow leads to disturbed shear stress distribution, which plays a major role in atherosclerosis development. Once anchored, the atherosclerotic lesion further alters blood flow distribution, promoting the growth and propagation of the disease condition, by causing endothelial dysfunction, platelet activation and thrombus formation.

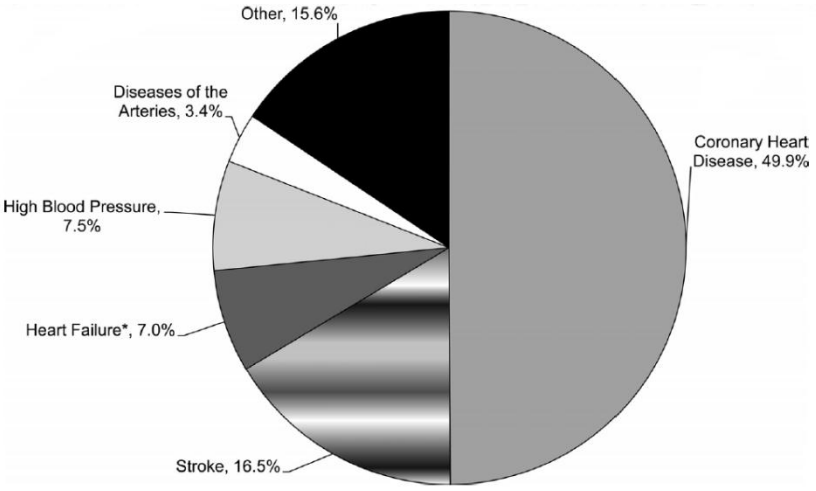

Figure 1. Percentage breakdown of deaths due to cardiovascular disease in the US (2008)[1]

In the coronary circulation, atherosclerotic plaques are most prevalent in the left coronary arteries (LCA), especially in the left anterior descending (LAD) branch near the left main (LM) bifurcation. Increasing evidence suggests the critical role of disturbed shear stress in the initiation and development of atherosclerotic plaques in coronary arteries. The complex blood flow patterns inside these arteries, arising due to the geometrical complexity, could induce highly disturbed shear stress. Endothelial cells (EC) present at the vessel wall and the platelets that are circulating in the blood flow are sensitive to these altered shear forces. The activation of these cells, along with their interactions, could affect the initiation and propagation of CHD and other related clinical conditions like thrombosis and stroke.

Thrombus formation (blood clot) inside the coronary circulation may completely block blood supply to cardiac muscles, resulting in cardiac ischemia (lack of oxygen).

Computational fluid dynamics is an efficient tool to analyze blood flow inside complex vasculature and can help to estimate various hemodynamic parameters. A number of studies have been conducted in the past decades to analyze the coronary blood flow, but most models were geometrically simplified. The activation and response of both EC and platelets by shear stress have also been investigated *in vitro* by a number of researchers. One common drawback in many of these *in vitro* studies is the utilization of non-physiological shear stress conditions. Recently, the dependence of EC and platelet activation on both shear stress magnitude and exposure time has been established[2-4]. This underlines the importance of the use of physiologically relevant shear stress conditions.

The major goal of this study was to investigate the behavior of endothelial cells and platelets under physiologically relevant dynamic shear stress conditions. Computational fluid dynamics simulations were used to estimate dynamic shear stress conditions in normal and diseased coronary arteries. These shear stress waveforms were then applied to endothelial cells and platelets *in vitro* and their responses were measured. The results obtained from this study can significantly improve our understanding of the role of shear stress during the pathogenesis of CHD.

CHAPTER II

SPECIFIC AIMS AND SIGNIFICANCE

The major goal of this study was to investigate the role of physiologically relevant dynamic shear stress on the activation and function of vascular endothelial cells and circulating blood platelets, as well as their interactions.

Global Hypothesis: Disturbed shear stress may activate endothelial cells and platelets, and promote their interactions, contributing to the pathogenesis of CHD and other related complications. This hypothesis was tested through the following specific aims.

Specific Aim 1: To conduct numerical simulation of blood flow with platelets as a discrete phase, inside a human left coronary artery and to estimate the shear stress history on the vessel wall and platelets under normal and disease conditions**.**

Specific Aim 2: To study the effect of physiologically relevant dynamic shear stress (obtained from numerical simulations from SA1) on vascular endothelial cells *in vitro*. Confluent endothelial cells were exposed to various pulsatile shear stress waveforms. Cell activation (ICAM-1 expression) and inflammatory response (tissue factor and thrombomodulin expression) were examined at both the protein level and RNA level.

Specific Aim 3: To investigate the effect of physiologically relevant dynamic shear stress on platelets. After dynamic shear stress treatment, platelet surface complement activation was measured. Changes in platelet proteome was also examined.

Specific Aim 4: To examine the interaction between endothelial cells and platelets *in vitro* under physiological/pathological shear stress conditions. Vascular endothelial cells were exposed to dynamic shear stress in the presence of platelets. EC and platelet activation and associated inflammatory/thrombotic responses were examined.

In this study, numerical simulation and *in vitro* experiments were combined to investigate the effects of dynamic shear stress on endothelial cells and platelets. Cell-cell interaction was investigated using a coupled-shearing system. Results obtained from this study can help us to better understand the mechanisms of dynamic shear stress induced endothelial cell and platelet activation, which may help us to better characterize CHD and search for potential therapeutic solutions.

CHAPTER III

BACKGROUND

Atherosclerosis, a common vascular inflammatory disease condition, is characterized by the localization and growth of atherosclerotic lesions that results in the narrowing of blood vessels. This alters blood supply to the downstream region. Atherosclerosis is the leading cause behind most cardiovascular diseases, including coronary heart disease (CHD). Endothelial cells (EC) located in the innermost layer of blood vessels, are in direct contact with the flowing blood, and play critical roles in the pathogenesis of atherosclerosis.

In our current level of understanding, the first step in initiation of atherosclerosis includes leukocyte sub-endothelial migration and deposition of lipids [especially low density lipoproteins (LDL)][5;6]. This is facilitated by activation and/or damage of EC by biochemical or biomechanical stimuli or a combination of both. The resulting changes in EC permeability and surface adhesion molecule expression directly assist trans-endothelial migration of leukocytes.

3.1 Shear Stress

Shear stress, the tangential friction force exerted by blood flow on adjacent fluid lamina and on the vessel wall, is one of the major contributors for the localization of atherosclerosis. Shear stress (τ) applied on any fluid element in a three dimensional space can be represented in tensor notation as shown in Equation 3.1.

$$\tau_{ijk} = \mu_{eff}\left(\frac{\partial v_i}{\partial X_j} + \frac{\partial v_j}{\partial X_k} + \frac{\partial v_k}{\partial X_i}\right) \qquad \text{.....(3.1)}$$

Where i, j, k = (x, y, z), v is velocity and μ_{eff} is the local effective viscosity.

Under laminar flow conditions, the maximum shear stress at a particular cross section of a blood vessel is found at the vessel wall, and it decreases towards the center of the blood vessel. A typical velocity profile and shear stress distribution under laminar fully developed flow is presented in Figure 2. In the case of a continuous laminar flow, effective viscosity is the same as the dynamic viscosity. However, under turbulence conditions, effective viscosity is the sum of laminar and turbulent viscosity. Turbulent viscosity, which results from the local disturbances, depends on total turbulent energy and length/time scale.

In general, shear stress at physiological levels helps to maintain the proper functioning of the endothelium and hemostasis, such as promoting anti-inflammatory and anti-thrombotic activities of the vessel wall[7;8]. Furthermore, platelet functions, including activation, adhesion and aggregation, are regulated by shear stress.

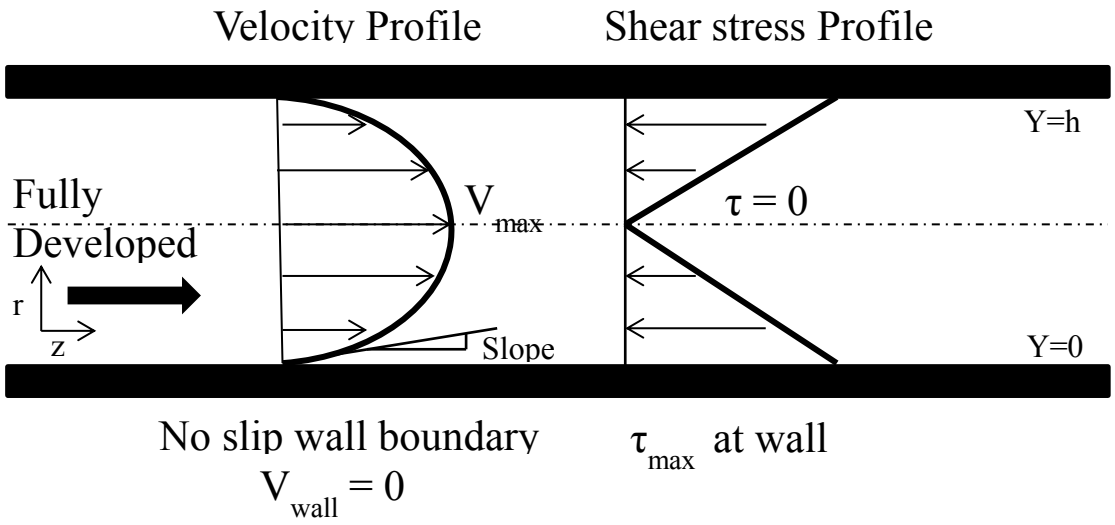

Figure 2. Velocity profile and shear stress distribution of a 2D fully developed laminar flow.

The pathogenesis of atherosclerosis is highly regulated by local blood flow and shear stress conditions. Atherosclerotic lesions are predominantly localized to a few major arterial beds, including coronary arteries, major branches of the aortic arch, the abdominal aorta, carotid arteries and iliac arteries[9]. The pulsatile nature of blood flow along with the complex anatomical geometry of these arteries (including twists, bends, curvature and bifurcations) produce regions of disturbed blood flow patterns.

For instance, Figure 3 (taken from Chandran et al.) compares the flow patterns at a 60˚ (representing near symmetrical aorta-illiac) and a 90˚ (representing renal arterial branches) arterial bifurcation[10]. At the point of bifurcation, as the flow divides into the two daughter vessels, regions of flow separation and corresponding flow skewing are produced. In case of a symmetric bifurcation (Figure 3A), the majority of the flow is concentrated towards the bifurcation with secondary flow forming near the outer wall. For an asymmetric bifurcation (Figure 3B), the branch with a reduced flow has a large

flow separation zone and low- magnitude shear zone. Blood flow in the coronary arteries can be subject to both patterns, causing flow separation, recirculation, vortex and eddy formation[11].

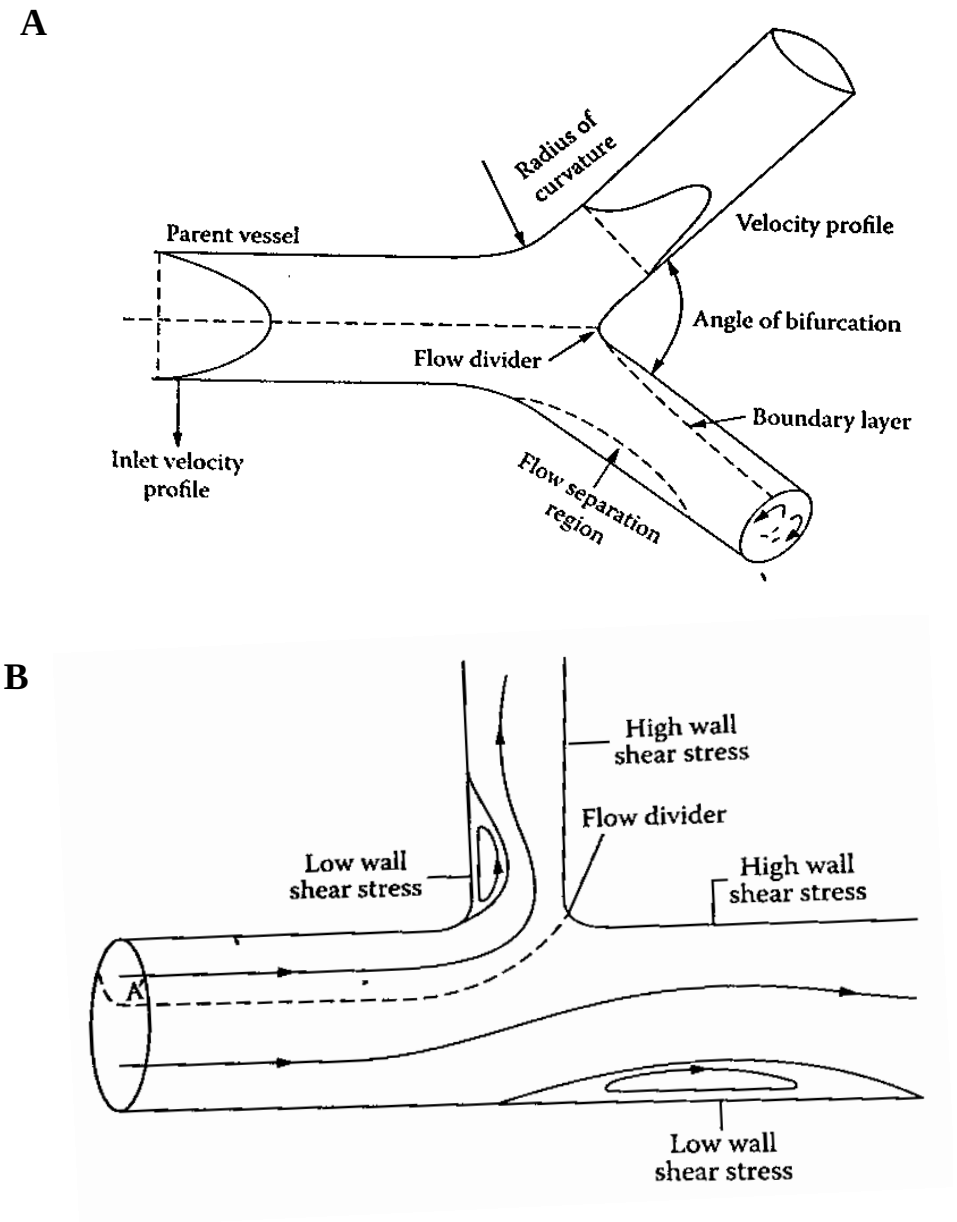

Figure 3. Flow distribution near an arterial bifurcation. (A) Representing a near symmetric aorto-iliac bifurcation, (B) Representing asymmetric (90°) renal arterial bifurcation.[10]

Altered shear stress associated with these disturbed flow patterns may affect the functions of vascular wall endothelial cells and platelets greatly. Typically, low shear stress induces endothelial cell activation by altering the surface expression of adhesion molecules which play a key role in pathogenesis of atherosclerosis. In addition, platelets exposed to low magnitude shear stress for an extended duration have been shown to activate and aggregate[3;4;12]. Elevated shear stress may induce vessel wall damage[13], platelet activation and thrombus formation[14]. Therefore, given the bipolar nature of shear stress, atheroprotective and atherogenic, it is important to understand the nature of shear stress (physiological or pathological) and its effects on various cellular functions pertaining to vascular disease conditions.

3.2 Coronary Circulation

Coronary arteries, originating from the base of the aorta, perform the critical function of supplying oxygen and nutrients to the cardiac muscles. The left coronary artery (LCA) supplies more than 50% of the heart muscles with blood[15]. The major branches of the LCA include the left main (LM), the left anterior descending (LAD) and the left circumflex (LCX) (shown in Figure 4) arteries. LCA has the highest probability for anchoring atherosclerosis. This is possibly due to the presence of LM bifurcation (which does not lie in a single plane)[16] and the curvature of LAD (replicating the curvature of the heart)[17], which may produce complex secondary flow[11].

The flow near the LM bifurcation is skewed towards the flow divider (inner wall), which creates a region of elevated wall shear stress at the point of bifurcation. In addition, near the entrance of LAD and LCX, flow separates, creating regions of varying

shear stress. Downstream (inside both LAD and LCX), the flow reattaches and re-develops. Furthermore, if an atherosclerotic lesion grows inside LAD, it can gradually decrease the vessel diameter and introduce additional disturbances to the local blood flow, creating regions of high, low and oscillatory shear stress and recirculation flow. This emphasizes the importance of estimation of shear stress distribution inside the LCA under normal and disease conditions.

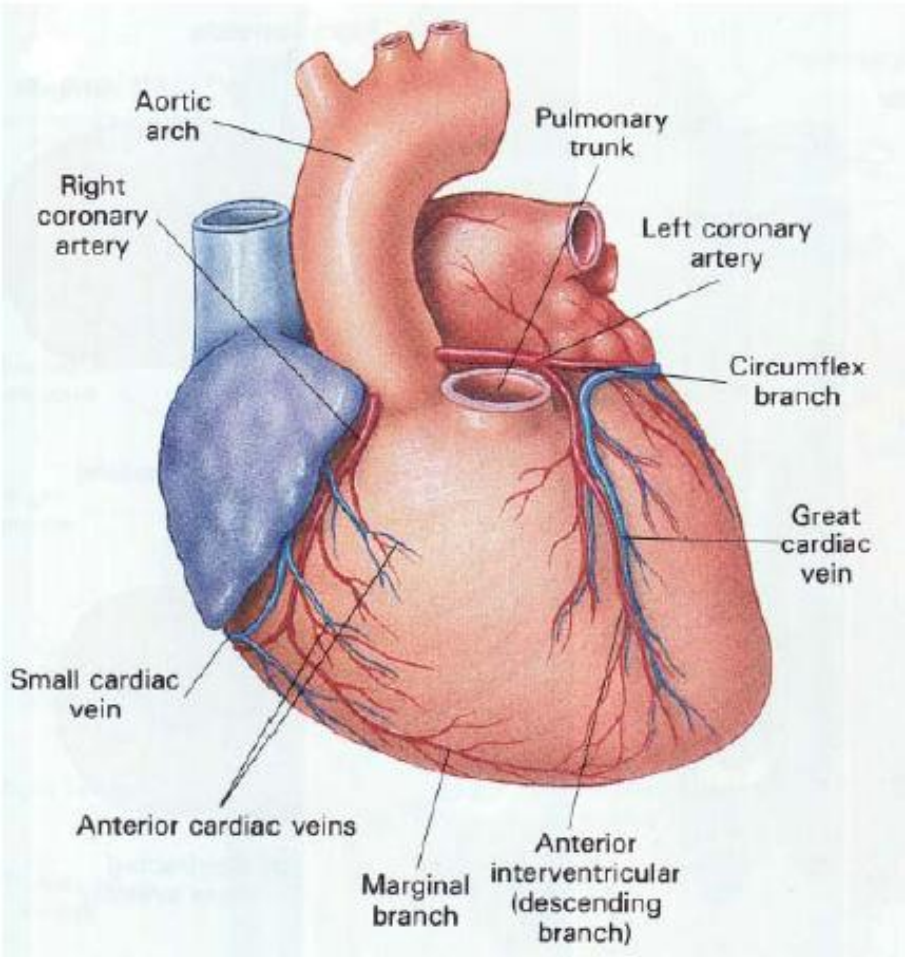

Figure 4. Human heart showing coronary vasculature. Taken from Martini et al.[15]

3.2.1 CFD of coronary flow

It is not possible to directly measure shear stress *in vivo*. Recently, non-invasive phase contrast magnetic resonance imaging (MRI) or pulsed ultrasound techniques have been used to measure the velocity gradient near the vessel wall, and from which shear stress can be calculated[18;19]. Carvalho et al. used a modified MRI technique to obtain wall shear rates in the carotid arteries[20]. The major drawback with this estimation is the assumption that the velocity profile is parabolic (fully developed), which is not true both spatially and temporally, and that the viscosity is constant. Such techniques are expensive and still need more validation. As an alternative, computational fluid dynamics (CFD) simulation of blood flow provides an efficient way to estimate shear distribution based on local blood flow conditions. CFD can account for the complex vasculature, pulsatile nature of blood flow and non-Newtonian behavior of blood. The ability of CFD to provide accurate results with high spatial and temporal resolution has been well established. One of the major considerations in numerical estimation of shear stress is whether the computational model can closely mimic the *in vivo* physiological conditions. Other things that need be considered are flow assumptions and the computational capacity.

Many studies have been conducted to analyze blood flow inside LCA using CFD and to estimate the magnitude and distribution of shear stress. The major limitation of many of these studies is the use of simplified arterial geometry. The simplification generally included the avoiding of changes in blood vessel diameter (taper), complex bends and the multi-planar curvature of the LM bifurcation, which could lead to inaccurate estimation in shear stress. In a study conducted by He et al., a simplified 3D

LCA model was used, and the time-averaged wall shear stress (WSS) was found to vary between 0.3 and 9.8Pa[16]. In a similar study by Perktold et al., a more realistic coronary artery model was employed and the average shear stress inside LM was found to be 0.42Pa and that inside LAD was found to be 1.14Pa[21], very different from He's study.

As mentioned earlier, an atherosclerotic lesion (stenosis) can significantly alter the local blood flow conditions, and hence shear stress distribution. A study conducted by Varghese et al., using Ahmed's stenosis model[12], revealed an elevated shear stress of 120Pa before the stenosis throat and around 2Pa downstream of the stenosis[22]. Yao et al. compared the variation in shear stress distribution due to bend angle and stenosis severity. Their results indicated that the maximum WSS at stenosis throat in a curved vessel reached as high as 300Pa (with 60˚ and 120˚ bends, and 60% stenosis)[23]. In a similar study, Nosovitsky et al. investigated the effect of the presence of a stenosis inside a simple curved LCA model and revealed that the maximum WSS reached 125Pa at the stenosis throat[24]. The variation in shear stress magnitude estimated by these studies is due to their variation in the geometrical considerations and nature of blood flow assumptions (steady or unsteady).

3.3 Endothelial cells and shear stress

Endothelial cells (EC) are one of the most essential and functional component of blood vessels. Lying in the innermost layer, EC provide an interface between blood and the vessel wall. Under normal conditions, the integrative functions of vascular endothelium include: monitoring sub-endothelial migration of micro/macromolecules (vascular permeability), regulating the coagulation cascade (hemostasis/prevention of

excessive blood loss), maintaining vascular tone (production of vasomodulators) and promoting atheroprotective environment (secretion/expression of anti-atherogenic factors). EC have the ability to temporarily respond to intra/extra-vascular changes in the environment, such as localized inflammation, by changing their surface expression of adhesion molecules (E- and L- selectin, ICAM-1, VCAM-1) or releasing cytokines (TNF-α, IL-1)[25]. Most of the time, these changes occur during immune responses and are reversible. But under some pathological conditions, EC undergo an irreversible activation which plays a pivotal role in vascular disease initiation.

EC are sensitive to blood flow induced shear stress. Even though several studies reported that the lack of shear stress may induce EC apoptosis[26], many studies have shown that shear stress is one of the agonists that can cause endothelial activation, injury and dysfunction. Through various mechanotransduction pathways, EC sense changes in shear stress. In large- to medium-sized arteries, locations with laminar blood flow usually possess a pulsatile shear stress with net positive amplitude, varying between 0.1-1Pa. Around bifurcations or downstream of a stenosis, low unidirectional pulsatile shear stress or oscillatory shear stress (bidirectional with the time-averaged shear stress approaching zero) can occur.

Shear stress within the physiological range is generally regarded as atheroprotective while altered shear stress (either high or low) as atherogenic. Physiological shear stress preferentially induces EC elongation and the alignment of cytoskeletal components to the direction of blood flow[27]. This orientation helps to reduce the effective resistance and shear stress on EC. In a study conducted by Partridge et al., HUVECs were exposed to steady shear stress (1.2Pa for 16hr) and then treated with a

cytokine, TNF-α[28]. The nuclear factor κB (NF-κB, a major cytoprotective and proinflammatory transcription factor) activity was measured. Further NF-κB also plays a major role in generation of ICAM-1. It was found that the pre-exposure to shear stress enhanced the NF-κB dependent cytoprotective transcription, while inhibiting the proinflammatory transcription. On the other hand, EC do not undergo realignment under disturbed blood flow patterns, which could be attributed to the low magnitude of time-averaged shear stress in a particular direction[29]. In addition to the structural change, disturbed shear stress is also known to activate EC and cause endothelial dysfunction.

3.4 Shear stress induced endothelial cell activation in atherosclerosis

The role of shear stress induced EC activation in the initiation and propagation of atherosclerosis is well established. Earlier studies relating shear stress to localization of atherosclerotic lesions resulted in two major opposing hypotheses. The high shear stress theory, proposed that the elevated shear stress would induce actual physical damage to the endothelium and expose the sub-endothelial layer to blood flow, leading to atherosclerosis initiation; and the low shear stress theory states that low shear stress activates the endothelium and leads to atherosclerotic lesion growth[10].

Shear stress induced EC activation responses, especially those pertaining to atherosclerosis, have been one of the major areas of research in the past couple of decades. One of the earliest studies on EC response to shear stress demonstrated that cellular damage would occur when exposed to elevated shear stress even for a short duration of time (37.9Pa for 60min)[13]. The results from this study formed the basis for high shear stress theory. However, a number of follow up studies confirmed the low shear

stress hypothesis[30]. Through clinical observation, Gibson et al. established a strong correlation between low magnitude wall shear stress and rate of atherosclerotic progression in human coronary arteries[31]. The major EC responses upon activation include loss of vascular integrity, enhanced surface adhesion molecule expression, EC surface phenotypical change from anti-thrombotic to prothrombotic, cytokine production and elevated immune responses[32]. Among all these responses, increased expression/activation of adhesion molecules is of primary concern due to their role in leukocyte adhesion, leading to initial anchoring and growth of atherosclerotic lesions. Intercellular adhesion molecule - 1(ICAM-1) assists leukocyte trans-endothelial migration[32]. In addition, modulation in EC surface pro-/anti-thrombotic protein expression, including tissue factor (interacts with the coagulation cascade) and thrombomodulin (inhibits thrombin production), can lead to localized thrombus formation[33;34]. Further, changes in EC surface von Willebrand Factor (vWF) facilitates platelet adhesion and subsequent activation[35]. The expression and activation of all these EC proteins can be greatly affected by shear stress.

3.4.1 ICAM-1

ICAM-1 is a 95kDa transmembrane glycoprotein present on EC membrane, which assists in trans-endothelial migration of leukocytes[36]. Injured endothelium present near athero-prone sites express an increased amount of ICAM-1 compared to a healthy intact endothelium. *In vivo* coronary examination has also revealed an elevated ICAM-1 expression near atherosclerotic lesions[37]. Elevated ICAM-1 expression was detected when EC were exposed to steady shear at 1Pa for 48hrs[38]. In a study conducted by Nagel et al., when exposed to low steady shear stress (0.3Pa) and varying shear stress (between

0.25Pa and 4.5Pa over 24hrs), EC expressed a similar ICAM-1 distribution, in a magnitude independent - time dependent manner[38]. Interestingly, when exposed to oscillatory shear stress (between +0.5 and -0.5Pa at a frequency of 1Hz), EC had a 11-fold increase in ICAM-1 expression[39]. Morigi et al. found an elevated ICAM-1 expression on HUVECs exposed to constant shear stress at 0.86Pa[40]. The functional significance of ICAM-1 increase was verified by an increase in leukocyte adhesion on EC exposed to laminar shear compared to static conditions. Furthermore, Tsuboi et al. detected a 1.27-fold increase in EC surface ICAM-1 expression (1.5Pa for 4 hrs) and the result was supported by an elevated expression of mRNA, quantified using real time PCR analysis[41].

These *in vitro* studies suggest that EC exposed to physiological-level shear stress may have elevated ICAM-1 expression, which contravenes the *in vivo* observations that elevated ICAM-1 expression occurred at lesion prone sites characterized with disturbed blood flow patterns and altered shear stress[42]. This variation could be attributed to the shear stress used in the above studies (most of these studies used constant shear stress). Therefore, it is important to investigate ICAM-1 expression under physiologically relevant dynamic shear stress conditions.

3.4.2 Tissue factor

Tissue factor (TF) is a major inflammatory glycoprotein (47kDa), synthesized by EC and leukocytes. One important function of TF is its role in coagulation cascade through interactions with factor VIIa. When a vessel is injured, EC upregulate TF expression, which binds to coagulation factor VIIa (present in plasma) and catalyzes the

conversion of Factor X to Factor Xa[43]. The end product of coagulation cascade is the formation of fibrin which helps to prevent excessive blood loss. In order to prevent uncontrolled TF activity, EC also secrete tissue factor pathway inhibitor (TFPI). In general, TFPI blocking studies have demonstrated that the modulation of TF expression/activity due to shear stress was primarily governed by the amount of TFPI released by EC[44]. Immunohistochemical observations of human atherosclerotic vessel sections have identified an over production of TF near the regions of plaque[45], establishing its role in thrombotic complications during vascular inflammation.

In a study conducted by Houston et al., EC were exposed to constant shear stress at 1.5Pa, and the result showed a time-dependent increase in TF gene expression[46]. Grabowski et al. reported a down regulation of TF mRNA in EC, when they were exposed to constant shear stress at 0.068 and 1.32Pa[44]. Also, the binding of monocytes to cytokine-activated EC was found to induce TF generation (approximately 10-fold increase) in a time-dependent manner[47]. TF activity can be measured through its ability to convert Factor X to Factor Xa. Lin et al., observed a time-dependent increase in EC TF procoagulant activity (by both mRNA level and through Factor Xa formation) when EC were exposed to steady shear at 1.2Pa[48].

These studies reflect the ability of shear stress to modify TF expression on EC. Since most of the previous work has investigated EC response to constant shear, it is important to understand the role of physiological and pathological dynamic shear stress on TF expression and activity.

3.4.3 Thrombomodulin

Thrombomodulin (TM), a cell surface glycoprotein, is predominantly produced and expressed by vascular endothelial cells. TM plays a critical role as a cofactor for thrombin, forming a 1:1 stoichiometric complex which serves as a catalyst for activation of protein C[49]. Protein C is a plasma glycoprotein. Thrombin activates Protein C into its activated form activated protein C (APC) which is amplified by the presence of TM (by >1000 fold). APC is an effective anti-coagulant which in the presence of protein S suppresses further thrombin generation by proteolytic inhibition of Factor Va and Factor VIIIa. The ability of TM to block thrombin was first proposed in a study conducted by Esmon et al., which established the physiological role of TM in inhibiting platelet activation[33]. The antithrombotic effect of TM was substantiated in a study by Gomi et al., where the effect of recombinant human TM was tested both *in vitro* and *in vivo*[50]. Recombinant human TM produced in Chinese hamster ovary cells revealed a dose-dependent increase in platelet clotting time (thrombin induced). Mice injected with both TM and thrombin (extracted from human) had a greater survival ratio when compared to those injected with only thrombin.

One of the major atheroprotective responses of EC during endothelial dysfunction is the modulation of surface expression of TM. EC expression of TM can be greatly regulated by fluid shear stress. In a study by Malek et al., there was a 37% decrease in TM mRNA expression in bovine aortic endothelial cells (BAEC) when they were sheared at 1.5Pa. At the shear stress level of 3.6Pa, TM mRNA expression decreased further to about 16%[51]. Total protein expression measured by Western blot indicated that EC exposed to shear stress at 1.5Pa for 36hrs had a significant decrease (33%) in TM

expression. In a similar study conducted by Takada et al., human umbilical vein endothelial cells (HUVEC) were exposed to two different shear stress (low - 0.15Pa and high - 1.5Pa) and the TM expression was measured at both protein and mRNA levels[52]. EC had an increased surface TM expression as shear stress magnitude and shear exposure time increased, compared to that of control (measured by flow cytometry and ELISA). RT-PCR revealed an approximate 300% increase in TM mRNA levels. The contradicting results from both these studies could potentially be attributed to the variation in cell origin. However, these experiments have demonstrated that shear stress can modulate TM expression, at both protein and mRNA level. EC TM expression under physiologically relevant dynamic shear stress conditions is yet to be investigated.

3.4.4 von Willebrand Factor

Platelets interact directly with EC through von Willebrand factor (vWF). vWF is an ultrahigh molecular weight protein (more than 10,000kDa) synthesized by EC and stored in Weibel Pallade bodies (WPB)[53]. Activated EC have increased secretion of vWF, which leads to an increased local vWF concentration[54]. The vWF subunit comprises of several domains, of which the A1 domain is the only binding site for platelet receptor, GPIbα. The binding of platelet GPIbα to vWF can trigger a series of platelet intracellular signaling pathways that contribute to platelet activation. Localized secretion of vWF was found to occur in areas of vascular inflammation and injury[55;56].

A few recent studies have established the role of hemodynamic shear stress on the accessibility of the vWF binding site. Locally elevated shear forces were found to induce structural changes on vWF expressed on EC surface, aligning them with the shear

direction and increasing their adhesive nature. This shear-dependent structural change in vWF (at shear stress of 35±3.5 Pa) was verified by atomic force microscopy[57]. In flow fields with shear rates around $1000s^{-1}$, platelet adhesion to EC is greatly governed through surface immobilized vWF[58]. In addition to its role in shear induced platelet adhesion to vessel wall, the intracellular signal triggered by vWF-GPIbα binding plays a significant role in GPIIb/IIIa mediated platelet aggregation.

Given the role of vWF in initiating thrombogenic response, especially in the regions of pathological shear stress, it is essential to investigate how dynamic shear stress regulate EC vWF expression. Furthermore, the regions of vasculature with low pulsatile and oscillatory shear stress (for example, inside a recirculation zone) tend to have more platelet retention times than the other regions of vasculature. EC activation in these regions, specifically an increased expression in vWF, may promote platelet adhesion and subsequent aggregation.

The literature review presented above reveals the importance of shear induced EC expression of ICAM-1, TF, TM and vWF and the discrepancies in our current understanding. In general, the alteration of these proteins at mRNA and protein levels has not been investigated under physiologically relevant dynamic shear stress conditions. The modulation of these proteins may have a significant role in pathogenesis of atherosclerosis and related complications. One of the major goals of this study was to investigate the activation of EC and their cellular responses to physiologically relevant dynamic shear stresses.

3.5 Platelets

3.5.1 Physiology and functions

Platelets are non-nucleated cells produced in the bone marrow. They circulate in the blood stream for about 7-10 days at a physiological concentration of 150,000-500,000/μL. Platelets, as sub-cellular fragments released from megakaryocytes, are packaged with platelet specific granules (α-granules and dense bodies) and cellular organelles. Platelet α-granules contain a number of secretory proteins such as growth factors (platelet derived growth factors, PDGF), coagulation co-factor (factor V), angiogenic factors and adhesion molecules (P-selectin, vWF and thrombospondin). Platelet dense bodies contain a large amount of ADP, which can provide a positive feedback for platelet activation. The platelet plasma membrane is occupied by a number of transmembrane glycoproteins, including GPIb complex and GPIIb/IIIa, etc., which act as receptors and contribute greatly to platelet functions. Apart from the glycoproteins, the platelet membrane also contains phospholipids, especially phosphatidylserine (PS). Under resting conditions, PS is present on the inside of the plasma membrane and is not exposed to blood flow. When activated, PS is relocated to the outside of the cell membrane and facilitates coagulation.

Platelets play a major role in hemostasis and thrombosis. Under physiological conditions, at the site of vascular injury, tissue factor (TF) expressed by the vascular wall endothelial cells interacts with Factor VIIa and forms TF-VIIa complex. The TF-VIIa complex triggers the coagulation cascade and leads to the formation of insoluble fibrin, which is the key component in a blood clot. The two important components for

coagulation that are provided by platelets include (1) negatively charged phospholipid membrane (PS translocated to outer surface) (2) coagulation factor V released from platelet α-granules. At the site of vessel injury, platelets adhere to the sub-endothelium through surface adhesion molecules. Upon initial adhesion, platelets also adhere to other activated platelets in the vicinity leading to thrombus formation.

Platelets can be activated by a number of agonists - both biochemical and biomechanical. Some of the important platelet agonists include ADP, thrombin, collagen (biochemical) and shear stress (biomechanical). The major platelet responses during activation include shape change, PS translocation and α-granule secretion. When activated, coagulant proteins stored in α-granules are released, this can lead to the activation of nearby quiescent platelets. Furthermore, thrombin generated as a byproduct of coagulation, is also a potent agonist for platelet activation.

3.6 Platelets and shear stress

3.6.1 Shear induced activation and aggregation

Blood flow induced shear stress plays a major role in platelet activation, especially during the pathogenesis of thrombosis. It was found that altered shear stress could trigger platelet activation and aggregation. A number of investigators have examined the effects of shear stress on platelet activation *in vitro*. When exposed to shear stress of 5Pa, platelets secrete small amounts of ATP, ADP and serotonin[59]. Higher shear stress may lyse platelets. Anderson et al. reported platelet lysis at two different shear stress levels (16 and 60 Pa) after different durations of exposure[60]. In a recent study by Yin et al., platelet activation (based on prothrombinase activity and P-selectin expression)

was found to increase in a shear stress-dose dependent manner (increase in magnitude and duration)[3]. In addition to directly activating platelets, shear stress was found to act synergistically with other agonists (such as ADP, TRAP, epinephrine, etc.) and plasma cofactors to activate platelets[61].

Besides activating platelets, shear stress also affects platelet aggregation. The current understanding of the mechanism behind shear stress-induced platelet aggregation is that at shear rates more than $1000s^{-1}$, platelets initially bind to the vessel wall or exposed extracellular matrix by the binding of platelet GPIbα to vWF[62;63]. This binding triggers an intracellular signaling pathway and activates platelets. Activation causes an increase in cytoplasmic Ca^{2+} concentration and the resulting ADP release triggers the binding of vWF/fibrinogen to GPIIb-IIIa which sustains platelet aggregation[64]. Despite the primary role of GPIIb/IIIa in platelet aggregation, blocking of vWF binding to GPIbα has been shown to result in inhibition of platelet aggregation[65]. Elevated shear stress could induce the binding of plasma soluble vWF to platelet surface receptor GPIIb/IIIa and to the GPIbα complex, and promote platelet aggregation.

3.6.2 Shear exposure time

One of the major drawbacks of the above discussed studies is the usage of steady shear to induce platelet activation, which is not physiologically relevant. Shear-induced platelet activation depends on both the magnitude of shear stress and the duration of shear exposure. Platelets exposed to low shear stress for a long period of time, or exposed to high shear stress for a short time, can both be activated. Short duration exposure (30 sec) to elevated shear stress at 60Pa was found to induce platelet lysis, while a shear of 16Pa

for 5min was also found to induce a similar response[60]. Further, platelets exposed to a shear of 10Pa for less than 20sec were found to be minimally activated (based on P-selectin expression) and reversibly aggregated (rapid disaggregation after the removal of shear stress)[66]. But when the duration was increased to longer than 20sec, platelets were highly activated and they irreversibly aggregated. In an attempt to investigate the platelet response near an arterial stenosis, Dong et al. exposed platelets to a complex pattern of elevated shear stress (10Pa) for a short duration (2.5sec) followed by a low shear exposure and found an enhanced platelet aggregation with minimal activation[66]. In an attempt to understand the effect of exposure time, Hellums summarized the effects of both shear stress magnitude and shear exposure time on platelet activation (as shown in Figure 5)[67], i.e., both high shear stress and low shear stress can activate platelets, with high shear stress requiring short time while low shear stress requiring long time.

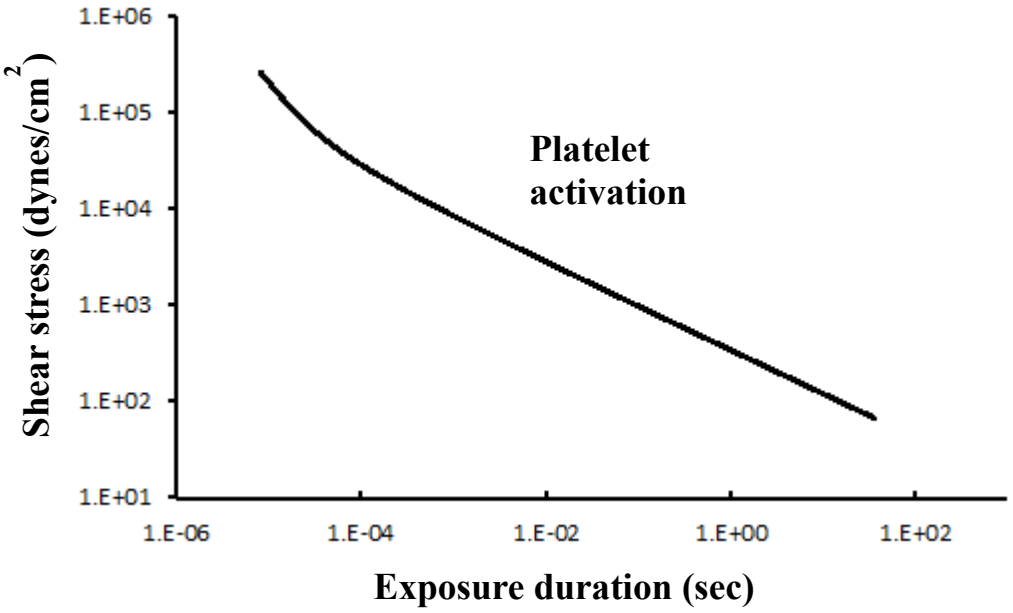

Figure 5. Platelet activation, function of serotonin release, presented as a relation between shear stress and exposure time. This is a compilation of results from different researchers using different devices. Modified and redrawn from Hellums et al.[67]

3.7 Shear induced platelet - complement interaction

Activated platelets mediate and support a number of inflammatory processes inside the circulatory system. Platelets are acclaimed as the agents for focusing inflammatory response to certain regions of vasculature and promoting inflammation during vascular disease conditions. They are presented with a number of surface molecules, including P-selectin, integrins ($\alpha_V\beta_3$, $\alpha_2\beta_1$, and $\alpha_{IIb}\beta_3$), CD40 ligand, CD40, and some junctional adhesion molecules[68], which link them to the immune system. In addition to these immune reactions, platelets also support complement activation.

3.7.1 Complement system

The complement system forms one of the major innate responses of the human immune system against the attack of any foreign bodies or pathogens. Complement is a complex biological system and consists of a group of serum proteases along with a set of regulatory proteins. The presence of foreign bodies or pathogens inside the human body will trigger complement activation and it plays a key role in clearing them from the system. The three major pathways of complement activation include the classical pathway, the alternative pathway and the lectin pathway (shown in Figure 6[69]).

Most of the components of the complement cascade are present in plasma and they circulate as zymogens. Under appropriate conditions, these zymogens become activated by proteolytic cleavage. The classical pathway is triggered by the binding of complement C1 complex (C1q-C1r-C1s) on the pathogen surface. This is followed by the cleavage of C4 and C2, leading to the assembly of C4b2b (known as C3 convertase). In the alternative pathway, low concentration of spontaneous activation of C3 happens in

plasma which binds with factor B and cleaved by factor D, leading to the formation of C3bBb or C3 convertase. Following either the classical pathway or alternative pathway activation, C3 is cleaved into C3b and C3a by C3 convertase. C3b binds with C3 convertase and forms the C5 convertase complex (C4b2b3b or C3bBb3b), which cleaves the successive components, finally resulting in the assembly of membrane attack complex (MAC) or C5b-9. The assembly of MAC on a cell surface will induce cell lysis, thereby the complement system clears pathogens from the human body.

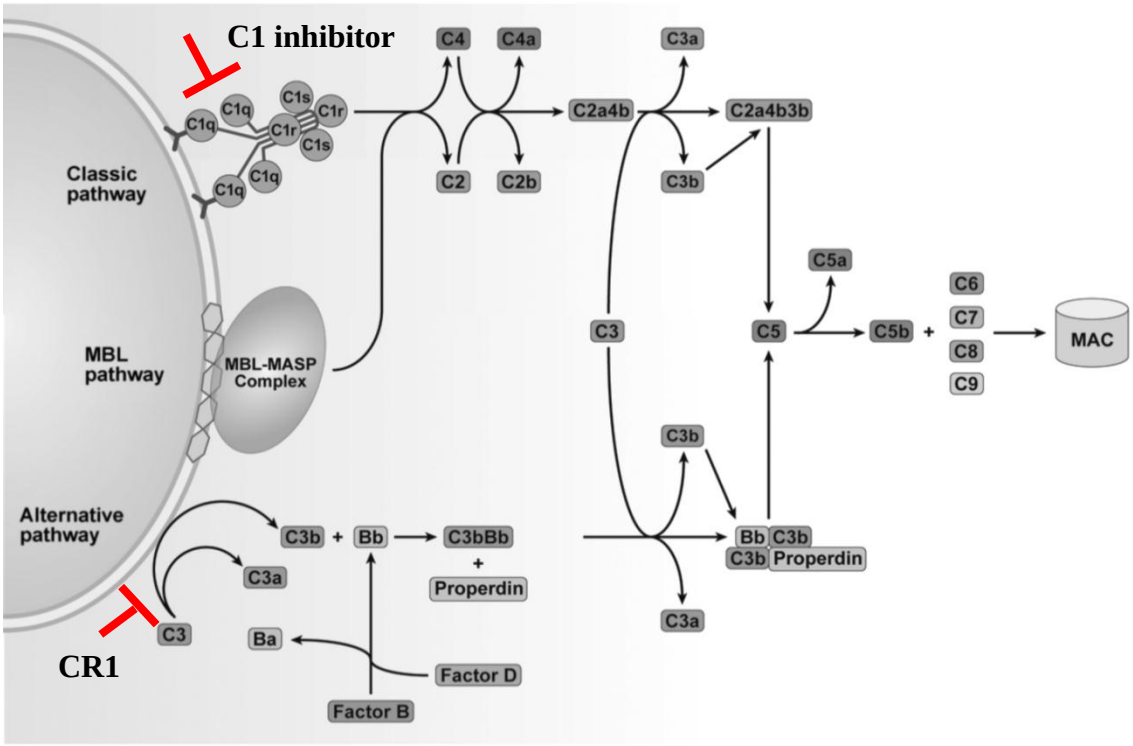

Figure 6. Complement cascade highlighting the classical, alternative and lectin pathway, resulting in the formation of membrane attack complex. Modified from Rutkowski et al.[69]

The effective regulation of the cytolytic potential of the complement system is carried out by a set of complement regulatory and inhibitory proteins. Some of the regulatory components include C1-inhibitor, C4b-binding protein, factor H, factor I, properdin, protectin and complement receptor 1. The two major inhibitory proteins that are involved in the classical pathway include C1-inhibitor (C1-INH) and the complement receptor 1 (CR1). C1-INH is present both in plasma and platelet α-granules. It can form covalent 1:1 complex with both C1r and C1s and inhibit the formation of C1 complex, thereby inhibiting the complement cascade at the initiation phase. Meanwhile, CR1 can bind to both C3b and C4b and form opsonized immune complex[70], which can be processed later by macrophages. Also, CR1 acts as a cofactor for factor I-mediated C3b cleavage[71]. Therefore CR1 functions as a regulator for both the classical and alternative pathway.

Complement activation has been found to play a major role in inflammation of various vascular disease conditions. The deposition of a number of complement proteins including C1q and C5b-9 have been found on atherosclerotic lesions[72-74]. Also, the plasma anaphylatoxins C3a, C4a and C5a that are released during the propagation of complement cascade can potentially alter the vascular permeability. In addition, atherosclerotic lesions, especially human coronary plaques, have revealed an increased level of C3a and C5a receptors[75].

3.7.2 Platelet complement activation

Recently, activated platelets were found to support complement activation to completion. Both classical and alternative pathway complement activation is supported

by platelets[76]. Platelets activated by elevated shear stress were found to induce classical pathway complement activation, by increasing C1q and C4d deposition on their surface[3]. In addition to the classical pathway, platelets were also found to support alternative pathway complement activation. P-selectin, a platelet activation marker protein, was found to facilitate the deposition and activation of C3, which could trigger the alternative pathway complement activation.

Furthermore, thrombin, which is a potent platelet agonist, also acts as a C5-convertase. Thrombin can biologically activate C5 even in the absence of C3 convertase[77]. On the other hand, the assembly of C5b-9 on platelet surface was found to induce platelet activation and subsequent secretion of procoagulant proteins[78;79]. These studies reveal the intrinsic ability of platelets to cross communicate with complement proteins. But the effect of dynamic shear stress on the interaction between platelets and complement cascade is yet to be investigated.

3.8 Platelet Proteomics

Proteomics can provide an efficient way for comprehensive analysis of protein expression under particular stimulation. Platelet proteomics follows two general approaches including global cataloging of all the proteins present in platelets and the functional characterization of subproteomes or changes within a proteome in response to a particular stimulation. In a recent study by Yin et al., platelet proteomic profiles in response to various agonists were analyzed using surface-enhanced laser desorption/ionization (SELDI) time of flight (TOF)[80] mass spectrometry. Distinct spectral

patterns were detected between resting and activated platelets in the low-molecular weight range (2-20 kda).

SELDI-TOF is a variation of conventional matrix assisted laser desorption ionization - time of flight (MALDI-TOF) mass spectrometry (MS), which enables a high throughout generation of protein profiles.

A SELDI protein chip array contains multiple spots composed of specific chromatographic configurations (cation/anion/hydrophobic/metal affinity). When a particular sample is applied to the chip, proteins/peptides in the sample are captured to this surface by electrostatic interaction, affinity chromatography or adsorption. After applying a suitable energy absorption matrix on the substrate, the captured proteins that are co-crystallized with the matrix are ionized using a nitrogen laser and a spectral profile is created by measuring TOF. The basic schematic of the SELDI system is shown below in Figure 7[81].

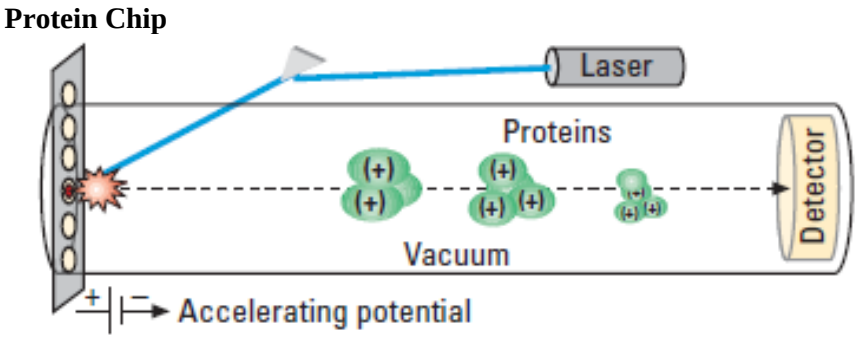

Figure 7. Functional schematic of the SELDI system showing protein chip, laser ionization and TOF measurement. Modified from Issaq et al.[81]

Proteomics technique can improve our understanding of platelet behavior at the post-translational protein level. Furthermore, this method can be used to analyze the variation in proteome and map various signaling cascades involved in different platelet functions. In this study, SELDI MS was used to investigate the effects of dynamic shear stress (at physiological and pathological level) on platelet proteomic patterns. Results obtained here can potentially lead to the identification of disease specific biomarkers for development of novel diagnostic procedures and interventional therapeutics.

3.9 Endothelial cell – Platelet interaction

EC and platelets interact in many ways. EC can express proteins (like TF, vWF) to attract platelets to the blood vessel wall. Under physiological conditions, this adhesion leads to platelet aggregation and clot formation to stop bleeding. Under disease conditions, platelet adhesion may induce thrombus formation.

EC and platelets can interact directly through their corresponding surface ligands and receptors. Activated platelets have elevated P-selectin expression on their surface, which mediates platelet rolling on activated EC[82], while elevated GPIbα expression enhances platelet interaction with EC surface vWF to enable platelet adhesion[58]. Both *in vitro* and *in vivo* studies have verified elevated adhesion of activated platelets to EC[83;84]. EC and platelets also interact through certain chemical messengers and proteins secreted upon activation. For instance, chemokines (such as TNF-α) released by activated EC are known to induce platelet microparticle generation[85]. With the advent of proteomics, platelet specific proteins were found localized to atherosclerotic plaques[86]. Activated

platelets are known to induce inflammation in EC, evidenced by elevated ICAM-1 and monocyte chemoattractant protein (MCP-1) expression[87;88].

Very few studies have investigated the direct interaction between EC and platelets, especially under shear stress conditions. P-selectin, expressed on activated platelet surface, is known to induce tethering and rolling of platelets on endothelium through its ligand PSGL-1, especially under low shear[82]. Also, an *in vivo* study with P-selectin double knock out (apoE-/- CD62P-/-) revealed a reduced atherosclerotic plaque occurrence compared to a normal mice[89]. In another *in vitro* study conducted by Macey et al., platelet microparticle formation was found to increase in whole blood flowing on TNF-α activated EC compared to flow on non-activated EC or after static co-culture[85]. Also, some *in vivo* studies have presented that platelets roll and adhere firmly to microvascular endothelium during postischemic reperfusion[84]. In addition to these direct interactions, platelets are responsible for a number of inflammatory response on ECs, especially on focusing responses to a particular vascular location under flow[90].

Based on the literature presented above, it is evident that the interaction between endothelial cells and platelets could be affected by flow. As a consequence, the altered interaction could affect the flow induced activation/response of EC and platelets individually. However, there is a gap in literature investigating EC-platelet interaction under physiologically relevant flow conditions. By filling this gap, our studies will help better characterize how EC-platelet communication/interaction affect cardiovascular disease progression.

The literature review above demonstrates that dynamic flow conditions and cell-cell interactions play very important roles in platelet and EC activities and disease development. The major focus of this project was to apply physiologically relevant dynamic shear stress to both endothelial cells and platelets and study their behavior. Also, their interactions were investigated in a EC-Platelet coupled shearing system. The results from this study will enable us to understand the interaction between EC, platelets and dynamic shear stress, especially during CHD initiation and development.

CHAPTER IV

MATERIALS AND METHODS

4.1 Numerical Modeling

4.1.1 LCA model

A physiologically realistic 3D human left coronary artery (LCA) model was developed using the computer aided design (CAD) software Pro-E Wildfire 4.0 (PTC). The LCA model was constructed based on the dimensions and geometrical information obtained through an anatomical study conducted by Dodge et al.[91;92]. In this study, the intrathoracic spatial locations of specific coronary artery segments were measured (on a normal human heart) through angiographic imaging. Dodge et al. presented an accurate measurement of both the spherical coordinates of centerline trajectory (left main - LM, left anterior descending artery - LAD, left circumflex artery -LCX and their branches) and the vessel diameters at different cross sections along the trajectory. This provided a way to build a physiologically realistic coronary artery model including the bifurcation, tapering and myocardial curvature.

The centerline trajectory of the LCA was first constructed using the spherical coordinates. Using various cross sectional diameters, the artery model was extruded through the trajectory. The branches in the model included LM, LAD, LCX, septals and diagonals. For this study, the 3D LCA model (presented in Figure 8) was constructed under both normal and disease conditions, which were modeled by adding a stenosis (30%, 60% and 80% reduction in vessel diameter) in the LAD branch downstream of the bifurcation (8mm from the apex of bifurcation). The key geometrical parameters including the vessel diameters, length of different branches and bifurcation angle are presented in Table 1.

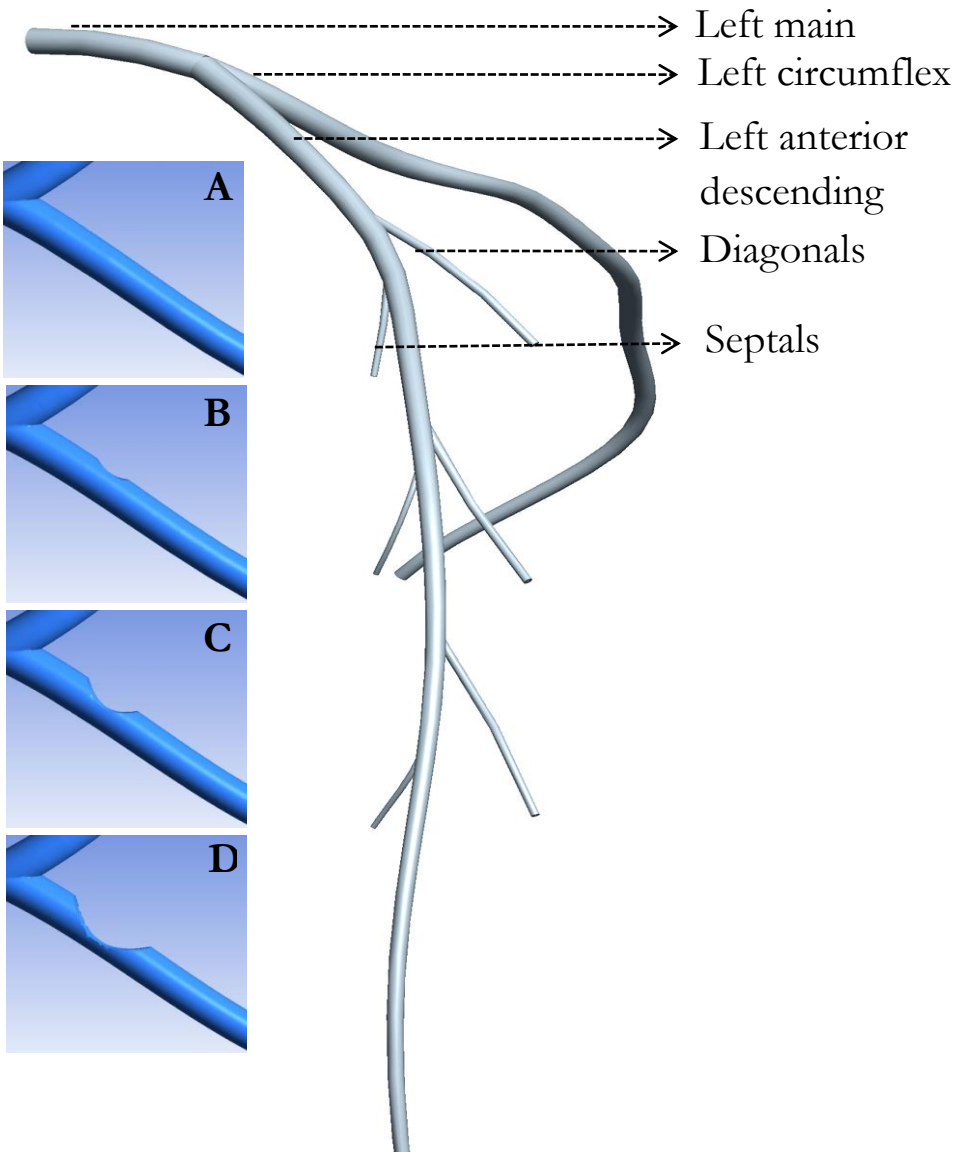

Figure 8. Physiologically realistic 3D computational model of the human left coronary artery used in this study. (A-D) represents LAD branch under normal, 30%, 60% and 80% stenosis condition respectively.

Table 1. Key geometrical parameters used for construction of human LCA model used in this study

	Parameter	Value (mm)
LM	**Inlet Diameter**	4.5
	Length	11
LAD	**Inlet Diameter**	3.8
	Length	118
	Outlet Diameter	1.9
LCX	**Inlet Diameter**	3.7
	Length	76.8
	Outlet Diameter	1.7
Bifurcation Angle		74.83˚

4.1.2 Computational Fluid Dynamics

Fluid flow in general is governed by three fundamental principles - conservation of mass, conservation of momentum and conservation of energy. The general equation for incompressible Newtonian fluid motion includes the continuity equation (mass balance – Equation 4.1) and the Navier-Stokes equation (momentum balance – Equation 4.2):

$$\boldsymbol{\nabla U = 0} \quad \textbf{.....(4.1)}$$

$$\boldsymbol{-\nabla P + \rho g + \mu(\nabla^2 U) = 0} \quad \textbf{.....(4.2)}$$

Where U is velocity vector [U ≡ (u, v, w)], P is pressure, ρ is fluid density and μ is dynamic viscosity of the fluid. In this case, a constant density of 1.06g/mL was used to model blood, while the local effective viscosity estimated by the solver was used to determine shear stress.

Computational fluid dynamics (CFD) provided a suitable way to qualitatively analyze the blood flow. In general, the fluid domain was subdivided into small elements (discretization) and the general equations were iteratively solved for each element (numerical solutions). For each time step, each node was updated (locally) with a new set of values. The accuracy of solution was dependent on the convergence of a set of predetermined variables, usually momentum and continuity variables. Based on the maximum Reynolds number (Re) in the domain (directly proportional to fluid velocity and cross sectional diameter shown in Equation 4.3), the type of flow (laminar /

turbulent) was determined (laminar flow if Re < 2300, transition to turbulent flow if Re > 2300) and suitable solvers were utilized (modified Navier-Stokes equations) accordingly.

$$\boldsymbol{Re = \frac{\rho.V.D}{\mu}} \text{ ..... (4.3)}$$

where ρ is fluid density, V is the fluid velocity, D is the length scale (cross sectional diameter for a circular cross section) and μ is dynamic viscosity of the fluid.

In the case of non-circular cross sections, Reynolds number (Re_{ij}) was calculated for each mesh element using the fluid velocity ($V_{i,j}$) and the length scale of that particular element (ΔX_{ij}), as shown in Equation 4.4.

$$\boldsymbol{Re_{ij} = \frac{\rho.V_{ij}.\Delta X_{ij}}{\mu}} \text{ ..... (4.4)}$$

In this study, the Reynolds number indicated that the flow was well within the laminar regime for normal, 30% and 60% stenosis conditions; hence a laminar solver was used. However, as complex flow patterns emerged under the 80% stenosis condition, a low Reynolds number k-ω turbulent solver was used.

4.1.3 Meshing

The LCA model (Figure 12) was meshed using a computational meshing package ICEM CFD v13.0, a preprocessor program for CFD solvers. A hybrid meshing scheme involving a combination of both hexahedral and tetrahedral elements was used to discretize the model. Particular regions of interest (bifurcation and stenosis region) were finely meshed compared to the rest of the model in order to optimize the memory loads and computing capacity while providing a feasible spatial resolution. All the results from

this study were tested for mesh independence. The total number of discretized elements for each model is listed in Table 2.

Table 2. Total number of nodes and elements under each condition that were used in this study.

Condition	No. of nodes	No. of elements	Element size range (mm)
Normal	209,520	961,733	0.014 – 0.432
30% stenosis	184,277	857,582	0.006 – 0.471
60% stenosis	168,182	761,719	0.072 – 0.536
80% stenosis	233,049	1,062,421	0.063 – 0.473

4.1.4 Coronary blood flow analysis

Solvers

The 3D human LCA CAD model (normal, 30%, 60% and 80% stenosis), constructed using Pro-E (WF 4.0, PTC) and discretized in ICEM CFD (ANSYS, v13.0) was imported into CFX-Pre (ANSYS v13.0), where the physical parameters of the model was configured. The flow was assumed to be laminar under normal, 30% and 60% stenosis conditions, while a k-ω turbulent solver was used to solve the flow field under the 80% stenosis condition. After defining all necessary assumptions and boundary conditions (given below) the model was exported to the CFX solver. Upon convergence

of momentum and continuity, the results were exported and analyzed using the CFD post package.

Assumptions

The coronary blood flow was solved using the following assumptions:

- **Fluid medium**: Blood was modeled as a continuous phase fluid with density of 1.06 g/cc.
- **Fluid inlet**: A transient coronary inlet velocity waveform was used (Figure 9)[93], and a fully developed parabolic inlet velocity profile (Figure 10) was defined at the inlet.
- **Walls**: The vessel wall was assumed to be rigid and non-porous, neglecting the viscoelastic property of the blood vessels.
- **Transient flow**: All simulations were conducted for a total of 3 cardiac cycles (0.9sec per cardiac cycle) with a time step size of 0.1 sec.
- **Convergence**: The convergence criteria for velocity components and continuity variables were set at 1.00E-6, while that of turbulence variables (k and ω) was set at 1.00E-3. A minimum of 600 iterations was required for each time step to reach convergence.

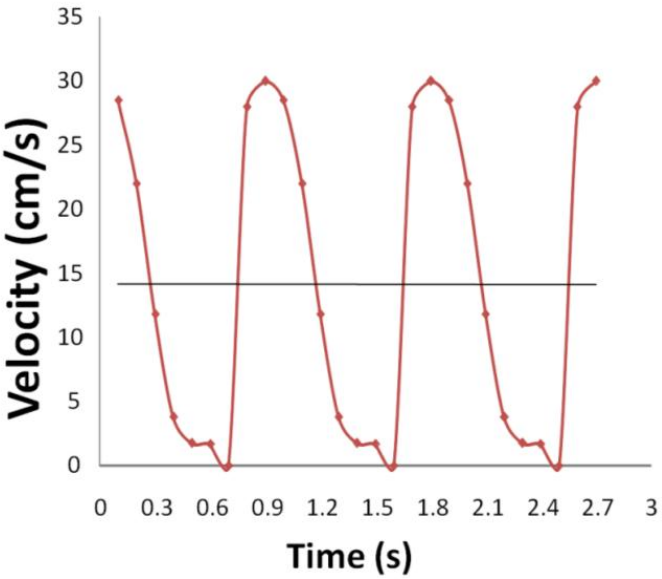

Figure 9. Inlet velocity waveform used in CFD simulations. Based on coronary input velocity for 3 cardiac cycles.

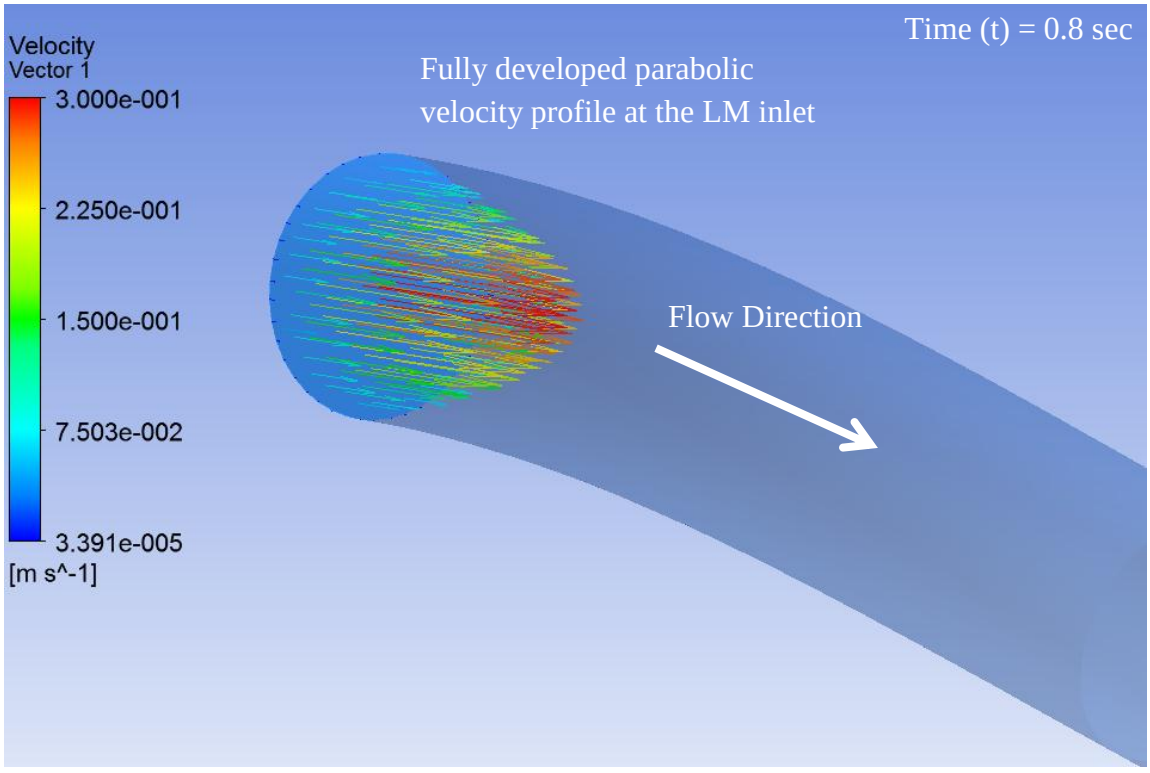

Figure 10. 3D fully developed velocity profile at the entrance of left main branch (t=0.8sec).

Boundary conditions

The discretized LCA model was exported to the CFX Pre software (pre-processing tool in the ANSYS CFX v13.0 package) and the following boundary conditions were defined.

- **Inlet**: The inlet surface boundary was defined as a velocity inlet (Figures 9 and 10). The maximum inlet velocity varied between 0.009 (at t = 0.7sec) and 30 cm/sec (at t = 0.9sec), at a normal heart rate of 72bpm.
- **Outlet**: The outlet surface was modeled as a pressure outlet and was set at atmospheric pressure. The distance of the outlet surface was sufficiently far away from regions of interest including the bifurcation and the stenosis (i.e., at least 9 times the inlet tube diameter from the bifurcation), hence the boundary condition should have negligible effect on the flow pattern.
- **Walls**: The rigid non-porous vessel wall boundary was defined as no-slip condition.

Shear stress history

After the simulation ended, shear stress at a particular wall node inside regions of interest (like stenosis throat, recirculation zone) was estimated in the solver (based on Equation 3.1). Shear stress history was constructed as shear stress at a particular node at every time step during one cardiac cycle. The computed shear stress history was then exported to a shearing device for the following *in vitro* studies.

4.1.5 Platelet Modeling

Platelets were modeled as a discrete phase and platelet trajectories as they traveled through the LCA were estimated using the Euler-Lagrangian approach. Platelets were seeded inside the LCA (released at LM inlet) at a rate of 1000 platelets per cardiac cycle and the simulations were conducted for at least 3 cardiac cycles. At the end of simulation, trajectories of platelets as they passed through the LAD branch of LCA, under normal and disease conditions, were calculated using the Lagrangian formulation in CFX (ANSYS, v13.0). The trajectories were calculated by integrating the particle force balance equation as shown in Equation 4.5.

$$\frac{du_i^p}{dt} = F_D\left(u_i - u_i^p\right) + \frac{g_i(\rho_p - \rho)}{\rho_p} + \frac{F_i}{\rho_p} \quad \text{..... (4.5)}$$

Where F_D is drag force, $\left(u_i - u_i^p\right)$ is particle relative velocity, and F_i accounts for additional forces like pressure gradient, Brownian motion and Saffman lift. At every time step, after iteratively solving the particle location, the shear stress value for that particular location (mesh element) was computed by the solver (based on Equation 3.1). By plotting the change in shear stress magnitude for every time step (along their trajectory), the shear stress history of platelets inside LCA was calculated.

Assumptions

- **Platelets**: Platelets were modeled as solid particles with a diameter of 4 μm, density of 1.2g/ml and viscosity of 1.2cP. A shape factor of 0.2 was defined to account for the flattened shape of platelets.

- **Seeding density**: 1000 platelets per cardiac cycle were released at the left main inlet surface and it was assumed that the initial velocity and acceleration (at time t=0) of platelet-like particles was 0.
- **Reactivity**: Platelet-like particles were chemically and biologically inert.

Two-way coupling: A two-way coupling scheme was employed, where the fluid phase influenced the drag and turbulence of particulate phase, and the particulate phase influenced the source terms (mass, momentum and energy) of the continuous phase.

4.2 Detailed methods section

Platelets: Fresh platelet rich plasma (PRP), anti-coagulated with 0.32% sodium citrate, was purchased from Oklahoma Blood Institute (Oklahoma City, OK) and platelets were separated from plasma by centrifugation (3000 rpm for 9 min). Washed platelets were prepared by resuspension of platelet pellets in HEPES (hydroxyethyl piperazine ethanesulfonic acid) buffered modified Tyrode's solution (HBMT: 0.137M sodium chloride, 2.7mM potassium chloride, 0.36mM monobasic sodium phosphate, 12mM sodium bicarbonate, 2mM magnesium chloride, 0.2% BSA, 5.5mM dextrose and 0.01M HEPES, pH to 7.4). The final platelet concentration was adjusted to 250,000/µl for all experiments. Platelet poor plasma (PPP), collected as supernatant after centrifugation of PRP, were aliquoted and stored at -80˚C until use.

Cell Culture: Human coronary artery endothelial cells (HCAEC) were purchased from Lonza (Walkersville, MD) and used between passages 2 and 8. HCAECs were grown to confluence on 6-well plates or petri dishes (6 cm) according to experiment requirements.

The cells were maintained in endothelial cell basal medium, supplemented with growth factors, including 2% fetal bovine serum (FBS), 0.1% hydrocortisone, hFGF, VEGF, R3-IGF-1, ascorbic acid, hEGF, GA-1000 and heparin (Lonza, Walkersville, MD). **Shearing Device:** Dynamic shear stress waveforms estimated from numerical simulations were applied to endothelial cells and platelets using two shearing devices: a cone and plate shearing device and a parallel-plate flow chamber.

Cone-Plate Shearing Device: A modified cone and plate viscometer, customer-built to accommodate 6-well plates (shown in Figure 11A), was used to apply various shear stress to platelets and endothelial cells[3;94;95]. The cones were made of ultra-high molecular weight polyethylene (UHMWPE), attached to the bottom of 4 stepper motors which were controlled by a PC. By adjusting the speed of the cones, shear stress generated in the wells could be precisely controlled. The cone-plate device used in this study had a cone angle of 0.5˚ and a radius of 1.733cm. This shearing device was primarily used to shear endothelial cells (EC) since they were usually cultured in 6-well plates. To apply shear stress to platelets, a cone-and plate system with a single cone was often used (Figure 11B, cone angle: 2˚ and radius: 2.455cm).

A uniform shear stress profile was generated in these devices, and it was directly proportional to the angular velocity of the cone. A schematic cross sectional view of the cone-plate device depicting the flow domain is shown in Figure 12.

The modified Reynolds number of the cone and plate shearing system can be calculated using Equation 4.7. The flow was laminar when $\tilde{R} < 1$.

$$\widetilde{R} = \frac{r^2 \omega \alpha^2}{12\nu} \text{..... (4.7)}$$

Where r is the radius of the cone and ν is the kinematic viscosity (ν=μ/ρ).

Under laminar conditions, shear stress generated by the cone-plate device can be calculated by Equation 4.6.

$$\tau = \frac{\mu.\omega}{\alpha} \text{.....(4.6)}$$

Where μ is dynamic viscosity of the fluid, ω is the angular velocity of the cone and α is the cone angle. While remaining in the laminar regime, the 6-well plate shearing device used in this study was capable of generating a maximum shear stress of 12Pa and the single cone shearing device was capable of generating a maximum shear stress of 7.2Pa.

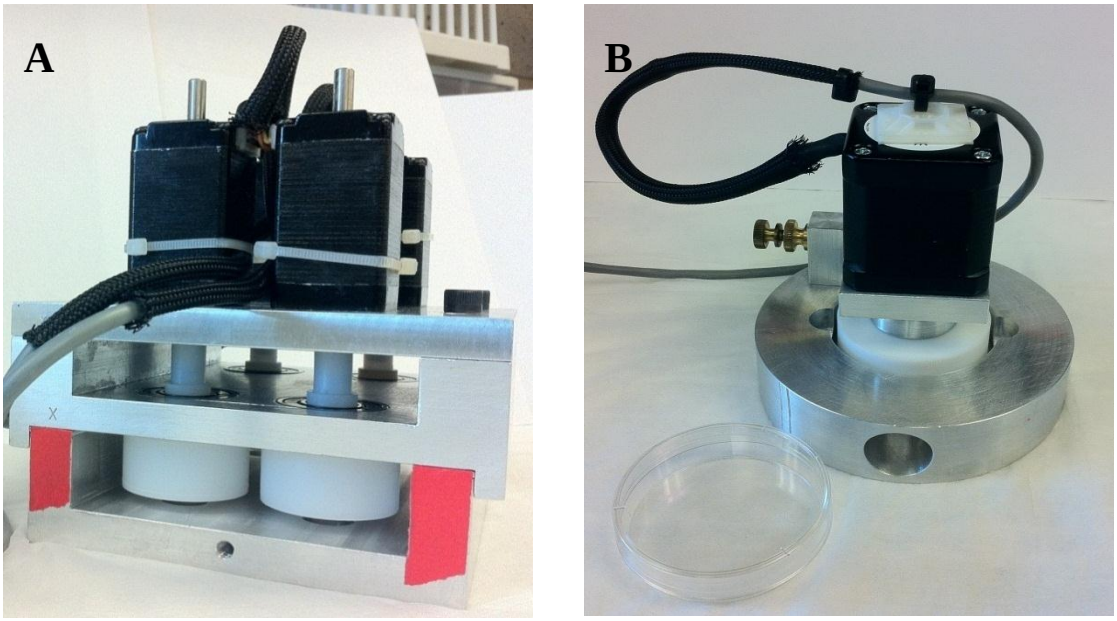

Figure 11. Modified cone and plate hemodynamic cell shearing device. Assembly of cones with the microstepper motor in a (A) 6-well plate used to shear EC and (B) single cone plate system used to shear platelets.

Shear stress history, estimated from the CFD simulation, was programmed into this cone and plate system to mimic the physiologically relevant dynamic shear stress conditions *in vitro* on a monolayer of EC or platelets. All experiments were conducted at 37˚C. For some experiments, platelets and EC were exposed to shear stress simultaneously, which was referred to as the coupled shearing experiments.

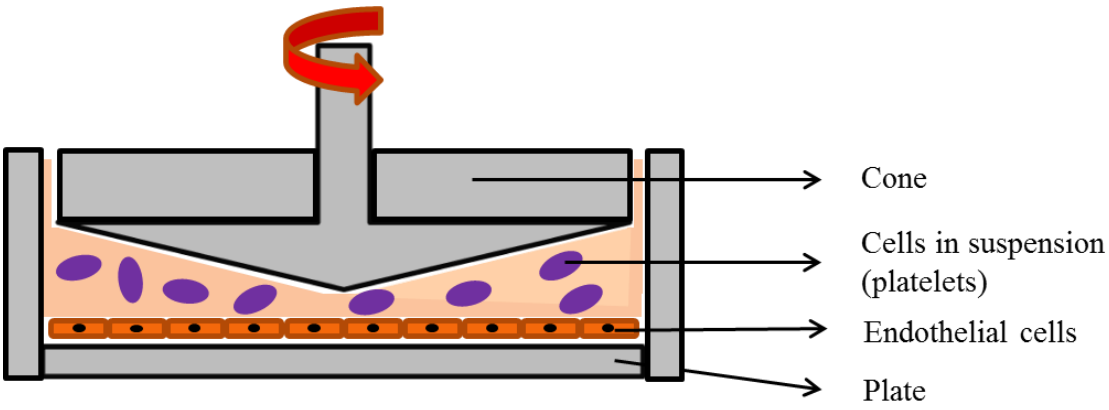

Figure 12. Cross sectional view of the cone-plate device used in this study to apply shear stress to endothelial cells (cultured on the bottom stationary plate) and platelets suspended in the flow domain. The device applies constant shear to both the cells attached on the bottom and also to the cells that are in suspension.

Parallel Plate Flow Chamber: A parallel-plate perfusion chamber was used alternatively to apply shear stress simultaneously to platelets and EC. The flow chamber was made of transparent polyvinyl chloride (channel height – 1mm, Figure 13A). The inlet and outlet of the chamber were connected to a peristaltic pump through tygon tubing, forming a flow loop (Figure 13B). The maximum shear stress generated in this chamber is calculated based on Equation 4.8 as given below.

$$\tau = \frac{6\mu Q}{bh^2} \quad \text{..... (4.8)}$$

Where μ is the fluid viscosity, b is the width of the chamber, h is the height of the chamber and Q is the flow rate inside the chamber. By adjusting the flow rate of the

pump, shear stress generated in the flow chamber can be precisely controlled. The flow chamber used in this study can generate shear stress ranging from 0.01 to 4.5Pa (by adjusting the flow rate up to a maximum of 660mL/min). Endothelial cells were grown to confluence on a glass coverslip (Electron Microscopy Sciences, Hatfield, PA), which was then placed on the bottom of the flow chamber. In the coupled shearing experiments, washed platelets were perfused through the chamber. The chamber was designed with sufficient entrance length such that the flow was fully developed as it reached EC on the cover slip, placed in the middle of the chamber. A schematic representation of the flow field is given in Figure 13C.

EC placed on the bottom of the chamber were exposed to a uniform shear stress (Equation 4.8), while platelets that were suspended in the flow field experienced a wide range of shear stress. For instance, in the region where flow was fully developed, platelets that were traveling close to the top and bottom wall experienced higher shear stress, compared to those travelling towards the center of the flow (as discussed in Section 3.1). This is a more physiologically relevant setup for EC-platelet interaction studies. However, due to the complex shear stress distribution on platelets, results obtained from these experiments, especially the platelet responses could be hard to interpret.

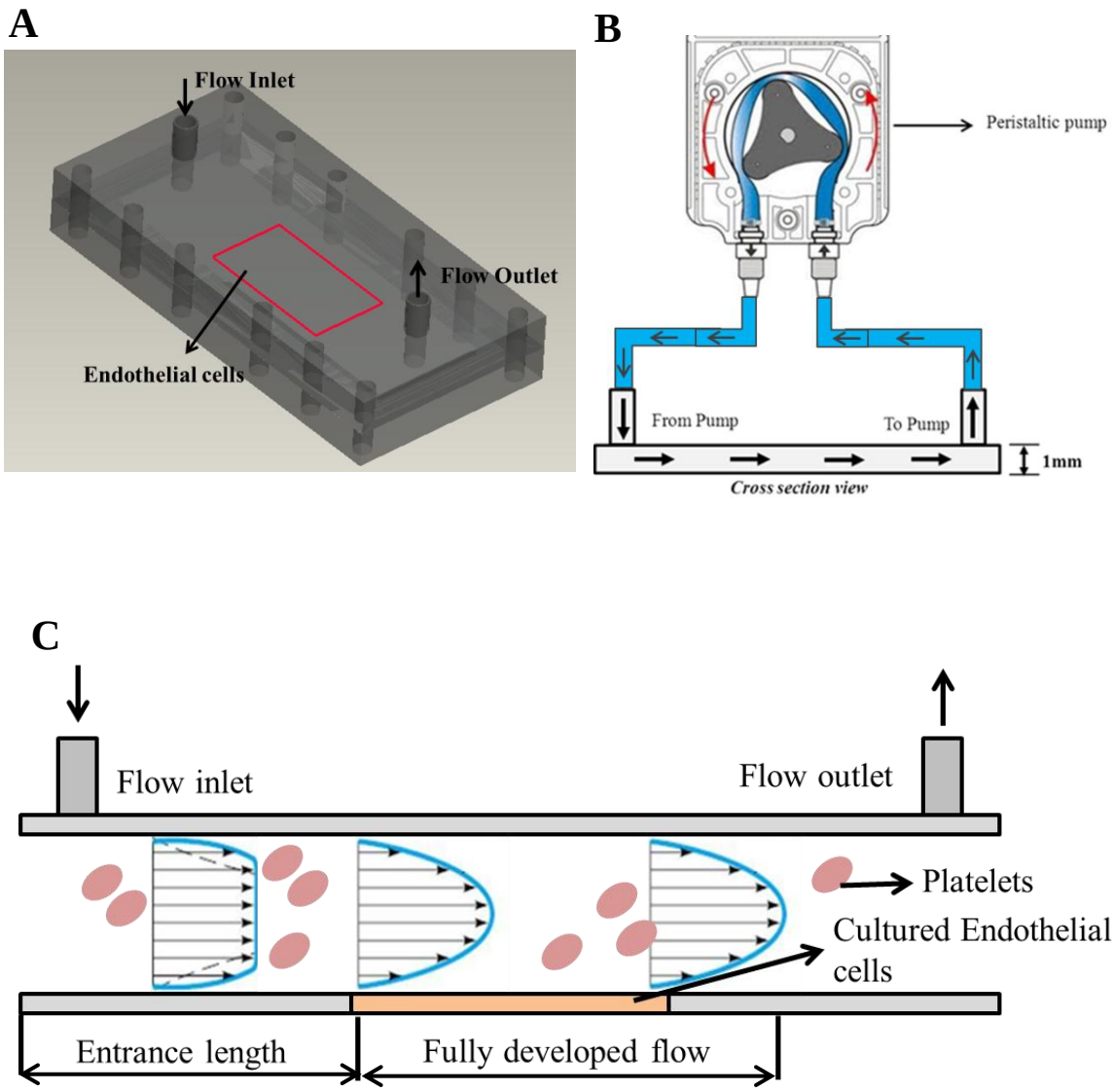

Figure 13. (A) Parallel plate flow chamber for shearing EC and platelets. (B) Complete flow loop set up with the chamber. (C) Schematic view of the flow development in the parallel plate flow chamber.

4.3 Effect of dynamic shear stress on EC

The wall shear stress estimated from numerical simulations was applied to EC in a cone and plate shearing device. The dynamic shear stress waveforms that were used in this study included normal, low-magnitude unidirectional, low oscillatory and high-magnitude pulsatile shear stress. Figure 14 depicts all four waveforms along with their corresponding locations. Normal shear represents the pulsatile shear stress history on a normal LCA wall (varies between 0.1 and 1 Pa), low magnitude unidirectional shear represents that inside the recirculation zone downstream of the stenosis (0.01 to 0.4 Pa), and high-magnitude pulsatile shear represents shear stress history on LCA wall at the stenosis throat (between 0.1 and 6 Pa, for 60% disease severity). The low oscillatory shear replicates shear history at certain regions near the bifurcation or in the recirculation zones where bidirectional flow occurs (±0.3 Pa, no net forward component). To measure changes in EC surface proteins and at mRNA level, EC were sheared for 60 min at 37°C. To measure changes in total proteins, EC were sheared for 120 min so as to ensure that the shear exposure time was long enough to induce changes in total protein expression, if any.

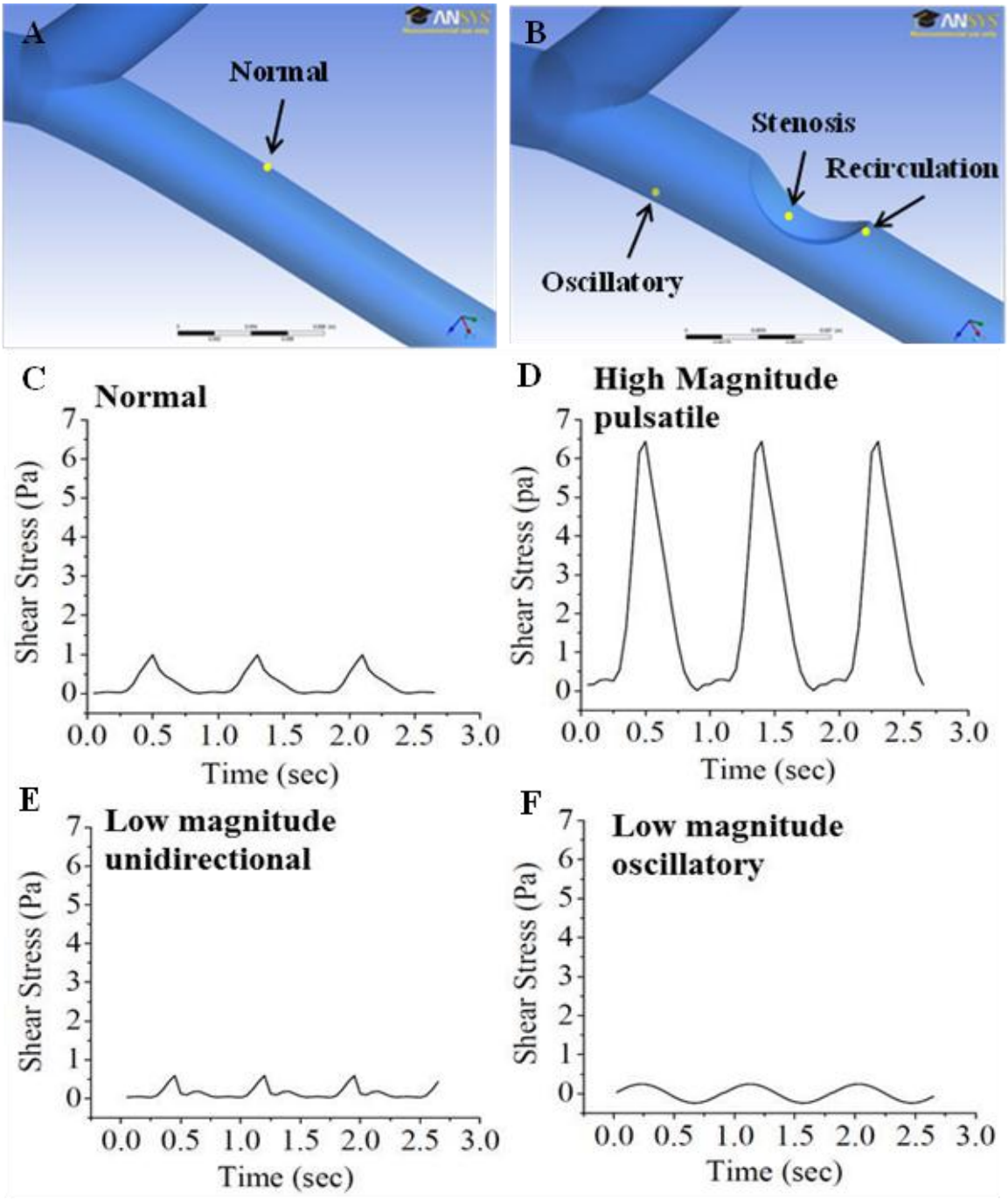

Figure 14. Shear stress history on EC vessel wall (over 3 cardiac cycles) inside LAD during CHD. (C) Normal waveform corresponds to WSS inside normal healthy LAD as shown in (A). (D) High magnitude pulsatile shear corresponds to WSS at 60% stenosis throat shown in B. (E, F) Low magnitude unidirectional and bidirectional shear waveform corresponding to WSS on EC present inside recirculation and oscillatory zone as shown in B. (oscillatory - bidirectional pulsatile shear with no net forward component)

4.3.1 Materials used

Antibodies: Mouse monoclonal anti-human ICAM-1 (1μg/mL, Ancell Corporation, Bayport, MN), tissue factor (1μg/mL, Abcam, Cambridge, MA), thrombomodulin (1μg/mL, Abcam) and von Willebrand Factor (1μg/mL, Abcam) antibodies were used to measure EC ICAM-1, TF, TM and vWF expression. For ELISA, primary antibody binding was detected using an alkaline phosphatase conjugated goat anti-mouse secondary antibody (1:1000 in PBS, Sigma Aldrich); for Western blot, primary antibody binding was detected using a horseradish peroxidase (HRP)-conjugated goat anti-mouse secondary antibody (1:1000 in PBS, Abcam). To detect total vWF expression in EC using Western blot, rabbit polyclonal anti-human vWF primary antibody (1μg/mL, Abcam) was used along with a HRP conjugated goat anti-rabbit secondary antibody (1μg/mL, Abcam).

Buffers:

- Phosphate-Buffered Saline (PBS)

  PBS contains 9% NaCl, 1M sodium phosphate dibasic, 0.5M sodium phosphate monobasic. The pH was adjusted to 7.4 using 1 M HCL.

- Tris-Buffered Saline (TBS)

  TBS was made with 19.97mM Tris and 0.15M of NaCl and set to the pH of 7.4.

- 0.5% Glutaraldehyde (Sigma Aldrich)
- 100mM Glycine – 0.1% BSA
- Lysis Buffer

0.1% Triton X – 100 (in PBS) containing proteolytic inhibitors aprotinin (1μg/mL), leupeptin (1μg/mL) and phenylmethylsulfonyl fluoride (PMSF, 1mM).

4.3.2 Shear stress induced EC activation – ICAM-1 expression

4.3.2.1 Surface protein expression measurement using a solid phase ELISA approach

EC exposed to different pulsatile shear stress waveforms (60min, 37°C) were examined for activation by measuring EC surface ICAM-1 expression using a solid phase ELISA approach. After shearing, cells were washed in PBS (2X) and fixed using 0.5% glutaraldehyde (15min, 37°C), followed by neutralization with 100mM Glycine – 0.1% BSA for 30 minutes. EC surface ICAM-1 expression was measured using a murine monoclonal anti-human ICAM-1 antibody (60min, 37˚C). After washing with PBS (2X), primary antibody binding was detected using alkaline phosphatase conjugated goat anti-mouse secondary antibody (60min, 37°C). After washing (2X), secondary antibody binding was detected using p-nitrophenyl phosphate substrate (pNPP, 1mg/mL) (Pierce biotechnology, Inc.) and color development was quantified by absorbance at 405nm in a microplate reader. For all experiments, untreated endothelial cells (EC maintained under static conditions) were used as control. EC incubated in PBS without primary antibody was assayed for non-specific antibody binding.

4.3.2.2 Total protein expression using Western blot

In addition to surface ICAM-1 expression, shear-induced changes in EC total ICAM-1 expression was measured using Western blot. For Western blot experiments, EC were sheared for a duration of 120min (37°C) to ensure shear exposure was long enough to affect total protein expression. After being exposed to different pulsatile shear stress

waveforms, EC were trypsinized and collected by centrifugation (3000rpm, 6min). The endothelial cell pellet was resuspended and incubated in lysis buffer (0.1% Triton X-100 in PBS) supplemented with proteolytic inhibitors including aprotinin (1μg/mL), leupeptin (1μg/mL) and PMSF (1mM) (at 4˚C, 60min) (volume normalized to cell count after shearing). Samples were then centrifuged at 14,000 rpm for 5min, and the supernatant containing cytosolic proteins was collected and stored at -80˚C until use. Gel electrophoresis was conducted on a 10% polyacrylamide gel, at 150V and 80mA (approx.) for 100 minutes. The protein bands were then transferred to a nitrocellulose membrane (0.2μm pore size, Whatman, Dassel, Germany) for Western blot analysis, using a mouse monoclonal ICAM-1 antibody (60min at RT). Primary antibody binding was detected using a HRP-conjugated goat anti-mouse secondary antibody. Secondary antibody binding was detected using a HRP chemiluminescent substrate (ECL, Thermo Fisher Scientific Inc., Rockford, IL) and read in a chemiluminescent imaging device (FluorChem HD2 system, Cell Biosciences, Santa Clara, CA). The intensity of protein bands was quantified using spot densitometry analysis (AlphaView software, Cell Biosciences). β-actin expression was used as loading control.

4.3.2.3 ICAM-1 mRNA expression

Shear stress induced changes in ICAM-1 expression at mRNA level was measured using RT-PCR. After exposure to shear stress (60min, 37˚C), the cells were collected in TriZol (Invitrogen) and the total RNA was isolated. RNA samples were then reverse transcribed using the cDNA synthesis kit from Quanta Biosciences (Gaithersburg, MD), following the manufacturers protocol. The forward and reverse primers for ICAM-1 were designed using Primer Express Software (Applied Biosystems, Inc., Foster City, CA).

The forward primer for ICAM-1 was 5' -AGACAGTGACCATCTACAGCTTTCC -3', and the reverse primer was 5' - CACCTCGGTCCCTTCTGAGA -3'. β-actin was used as endogenous control. The forward and reverse primer sequence for actin were 5' - TGCCGACAGGATGCAGAAG -3', and 5'- CTCAGGAGGAGCAATGATCTTGAT-3' respectively. For amplification of ICAM-1 expression, 2µl of cDNA was added to SYBR® Green PCR master mix (Applied Biosystems) containing 0.25µM forward as well as reverse primers. PCR was performed in a Step-One-Plus system (Applied Biosystems). Relative mRNA expression (RQ) normalized to control EC (cells that were not exposed to shear stress) was calculated using the ΔC_t method.

4.3.3 Shear stress induced EC injury – Tissue factor (TF) and Thrombomodulin (TM) expression

4.3.3.1 Surface protein expression using ELISA

After shear exposure, EC surface tissue factor and thrombomodulin expression was measured using monoclonal murine anti-human tissue factor and thrombomodulin antibodies, using a solid phase ELISA approach as described before.

4.3.3.2 Total protein expression using Western blot

Similarly, total tissue factor and thrombomodulin expression in EC was measured using Western blot as described previously. Alternatively, total tissue factor expression in EC was measured using a commercial sandwich ELISA kit (American Diagnostic Inc., Stanford, CT). Briefly, after shear exposure, cells were washed twice (PBS), trypsinized and collected. After normalizing the cell count, EC were resuspended in 0.1% Triton X-

100 (in TBS) and lysed by sequential freeze-thaw cycles (3X, 30min freezing at -80˚C followed by 30min thawing at 37˚C water bath). Cell membrane and debris were removed by centrifugation, and the supernatant containing cytosol proteins was collected. The samples were then applied to a 96-well microtiter plate pre-coated with mouse monoclonal TF capture antibody (overnight at 4˚C). The wells were washed with wash buffer (PBS with 0.1% Triton X-100, pH 7.4) and incubated with biotinylated anti-human TF $F(ab')_2$ antibody (60min at RT). After washing, antibody binding was detected using a streptavidin conjugated horseradish peroxidase (60min at RT) and developed using a tetramethylbenzidine (TMB) substrate. The reaction was stopped after 20min using 0.5M H_2SO_4 and color development was measured at 450nm using a microplate reader.

4.3.3.3 mRNA expression using RT-PCR

Shear stress-induced changes in TF and TM mRNA expression was measured using RT-PCR (as described before). The forward and reverse primers used for TF were 5'-GCGCTTCAGGCACTACAAATACT-3' and 5'-CCTGACTTAGTGCTTATTTGAACAGTGT-3' respectively, while those for TM were 5' - CTCATAGGCATCTCCATCGCG -3' and 5' - CCGCGCACTTGTACTCCATCT -3' respectively. β-actin was used as endogenous control.

4.3.4 Shear stress induced EC platelet adhesion receptor – von Willebrand factor (vWF) expression

4.3.4.1 Surface protein expression using ELISA

Shear stress induced changes in EC surface vWF expression was measured using a solid phase ELISA as described above, using a monoclonal murine anti-human vWF antibody.

4.3.4.2 Total protein expression using Western Blot

Post shearing, changes in EC total vWF expression was measured using Western blot as described before. A rabbit polyclonal anti-human vWF was used as the primary antibody (1μg/mL) to detect total vWF. Primary antibody binding was detected using a HRP conjugated goat anti-rabbit secondary antibody (1μg/mL) and developed using ECL substrate.

4.3.4.3 mRNA expression using RT-PCR

As described before, shear stress induced changes in vWF expression was measured using RT-PCR. The forward and reverse primers were 5'-GTTCGTCCTGGAAGGATCGG-3' and 5'-CACTGACACCTGAGTGAGAC-3' respectively. β-actin was used as endogenous control.

4.4 Effect of dynamic shear stress on platelets

Typical platelet shear stress histories (waveforms shown in Figure 15) obtained from numerical simulations were applied to platelets *in vitro* in the cone and plate shearing device. Platelets were exposed to three specific shear stress waveforms including normal (represents shear stress on platelets passing through a normal LCA, 0.1-1Pa), high magnitude pulsatile (platelet passing through the stenosis once every 90 sec, normal shear with intermediate exposure to 6Pa for 0.1 sec once every 90 sec) and low magnitude unidirectional shear (platelet caught in recirculation zone downstream of the stenosis, 0.04-0.1Pa) waveforms. In general, the concentration of platelets is higher near the vessel wall compared to that in the core flow. Therefore shear stress history of platelets that travel close to the vessel wall was chosen, which was very similar to the wall shear stress history used for endothelial cells. The major difference between EC and platelet shear stress history was in the stenosis shear waveforms. EC, due to their fixed spatial location, were continuously exposed to a peak shear of 6Pa every cardiac cycle. However, as platelets traveled through the stenosis throat they were momentarily exposed to a peak shear of 6Pa. As they passed the stenosis region, they were exposed to physiological level shear stress. We assumed that platelets traveled through the same stenosis throat once every 90 sec.

Pulsatile shear-induced platelet activation was measured by their ability to generate thrombin, using a modified prothrombinase assay. This experiment was conducted in our lab as a part of a study published earlier by Yin et al[4]. In the present study, shear stress-associated platelet complement activation was measured through platelet surface C1q, C4d, iC3b and sC5b-9 expression. Changes in platelet proteomic

profiles induced by shear stress was examined using the surface enhanced laser desorption ionization (SELDI) ProteinChip reader.

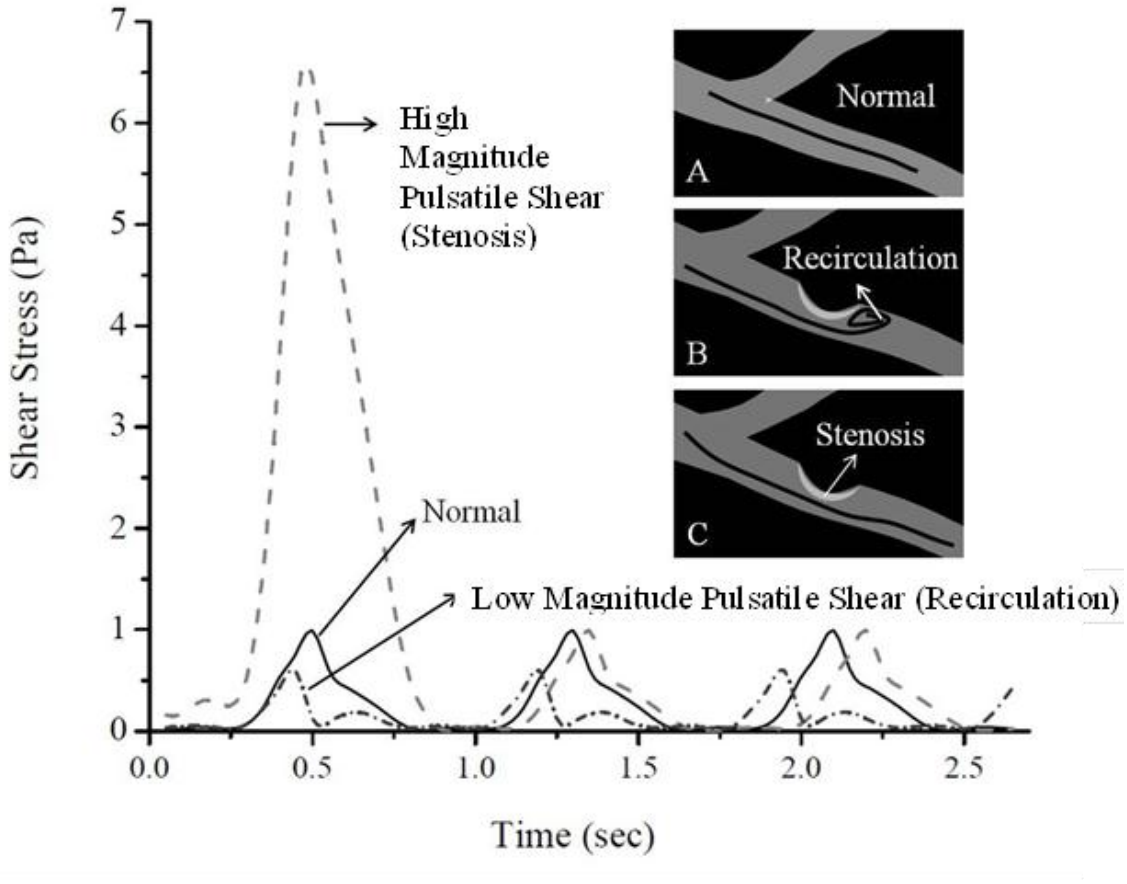

Figure 15. Shear stress history (3 cardiac cycles) on platelet passing through LAD under different conditions. Normal - platelet passing through healthy LAD, Stenosis - Platelet passing through 80% stenosis artery and Recirculation - platelet trapped inside recirculation zone.

4.4.1 Materials used

Antibodies: Mouse monoclonal anti-human C1q, C4d, iC3b and sC5b-9 (1μg/mL, Quidel Corporation, San Diego, CA) antibodies were used to measure platelet surface deposition of complement proteins – C1q, C4d, iC3b and sC5b-9. FITC conjugated goat anti-mouse secondary antibody (Sigma) was used to detect primary antibody binding for flow cytometry measurements. Non-specific binding was detected by incubating platelets with FITC-conjugated MOPC (Ancell Corporation, Bayport, MN). For ELISA, the primary antibody binding was detected using an alkaline phosphatase conjugated goat anti-mouse secondary antibody (Sigma-Aldrich). Platelet surface complement receptor–1 (CR1) expression was detected using a monoclonal murine anti-human CD35 antibody (Ancell).

Buffers:

- Hepes Buffered Modified Tyrode's solution (HBMT)
- 0.5% glutaraldehyde
- 100mM glycine with 0.1% BSA
- Tris-Buffered Saline (TBS) (described above)
- Phosphate-Buffered Saline (PBS) (described above)
- ProteinChip CM low-stringency buffer: 0.1M sodium acetate, pH 4.0 (BioRad)

4.4.2 Platelet associated complement activation

4.4.2.1 Platelet surface complement protein deposition

Washed platelets were exposed to above mentioned pulsatile shear stress waveforms for 30min and platelet complement activation (surface deposition of

complement protein C1q, C4d, iC3b and sC5b-9) was measured using a solid-phase ELISA. Platelets were sheared for only 30 minutes, as significant changes in platelet complement response were detected. Briefly, sheared platelet samples were immobilized into a 96-well microtiter plate pre-coated with poly-L-lysine (10µg/mL, 30min at 37˚C), fixed with 0.5% glutaraldehyde (15min, 37˚C) and blocked using 100mM glycine – 0.1% bovine serum albumin (BSA, 99% fatty acid free, Sigma-Aldrich). After washing (TBS), platelets were incubated with human plasma (PPP diluted 1:10 in HBMT, 60min, 37˚C). Platelet complement protein deposition was measured by incubating the samples with murine monoclonal anti-human C1q, C4d, iC3b and sC5b-9 antibodies (1:200 in HBMT, 60min, 37˚C). Primary antibody binding was detected using an alkaline phosphatase conjugated goat anti-mouse secondary antibody (1:1000 in HBMT, 60min 37˚C). Finally, complement protein deposition was developed using a p-nitrophenyl phosphate substrate (pNPP, 1mg/mL) (Pierce Biotechnology, Inc.) and measured at 405nm in a microplate reader.

Alternatively, complement protein deposition on platelets in fluid phase was measured using flow cytometry. Post shearing, platelet samples were treated with plasma in suspension (60min, 37˚C) and washed twice by centrifugation (1000x*g*, 5min). The samples were then incubated with murine monoclonal anti human C1q, C4d, iC3b and sC5b-9 antibodies (1:100, 30min, RT); primary antibody binding was detected using a FITC conjugated goat anti-mouse secondary antibody (1:100, 30min, RT). After incubation, platelet samples were fixed in 1% paraformaldehyde (AlfaAesar, MA) and read in a flow cytometer (Accuri C6, Ann Arbor, MI). Resting platelets were used as

negative control, while platelets incubated with MOPC antibody was used to measure non-specific binding.

4.4.2.2 Activation of complement inhibitors

The complement system is highly regulated by a set of complement inhibitors. For instance, C1 inhibitor (C1-inh) can form a covalent 1:1 complex with both C1r and C1s (sub-units of C1 complex) and prohibit the formation of C1 complex[96]. Similarly, complement receptor 1 (CR1) interacts with C3b and C4b, and regulates both classical and alternative pathway of complement cascade[71]. The amount of C1-inhibitor (C1-INH) released during shearing was also measured. After shearing, the platelet samples were centrifuged (3000rpm, 6min) and the supernatant was collected and assayed for C1-INH, using a C1-inhibitor ELISA kit (Quidel Corporation, San Diego, CA). Briefly, the samples were diluted 1:10 in specimen dilutent (0.035% ProClin 300 in PBS) and incubated with biotin conjugated C1-INH reactant to form C1-inhibitor:C1 reactant complex (C1-INH complex), which was fixed to avidin pre-coated microtiter wells. After washing (0.05% Tween20 and 0.035% ProClin 300 in PBS), the fixed C1-INH complex was incubated with HRP conjugated anti human C1-INH antibody. The samples were then treated with a chromogenic substrate and color development was read at 405nm using a microplate reader. Based on a standard curve, the amount of C1-INH released by platelets during shearing was quantified.

Shear-induced changes in platelet surface complement receptor 1 (CR1) expression was measured using a solid phase ELISA as described earlier, using a monoclonal murine anti-human CD35 antibody.

4.4.3 Platelet proteomics

Platelets stimulated with shear stress were examined for changes in proteomic profiles using the SELDI ProteinChip reader (BioRad, Hercules, CA). Washed platelets were exposed to two different types of shear stress conditions – constant shear (1 and 3Pa) and dynamic shear (normal, low magnitude unidirectional and high magnitude pulsatile shear) for 60min as described above. After treatment, platelet samples were washed with 0.9% NaCl containing 10mM EDTA (by centrifugation 1000x*g*) and resuspended in platelet lysis buffer (0.1% Triton X-100 in PBS) containing proteolytic inhibitors (1μg/mL aprotinin, 1μg/mL leupeptin and 1mM PMSF). After incubating on ice for 60 min, the insoluble cell membrane components were discarded by centrifugation (12000x*g*) and the cell lysate was collected and stored at -80˚C until use. Resting platelets were used as control, while platelets treated with thrombin receptor activator peptide (20μM TRAP, 5min, RT) were used as the positive control.

A weak cation exchange chromatographic substrate (CM 10 ProteinChip Array shown in Figure 16, BioRad) was prepared by washing the substrate with low stringency binding buffer (pH 4.0, BioRad). The lysate samples were then applied to these pre-activated surfaces and incubated at room temperature for 60min. After removing excess samples, the binding spots were washed using a CM low-stringency binding buffer (BioRad, 3X), followed by deionized water (2X). The chromatographic spots were allowed to air dry (~5 min, RT) and embedded in an electron-absorbing sinapinic acid energy absorption matrix (SPA-EAM, BioRad). The matrix was prepared by diluting lyophilized EAM in equal volumes of 1% trifluoracetic acid (Fisher Scientific) and sinapinic acid (Sigma). The ProteinChip arrays were then read in the SELDI ProteinChip

reader (BioRad). The threshold range was kept at 1500Da (corresponding to SPA-EAM matrix noise) and the signal to noise ratio was kept at 3.0. Based on the time of flight data collected, protein mass over charge (m/z) ratio was estimated. The m/z data was calibrated using a known peptide calibration chip containing 6 different peptide peaks in the range of 2-20KDa (BioRad) under same conditions. The peptide calibration peaks included Arg8-vasopressin (1084.25Da), somatostatin (1637.90Da), dynorphin A (2147.5Da), ACTH (3465Da), Beta endorphin (3465Da), Arg-insulin (5963.8Da) and cytochrome C (12230.92Da). Small proteins/peptides in the range of 2 to 20kDa (m/z) were of special interest in this study.

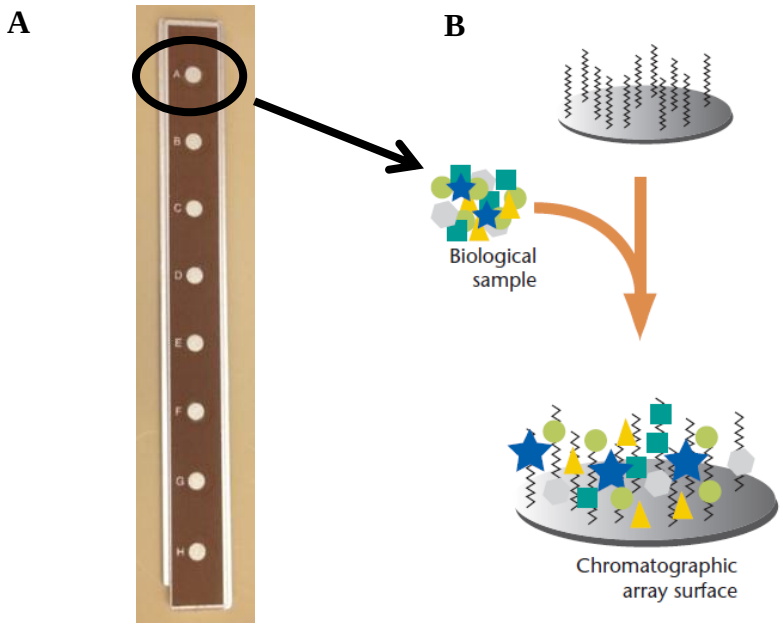

Figure 16. (A) SELDI protein chip with chromatographic spots/surface on which the samples were applied. (B) Capture of biological samples on a chromatographic surface.

The spectral data was analyzed using the ProteinChip data management software (BioRad). Baseline of each spectrum was adjusted to offset noises, and all spectral peaks were normalized. Spectral profiles obtained from sheared and resting platelet were compared by using peak cluster analysis provided by the software. Signal to noise ratio was set at 5 and mass tolerance at 0.3%. For statistical analysis, peak intensity was used.

4.5 Effect of dynamic shear stress on EC – platelet interaction

To examine how platelet-EC interaction affected cell responses to dynamic shear stress, confluent HCAEC were exposed to various shear stress waveforms in the presence of washed platelets (250,000/μL) *in vitro* in a cone and plate shearing device or a parallel-plate flow chamber. As discussed earlier (Section 4.4), normal and low magnitude unidirectional shear waveforms were similar for both EC and platelets. The high magnitude pulsatile shear was different for EC and platelets (shown in Figures 14 and 15). To study interaction, the platelet high magnitude pulsatile shear waveform was used in the coupled cone and plate shearing system. In the cone and plate shearing system, since shear stress was uniform everywhere, using the EC high shear waveform would have led to a significantly increased shear stress loading (shear-time integral) on suspended platelets, which might potentially induce fast cell activation or damage[3]. Hence the platelet high shear waveform was used for coupled shearing experiments. Effects of shear stress and cell-cell interaction on EC activation, EC inflammatory response, platelet thrombogenicity, and platelet complement activation were examined.

In the parallel-plate flow chamber, platelets and EC experienced different shear stress at the same flow rate. For platelets in the fluid phase, cells that were moving close

to the top and bottom boundary of the chamber experienced higher shear stress, while cells moving in the center of the chamber were exposed to a lower shear stress (as shown in Section 4.2 and Equation 4.8). For EC that were attached to the bottom of the chamber, as flow was fully developed (as described in Section 4.2), shear stress exerted on the cells was uniform and was proportional to the flow rate. The parallel-plate flow chamber provided a more physiological experimental setup to investigate direct interaction between EC and platelets under dynamic shear stress conditions. However, with platelets and EC exposed to different shear stress, the complexity of the experiment significantly increased. Flow rate in the chamber was adjusted to mimic normal (0-200mL/min), low (0-90mL/min) and high (0-660mL/min) magnitude pulsatile shear environment, with the maximum shear stress of 1, 0.4, and 3Pa generated on the bottom of the chamber on EC, respectively. To examine the effect of dynamic shear stress and platelet-EC interaction on individual cell responses, platelet adhesion to EC was directly examined using immunofluorescence microscopy.

4.5.1 Materials used

Antibodies**:** Alexa fluor 488 conjugated Phalloidin against F-actin (Invitrogen, Grand Island, NY), DAPI nucleic acid stain (Invitrogen) and TRITC conjugated antibody against GPIbα (CD42b, Ancell) were used to detect platelet adhesion to EC using immunofluorescence microscopy. PECAM-1 expression on both EC and platelets was detected using TRITC conjugated anti-human CD31 antibody (Ancell). Mouse IgG1 Kappa (MOPC) conjugated with FITC and TRITC was used as isotype negative control.

4.5.2 EC response to dynamic shear stress in the presence of platelets

EC and platelets were exposed to various shear stress waveforms simultaneously for 60min. After shearing, platelets were removed from the coupled-shearing system and EC were washed gently in PBS (2X). EC response was measured by cell surface ICAM-1 and TF expression using a solid phase ELISA approach (as described before); and EC ICAM-1 mRNA expression was measured using RT-PCR (as described before). In a parallel work conducted by other lab members, EC surface TM and vWF expression was examined after co-shearing with platelets, and no significant change was observed under all three shear conditions.

4.5.3 Platelet response to dynamic shear stress in the presence of EC

After exposed to shear stress with EC, platelet samples were removed from the coupled shearing system and platelet thrombogenicity was measured using a modified prothrombinase assay (PAS)[97]. In a previous study conducted by other lab members, platelets were exposed to all three pulsatile shear waveforms alone and their thrombogenicity was measured using PAS assay[4], which measured acetylated thrombin generation from acetylated prothrombin. This previous study demonstrated that after 30min of shear exposure high magnitude shear induced an elevated rate of thrombin generation compared to normal shear but no change was observed under low magnitude shear. However, at the end of 30min, low magnitude shear induced a 50% increase in thrombin generation compared to normal shear. This result indicated that a longer exposure to low magnitude shear could potentially lead to elevated platelet activation.

Here, similar experiments were conducted in the presence of EC to investigate if platelet-EC interaction would affect platelet response to dynamic flow conditions. Acetylated thrombin did not have a positive feedback on platelet activation, thus provided a one-to-one relationship between shear stress and thrombin generation. After shear exposure, platelet samples (collected from the shearing device) were incubated with factor Xa (100pM, Enzyme Research, MO), acetylated prothrombin (200nM, Enzyme Research) and $CaCl_2$ (50μM) for 10min at 37˚C. The amount of thrombin generated was quantified using a chromogenic substrate (Chromozym-TH, Roche Applied Sciences, IN) and the color development was measured at 405nm. Resting platelets incubated with EC were used as control.

In addition, to examine the effect of cell interaction on platelet complement response to dynamic flow, platelet samples were removed from the coupled shearing system and examined for their surface C1q deposition using flow cytometry (as described above). Resting platelets incubated with untreated EC were used as control.

EC (activation/inflammation) and platelet (activation, complement protein deposition) responses measured from these coupled shearing experiments were compared to those obtained from single cell shearing experiments.

4.5.4 Platelet adhesion to EC under dynamic shear stress

Platelet adhesion/deposition on EC was measured using immunofluorescence microscopy.

Following shear exposure, platelets were removed from the system. EC were washed gently with PBS (2X), followed by fixation in 0.5% glutaraldehyde (15min,

37˚C) and neutralized with glycine-0.1% BSA (30min, 37˚C). Platelets adhered to EC monolayer were detected using a TRITC (red) conjugated GPIbα antibody (Ancell) (10min, RT). After washing with PBS (2X), cells were permeablized with 1% Triton X-100 (5min, RT), and incubated with phalloidin (green, Alexa Fluor 488, Invitrogen) to detect F-actin in both EC and platelets (20min, RT). DAPI (blue) was used to detect EC nuclei (Invitrogen) (5 min, RT). The cells were washed (2X) and immediately examined using a fluorescence microscope (Nikon TE 2000U). Fluorescent images were captured at random locations using a Coolsnap fast cooled (ES2) digital camera interfaced with NIS Elements Software (Nikon). By overlaying images from different excitation, platelet adhesion was identified by co-localization of GPIbα and actin. Further, deposition of platelets or platelet microparticles was characterized (by size) by examining higher magnification images (up to 100X). Non-specific binding was probed using FITC/TRITC-MOPC binding. In addition, amount of platelet binding was quantified by measuring the ratio of area covered by platelets to the total image area using ImageJ (v1.46, NIH). By adjusting the image contrast platelet deposited area was isolated. After converting the image from RGB to black and white, the total area covered by platelets was quantified.

Due to the abundance of actin filaments in cytoskeleton, the fluorescence signal from actin staining might be overwhelming. Therefore, alternatively, the cells were incubated with TRITC conjugated anti-human CD31 antibody (to detect PECAM-1 on both EC and platelets). PECAM-1 is regarded as one of the potential target mechanosensing protein that is present on the membrane of both EC and platelets[98].

GPIbα is one of the key ligands that are involved in platelet adhesion to EC, through EC surface receptor vWF. To investigate whether GPIbα-vWF binding is responsible for platelet adhesion to EC and other related changes under dynamic shear stress, platelet GPIbα was blocked using a mouse anti-human GPIbα blocking antibody (30min, RT) before coupled shearing. In addition, platelet membrane GPIIb/IIIa is also involved in platelet adhesion to EC through vWF or ICAM-1 (secondary binding through fibrinogen). Platelets were incubated with tirofiban (50ng/mL, 5min RT) to block surface GPIIb/IIIa before being exposed to shear stress in the presence of EC. After shearing, EC were washed and incubated with TRITC-conjugated PECAM-1 antibody to detect platelet binding, and EC nuclei were detected using DAPI.

The adhesion studies were conducted using both the cone and plate shearing device and the parallel-plate flow chamber. For the cone and plate shearing device, EC were cultured directly on the 6-cm petri dish, and for the parallel-plate flow chamber, EC were cultured on coverslips (22 X 40 mm) and placed inside the chamber after EC were confluent. To achieve required high shear stress inside the chamber, washed platelet viscosity was increased by adding dextran (3% by weight). Using flow cytometry, no change in platelet activation (surface CD62P expression) was detected due to addition of dextran.

4.6 Statistics

The statistical analysis of the data obtained from all experiments were carried out using one way ANOVA or Student's *t*-test based on the treatment conditions. All

statistical analysis was conducted using the Primer of Biostatistics software package (v4.02, McGraw Hill) and Excel (Office 2010).

CHAPTER V

RESULTS

5.1 CFD analysis of coronary flow

A physiologically realistic 3D human left coronary artery model was developed using ANSYS CFX. Blood flow inside the artery was simulated under normal and disease conditions, i.e., 30%, 60% and 80% constriction in the LAD branch. The velocity and shear stress distribution, over one cardiac cycle, inside the LAD branch was estimated[99]. The main region of interest was the area in the LAD near the bifurcation, which is a well-established athero-prone region[16]. The velocity vector distribution (Figure 17) in this region indicated that flow was skewed towards the wall close to the bifurcation (20mm downstream from the bifurcation), resulting in a high velocity gradient. In contrast, the outer LAD wall away from the bifurcation experienced flow separation and lower velocity gradient. As the stenosis severity progressed, the magnitude of the mean centerline velocity at the stenosis throat increased from 19.65cm/sec under normal condition to 23.96cm/sec, 35.16cm/sec and 62.93cm/sec under 30%, 60% and 80% stenosis condition, correspondingly.

5.1.1 Estimation of wall shear stress history

Wall shear stress (WSS) along the LAD wall was calculated based on the velocity gradient and local effective viscosity. The major regions of interest inside LAD included oscillatory zone near the bifurcation, high shear stress area around the stenosis throat, and recirculation zone downstream of the stenosis. The contours of wall shear stress distribution (at t = 0.8 sec) near the regions of interest are shown in Figure 18. Wall shear stress history over one cardiac cycle (t = 0.9 sec), at every single node (of wall elements) in these regions was calculated. Some of the representative wall shear stress history waveforms at different locations were depicted in Figure 13 in the Methods section. These shear stress waveforms represent: 1) physiological pulsatile shear, which varied between 0.1-1Pa; 2) low magnitude unidirectional shear representing shear stress variation on LAD wall inside the recirculation zone, which varied between 0.01-0.4Pa; 3) low magnitude bidirectional shear representing wall shear stress variation inside the oscillatory shear zone opposite to the bifurcation, which varied between±0.3Pa; and 4) high magnitude pulsatile shear representing shear stress variation at the stenosis throat (60% severity), which varied between 0.1-6Pa once every cardiac cycle. The calculated shear stress waveforms were exported to a cone and plate shearing device or a parallel-plate flow chamber to conduct *in vitro* experiments on EC.

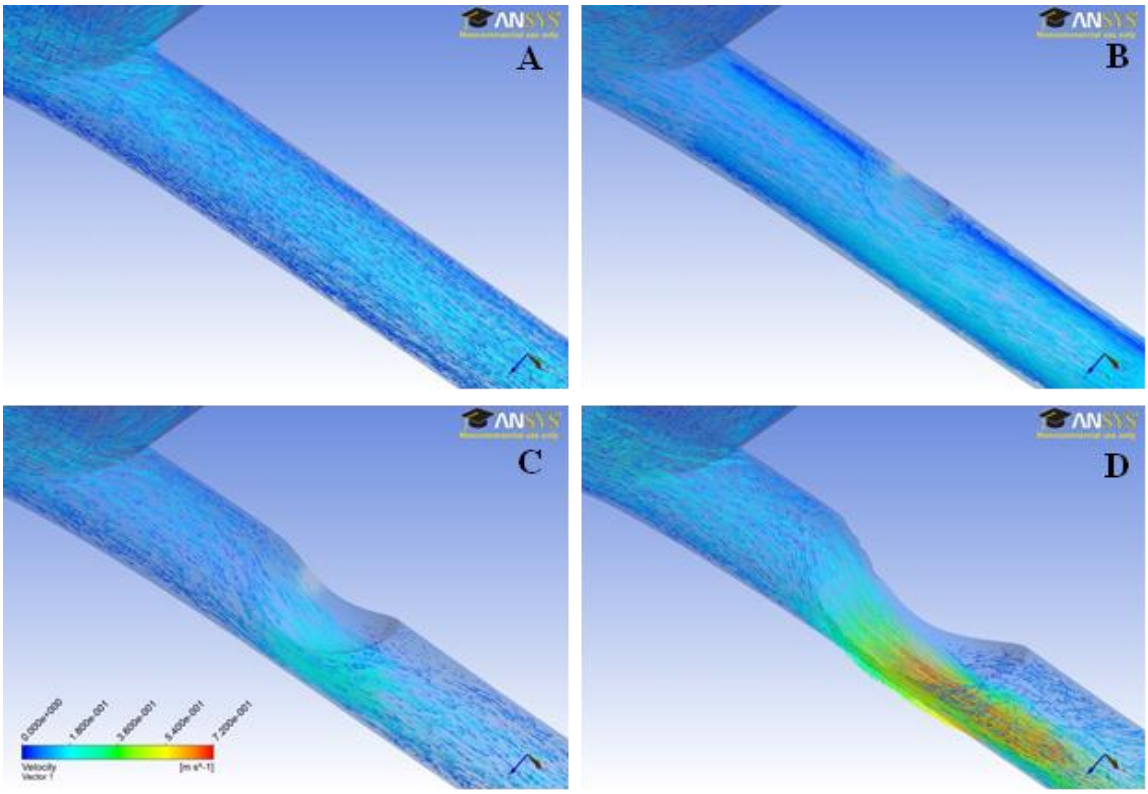

Figure 17. Velocity vector distribution inside LAD under (A) Normal, (b) 30% stenosis, (C) 60% Stenosis and (D) 80% stenosis condition. The vectors are representative of maximum inlet velocity at t = 0.8 sec.

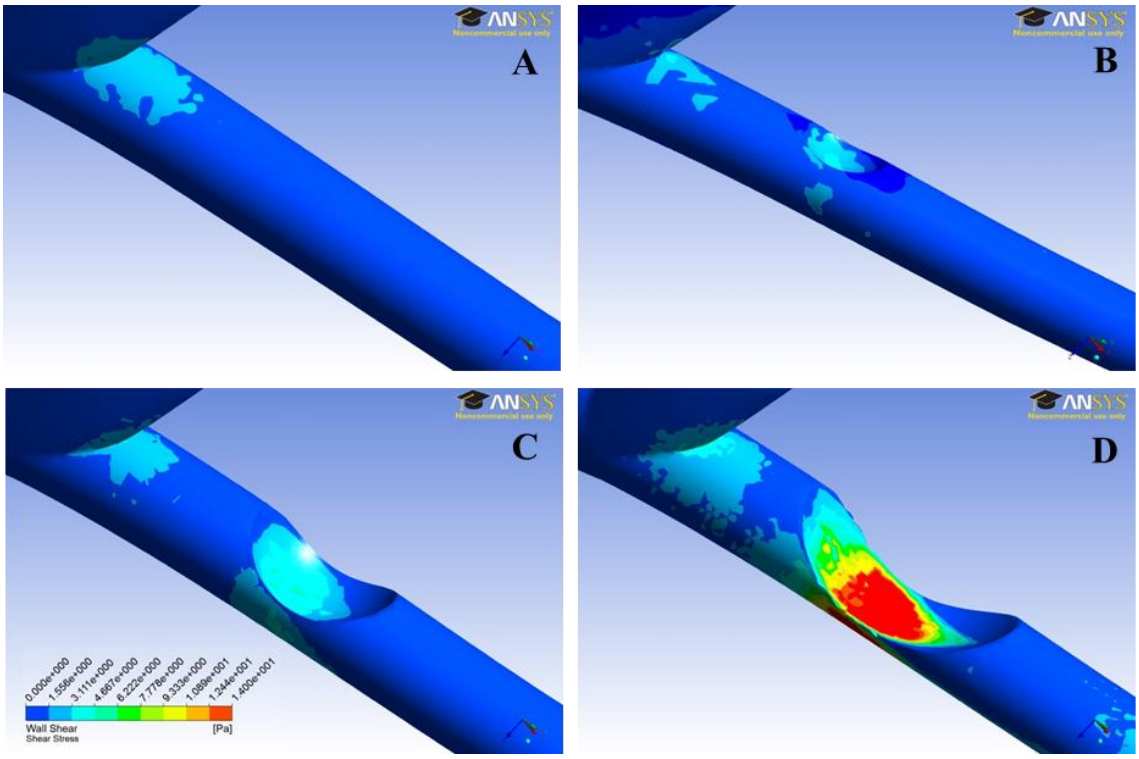

Figure 18. Wall shear stress contours on LAD wall under (A) Normal, (b) 30% stenosis, (C) 60% Stenosis and (D) 80% stenosis condition. The shear stress distribution is representative of maximum inlet velocity at t = 0.8 sec.

5.1.2 Estimation of platelet trajectory and shear stress history

Platelets seeded at the entrance of LCA were tracked at every time step and their trajectory was calculated using ANSYS CFX. Some representative platelet trajectories were plotted under both normal and disease conditions and shown in Figure 19. Shear stress applied to platelets along their trajectory was calculated using a discrete phase model. Platelets that were moving close the vessel wall were generally exposed to higher shear stress and had a higher chance to adhere to the vessel wall. Hence typical shear stress history of platelets that were travelling close to the blood vessel wall was chosen to direct the *in vitro* studies, which were depicted in Figure 15 in the Methods section. The three shear waveforms used in this study were 1) physiologically normal shear waveform, describing a platelet traveling through a normal LAD, which varied between 0.1-1Pa; 2) pathologically low magnitude unidirectional shear representing a platelet trapped inside the recirculation zone downstream of a stenosis, which varied between 0.01-0.4Pa; and 3) high magnitude pulsatile shear mimicking shear stress on a platelet traveling through a 60% stenosis very close to the wall once every 90sec, where the waveform had a peak shear of 6.5Pa for 0.1sec once every 90sec.

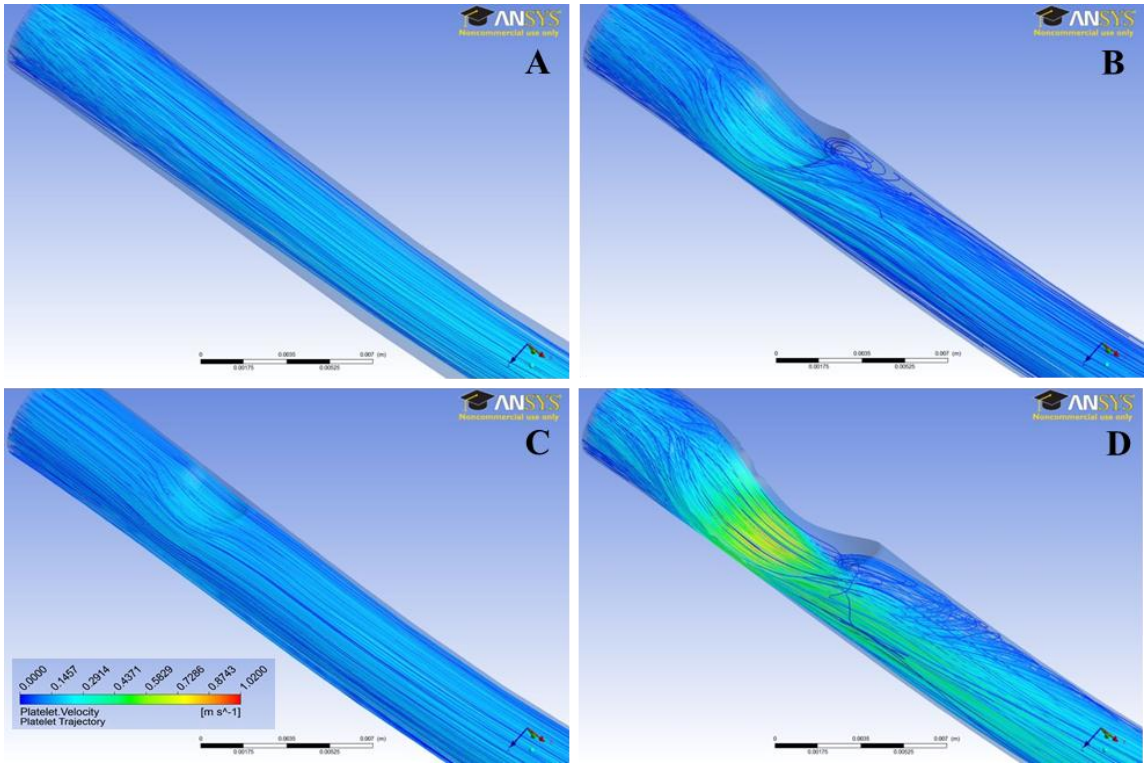

Figure 19. Platelet trajectory inside LAD under (A) Normal, (b) 30% stenosis, (C) 60% Stenosis and (D) 80% stenosis condition. The trajectories are representative of maximum inlet velocity at t = 0.8 sec.

5.2 Effect of dynamic shear stress on endothelial cells

Confluent monolayers of human coronary artery endothelial cells (HCAEC) were exposed to the four dynamic shear stress waveforms (Figure 13) using a cone-plate shearing device. Post shearing, cells were examined for their surface and total expression of athero-genic/protective protein markers including ICAM-1, TF, TM and vWF. In addition, changes induced by shear stress at mRNA level was also measured.

5.2.1 EC activation – ICAM-1 expression

EC were exposed to all four shear stress waveforms for 60min. EC surface ICAM-1 expression was measured using a solid phase ELISA. The results are presented in Figure 20A as normalized OD values (normalized to untreated EC). Compared to normal shear stress, low magnitude unidirectional shear stress induced a slight increase in ICAM-1 expression (Mean ± SD: 1.32±0.16, n=5 for normal, and 1.38±0.44 for low unidirectional shear, n=4), but no statistical significance was detected. Oscillatory shear stress induced a reduction in ICAM-1 expression (1.04±0.08, n=5) compared to normal shear, but no statistical significance was detected. EC exposed to high magnitude shear stress had a significant ($P<0.05$) reduction in ICAM-1 expression (0.82±0.11, n=5), compared to both normal and low magnitude unidirectional shear stress.

In addition, shear stress induced changes in EC total ICAM-1 expression were measured using Western blot techniques. The results (normalized band intensity) revealed an elevated ICAM-1 total protein expression in EC exposed to low unidirectional and oscillatory shear conditions. EC exposed to high magnitude pulsatile shear had a reduction in ICAM-1 expression. Representative images of the protein bands

are shown in Figure 21. For all experiments, the band intensity was quantified using spot densitometry and the average band intensity normalized to control is presented in Figure 20B. The intensity data indicated that the low magnitude unidirectional (Mean± SD: 1.35±0.29) and bidirectional shear (1.52±0.21) induced a statistically significant ($p<0.05$, n=4-5) increase in ICAM-1 expression compared to normal shear (0.96±0.37), while high magnitude pulsatile shear (0.66±0.11) led to a significant reduction in ICAM-1 expression.

To measure the changes in ICAM-1 at mRNA levels, post shearing (60 min), total cellular mRNA from each sample was isolated and examined using RT-PCR. Figure 20C represents the relative change in ICAM-1 expression (relative to β-actin) under four different dynamic wall shear stress conditions. ICAM-1 mRNA levels did not change under both low magnitude unidirectional (Mean ± SD: 2.34±0.78, n=6) and bidirectional (2.32±0.46, n=5) shear compared to normal shear (2.48±0.74, n=5). However, high magnitude pulsatile shear (1.42±0.68, n=6) induced a significant reduction in ICAM-1 mRNA expression compared to all the other shear conditions.

These results demonstrated that EC were sensitive to the variation in dynamic shear stress, in terms of ICAM-1 expression. Overall, low pathological shear stress could potentially increase EC ICAM-1 expression, while elevated shear stress would reduce ICAM-1 expression.

A. EC surface ICAM-1 expression

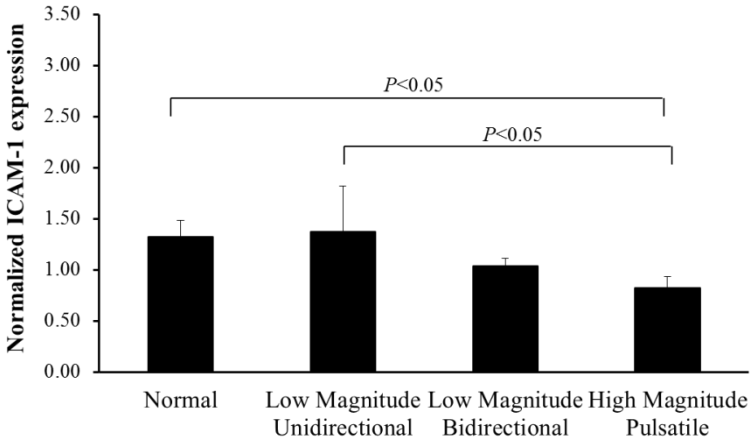

B. EC total ICAM-1 expression

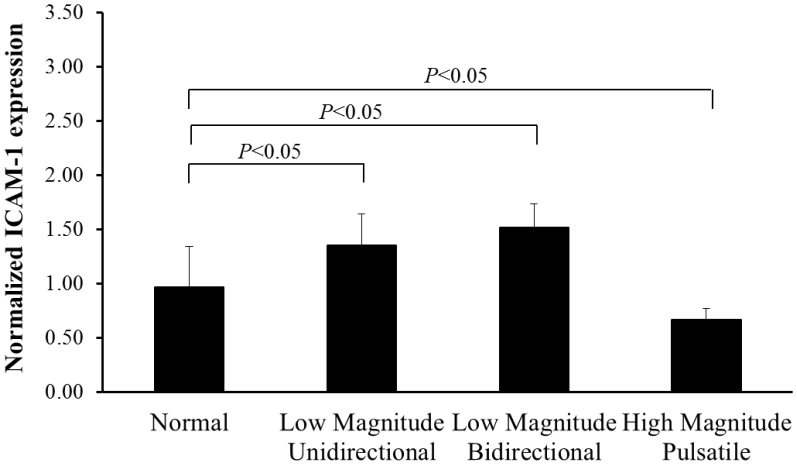

C. EC ICAM-1 mRNA expression

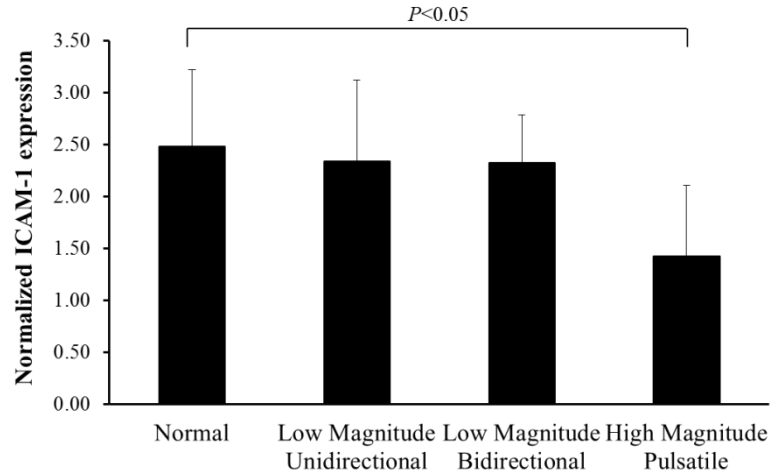

Figure 20. Shear stress induced changes in EC ICAM-1 expression at surface (A, using ELISA), total (B, using western blot) and mRNA (C, RT-PCR) levels. Data is presented as Mean± SD normalized to untreated EC.

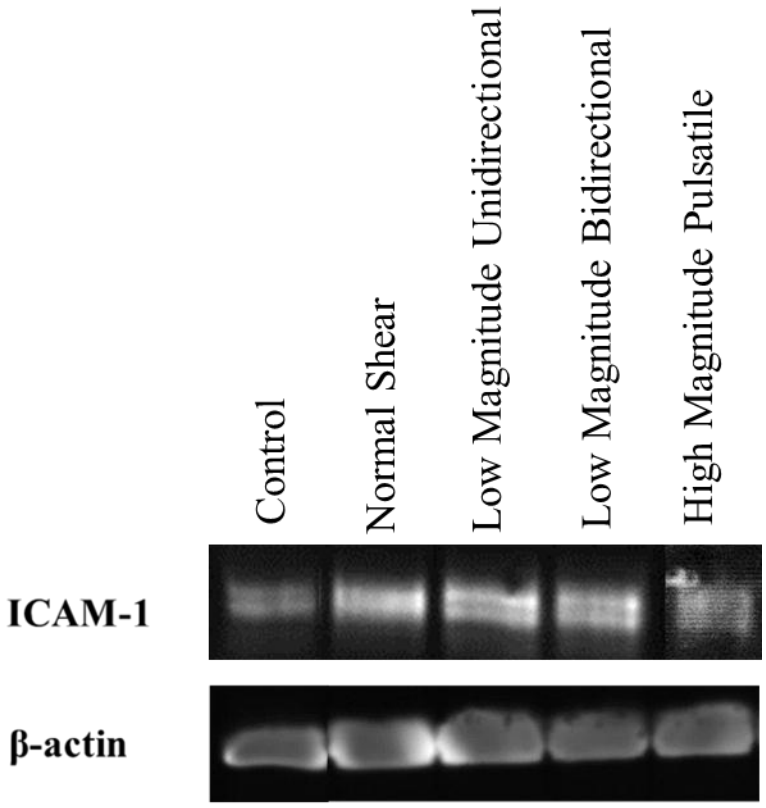

Figure 21. Representative Western blot showing ICAM-1 total protein concentration under different shearing conditions.

5.2.2 EC injury response – TF and TM expression

Dynamic shear stress-induced changes in EC inflammatory response were investigated by measuring changes in the surface expression of tissue factor (TF) using solid phase ELISA. Figure 22A represents the normalized O.D. value of TF expression under dynamic shear stress. For tissue factor expression, none of the pathological shear stress waveforms (low unidirectional, high magnitude, and oscillatory) led to any significant changes compared to physiological pulsatile shear stress. While among the three pathological shear conditions, oscillatory shear (Mean ± SD: 0.91±0.26, n=5) induced a statistically significant reduction (P<0.05) in TF expression compared to low magnitude unidirectional shear (1.425±0.153, n=4).

For total protein expression, using Western blot, no tissue factor bands were detected in cell lysates (Figure 23). Since clear TF bands were visible when recombinant TF was used, it was suspected that majority of TF was localized to the cell membrane which was discarded during the cell lysate preparation, and hence the remaining cytosolic TF protein concentration was minimal and could not be detected by Western blot. Therefore an alternative approach was taken to measure EC total tissue factor expression using a TF sandwich ELISA kit. Changes in total TF protein concentration is presented as normalized O.D. value (normalized to unsheared EC) in Figure 22B. Compared to normal shear (Mean ± SD: 1.451±0.154, n=4), both low magnitude unidirectional (1.067±0.035, n=4) and bidirectional (1.198±0.118, n=3) shear stress induced a significant (P<0.05) reduction in total TF expression.

In addition, TF expression was also measured at the mRNA level (Figure 22C). For TF mRNA expression, EC exposed to low magnitude unidirectional (Mean ± SD: 0.65±0.08, n=5) and high magnitude pulsatile shear (0.79±0.21, n=4) induced a statistically significant decrease compared to normal shear (2.78±0.94, n=6). Low magnitude bidirectional shear (2.30±0.57, n=4) induced no change in TF mRNA expression compared to normal shear, while significantly increased TF mRNA expression compared to low magnitude unidirectional and high magnitude pulsatile shear stress.

Together these results indicated that EC were sensitive to variation in dynamic shear stress. Even though responses (TF expression) we observed here were not consistent at the surface protein, total protein and mRNA level, it was clear that EC could respond to various pathological dynamic shear stress differently in terms of TF expression.

Similarly, EC surface TM expression was examined using solid phase ELISA. The results are summarized in Figure 24A. A statistically significant decrease was observed under low magnitude unidirectional (1.00±0.19, n=7), bidirectional (0.91±0.01, n=5) and high magnitude pulsatile shear (0.97±0.08, n=7), when compared to normal shear (1.19±0.2, n=6).

Further, shear stress induced changes in EC total TM protein expression was measured using Western blot. The protein bands (at 74KDa) developed on the blots indicated that all dynamic shear stress induced a slight decrease in TM expression, compared to normal pulsatile shear stress (representative blot shown in Figure 25). The

spot densitometry analysis (Figure 24B) revealed that the TM expression on low magnitude unidirectional (Mean ± SD: 1.10±0.15, n=3), bidirectional (1.09±0.16, n=3), and high magnitude pulsatile shear (1.34±0.14, n=3) was slightly reduced compared to normal shear (1.41±0.25, n=3). No statistical significance was detected.

No significant changes in TM mRNA expression were detected under any pathological dynamic shear conditions, compared to the normal pulsatile shear stress. (Figure 24C).

These results suggested that the exposure to pathological dynamic shear stress conditions led to changes (mostly reduction) in EC TM expression, compared to physiological pulsatile shear. This indicated that EC were sensitive to changes in dynamic shear stress, and could respond differently in terms of TM expression.

A. EC surface TF expression

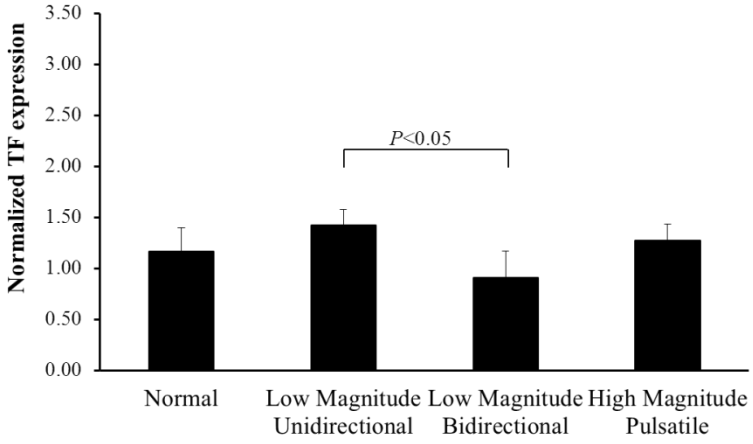

B. EC total TF expression

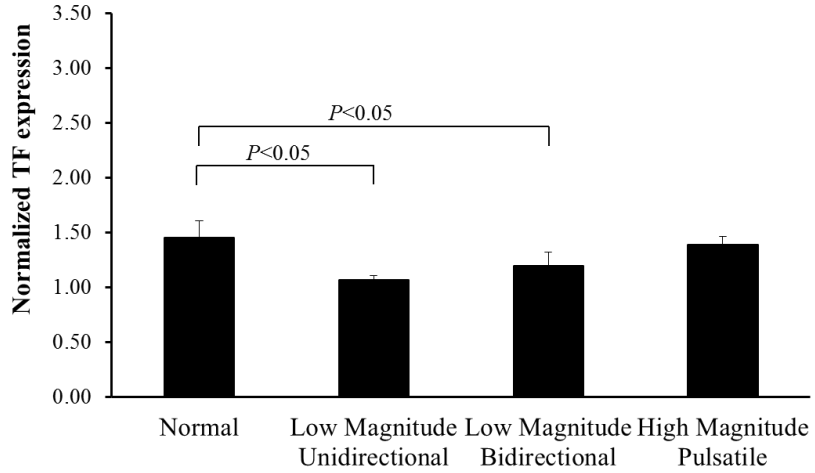

C. EC TF mRNA expression

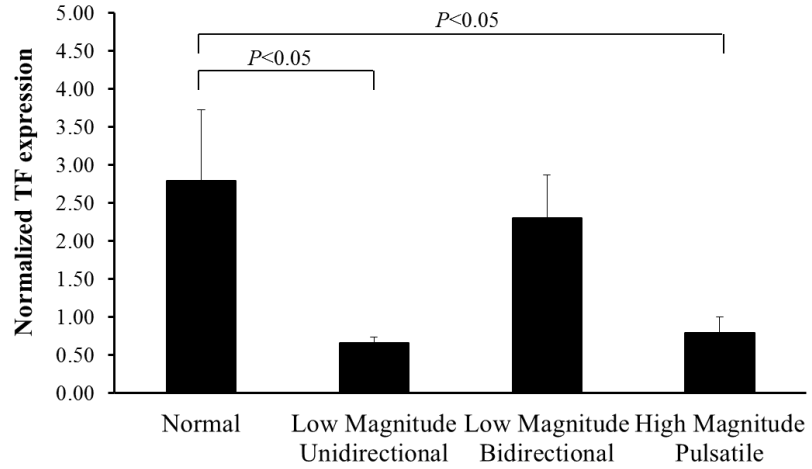

Figure 22. Shear stress induced changes in EC TF expression at surface (A, using ELISA), total (B, using sandwich ELISA) and mRNA (C, RT-PCR) levels. Data is presented as Mean + SD.

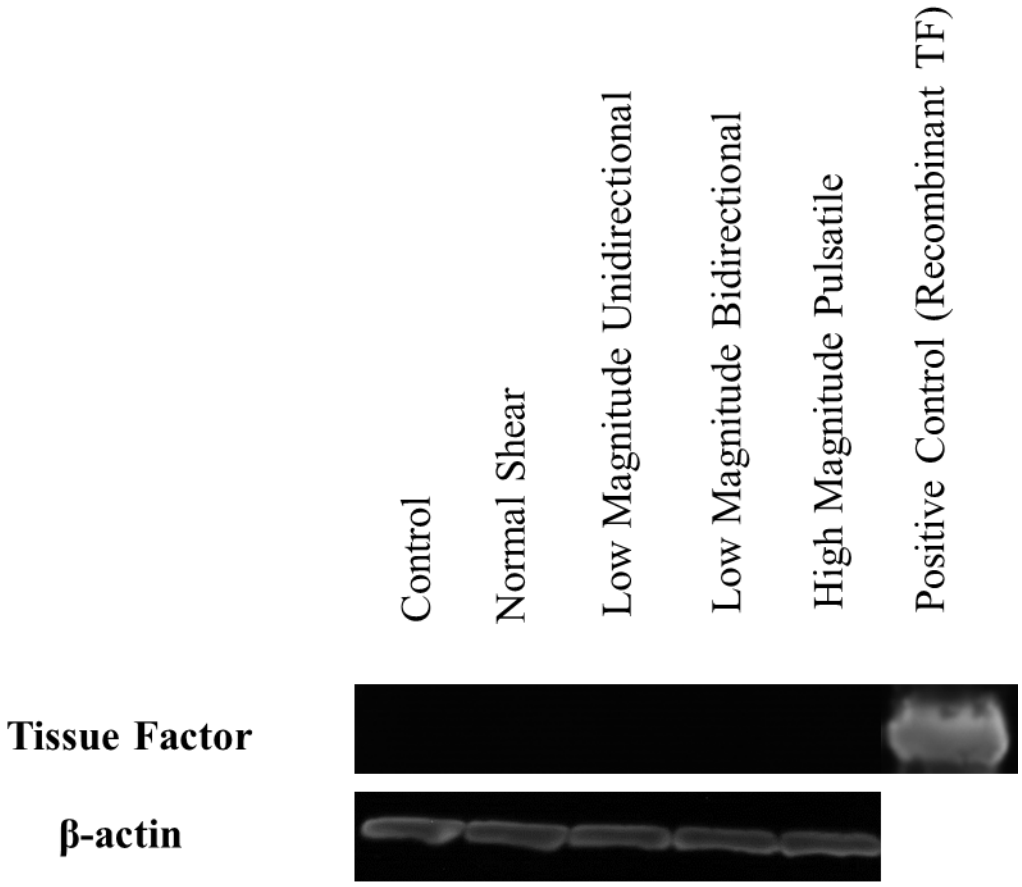

Figure 23. Representative western blot showing TF total protein concentration under different shearing conditions. As a positive control recombinant TF was used in the assay to validate the experimental design.

A. EC surface TM expression

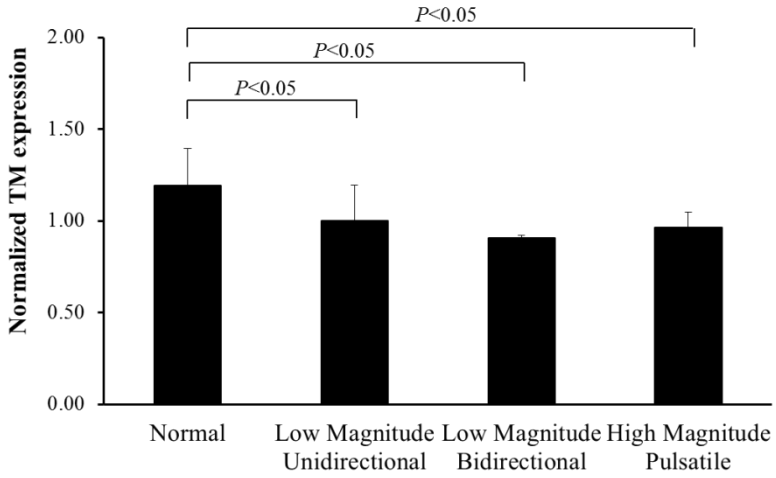

B. EC total TM expression

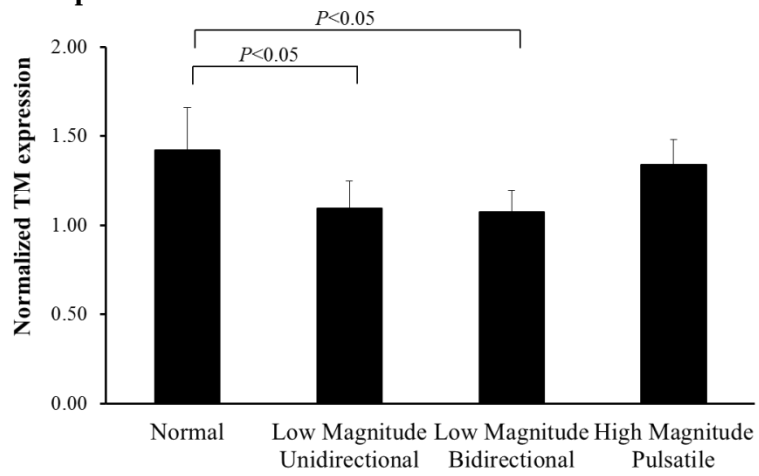

C. EC TM mRNA expression

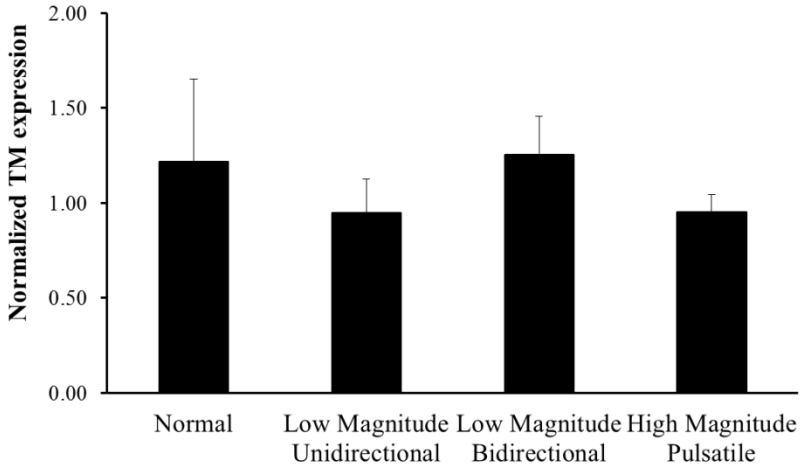

Figure 24. Shear stress induced changes in EC TM expression at surface (A, using ELISA), total (B, using western blot) and mRNA (C, RT-PCR) levels. Data is presented as Mean + SD.

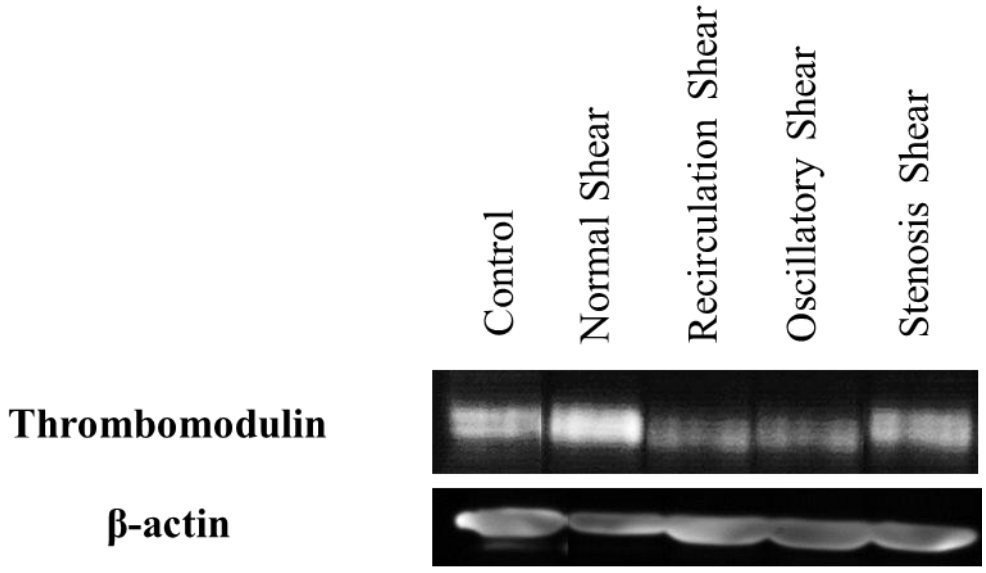

Figure 25. Representative western blot showing TM total protein concentration under different shearing conditions.

5.2.3 EC vWF expression

EC directly interact with circulating platelets through surface von Willebrand Factor (vWF) expression. Shear stress-induced changes in EC surface vWF expression was measured using solid phase ELISA. The results (presented in Figure 26A) indicate that the low magnitude unidirectional (Mean ± SD: 1.11±0.27, n=7) and oscillatory shear (1.12±0.22, n=5) induced an upregulation of surface vWF expression compared to normal shear (1.00±0.31, n=6), however no statistical significance was detected. High magnitude pulsatile shear (1.00±0.2, n=7) did not induce any changes in surface vWF expression compared to normal shear.

EC total vWF expression was measured using Western blot. No significant changes in EC total vWF expression was detected. The intensity data is presented in Figure 26B and a representative blot is presented in Figure 27.

In addition, vWF mRNA expression was measured on EC exposed to all four dynamic shear stress waveforms. The relative mRNA expression values are presented in Figure 26C. Except the low magnitude unidirectional shear stress (Mean ± SD: 2.23±0.71, n=6, $P<0.05$), none of the pathological dynamic shear stress induced any changes in EC vWF mRNA expression compared to normal shear (0.85±0.27, n=5).

Overall, these results suggest that EC did not respond to various dynamic shear stress conditions in terms of vWF expression. Altered shear stress did not have effect on vWF expression, or EC capability in accepting platelet binding.

A. EC surface vWF expression

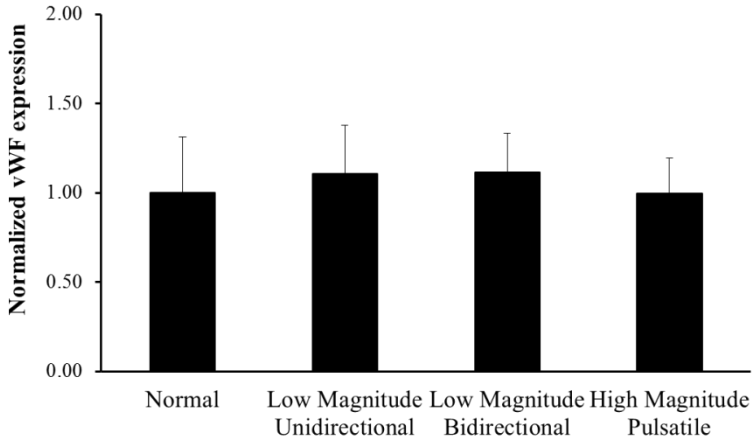

B. EC total vWF expression

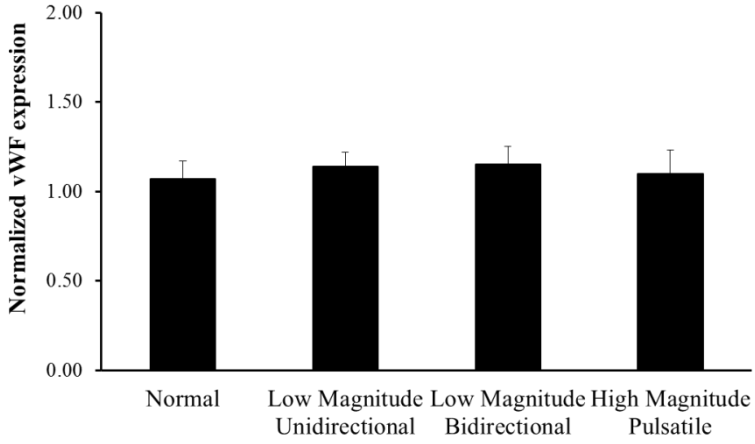

C. EC vWF mRNA expression

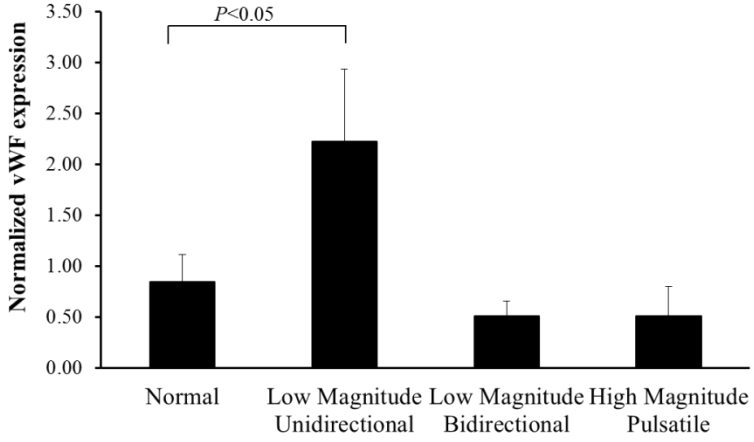

Figure 26. Shear stress induced changes in EC vWF expression at surface (using ELISA), total (using western blot) and mRNA (RT-PCR) levels. Data is presented as Mean + SD.

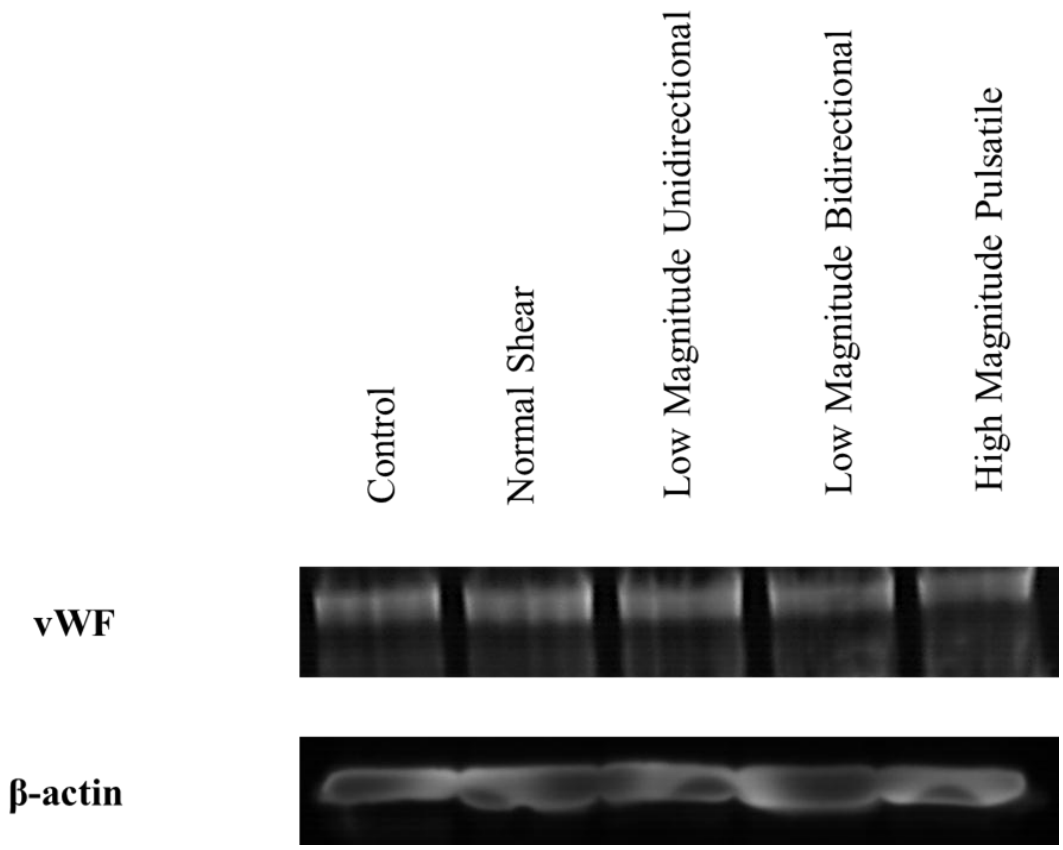

Figure 27. Representative western blot showing vWF total protein concentration under different shearing conditions.

5.3 Effect of dynamic shear stress on platelets

Platelets were exposed to three different shear stress waveforms *in vitro* using a cone and plate shearing device. The three waveforms (Figure 14) were selected from CFD simulations representing platelet passing through normal LAD near the vessel wall (referred to as normal), platelet passing through a 60% stenosis throat (once every 90 sec) (referred as high magnitude pulsatile shear), and platelets trapped inside the recirculation zone (referred to as low magnitude pulsatile shear).

Effects of these three dynamic shear stresses on platelet activation *in vitro* was studied and reported previously[4]. It was demonstrated that the rate of thrombin generation was not statistically significant under both low and high magnitude pulsatile shear compared to normal shear. However, flow cytometry measurement on platelet surface CD62P expression demonstrated that platelets exposed to all three dynamic shear stresses were not activated[100]. These results indicated platelets were not sensitive to changes in dynamic shear stress patterns, in terms of CD62P expression, or cell activation; but dynamic shear stress at any level was able to lead to thrombin generation, if shear exposure time was adequate.

5.3.1 Platelet complement activation

5.3.1.1 Platelet surface complement protein deposition

Post shearing, platelets were fixed to 96-well microtiter plates, incubated with human plasma and were examined for surface complement protein C1q deposition using solid phase ELISA (Figure 28). The results indicated that the platelets that were exposed to low magnitude pulsatile shear stress (Mean ± SD, 1.26 ± 0.06, $p<0.05$, $n=9$) had a

significant increase in C1q deposition compared to normal shear (1.07±0.09, n=9), while no noticeable changes were observed under high magnitude pulsatile shear. To determine if complement activation would proceed to completion, platelet surface deposition of other complement cascade proteins –C4d, iC3b, and SC5b-9 were examined using a similar solid phase ELISA approach. The results (Figure 29) revealed noticeable increase in C4d deposition under pathological shear stress conditions (0.81±0.19, n=9 for normal; 0.97±0.13, n=6 for low unidirectional; 0.91±0.04, n=8 for high magnitude pulsatile), but no significant changes were detected between the conditions. These results indicated that the downstream complement cascade was completely inhibited.

Alternatively, platelet surface complement C1q expression was measured in the fluid phase using flow cytometry. The representative fluorescence histogram is presented in Figure 30. Resting platelets (not exposed to shear stress) were used as experimental control, while MOPC was used to measure non-specific antibody binding. The results indicated that platelets exposed to low magnitude unidirectional shear expressed an elevated C1q deposition (population shift in fluorescence histogram shown in Figure 30) compared to both normal and high magnitude pulsatile shear ($P<0.05$). The normalized all mean fluorescence values quantifying complement C1q deposition from flow cytometry is summarized in Table 3. Similarly, no significant change in downstream complement protein (C4d) expression was detected using flow cytometry (mean fluorescence value shown in Table 3). To reduce the variation in platelet complement response from different donors, the all mean fluorescence value was normalized to that of resting platelets on the same day.

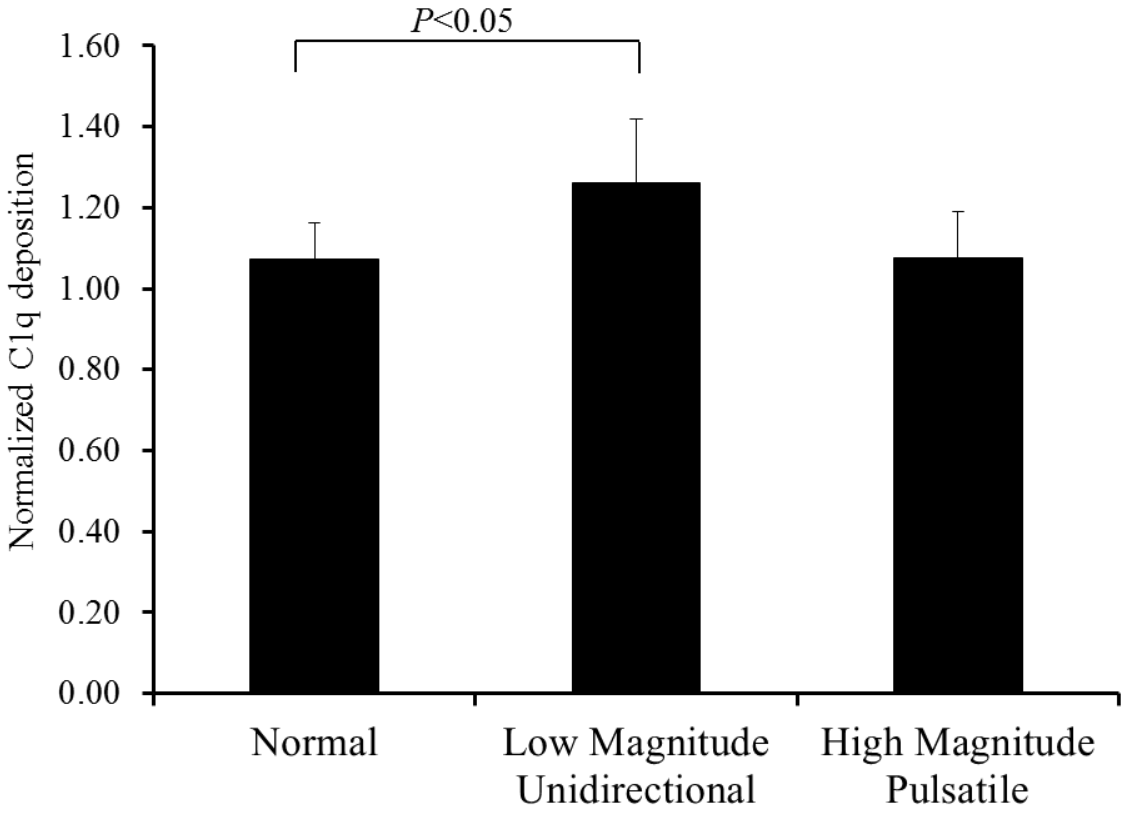

Figure 28. Normalized (to resting platelets) platelet surface C1q expression measured using solid phase ELISA. Data is presented as Mean + SD.

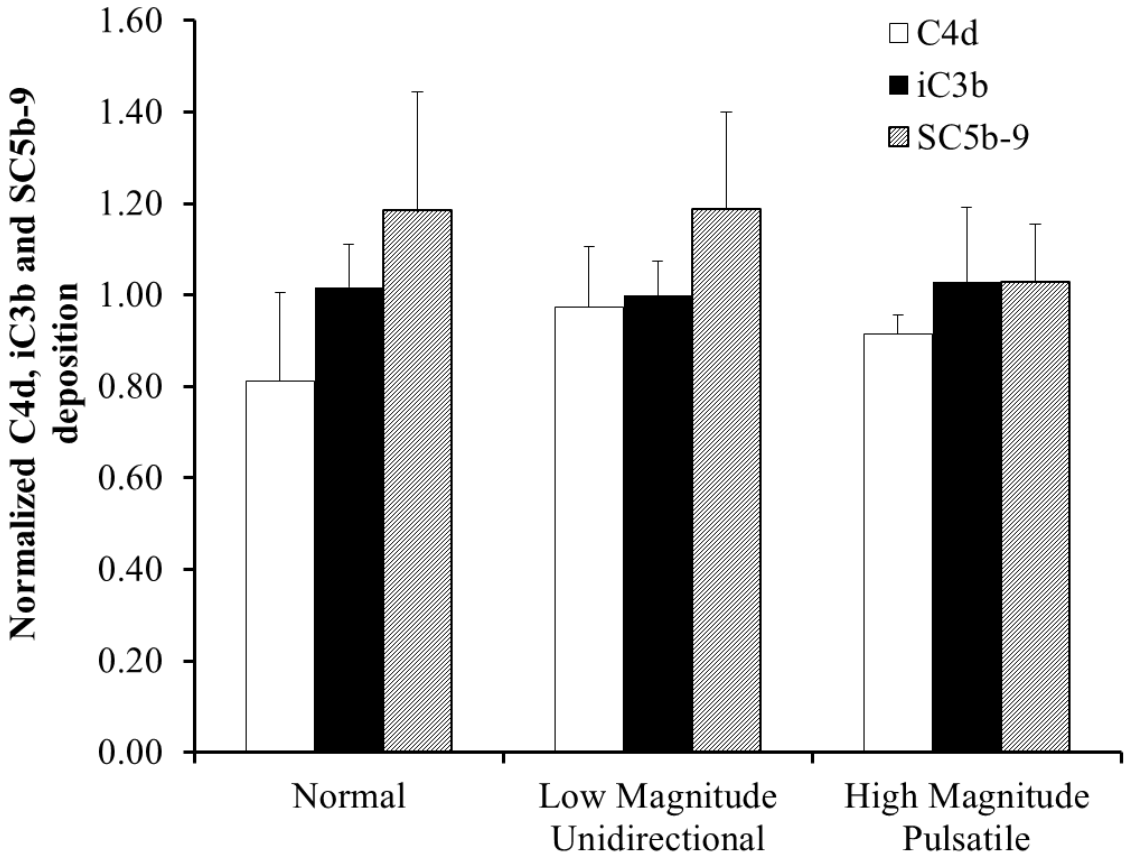

Figure 29. Normalized (to resting platelets) platelet surface C4d, iC3b and sC5b-9 expression measured using solid phase ELISA. Data is presented as Mean + SD.

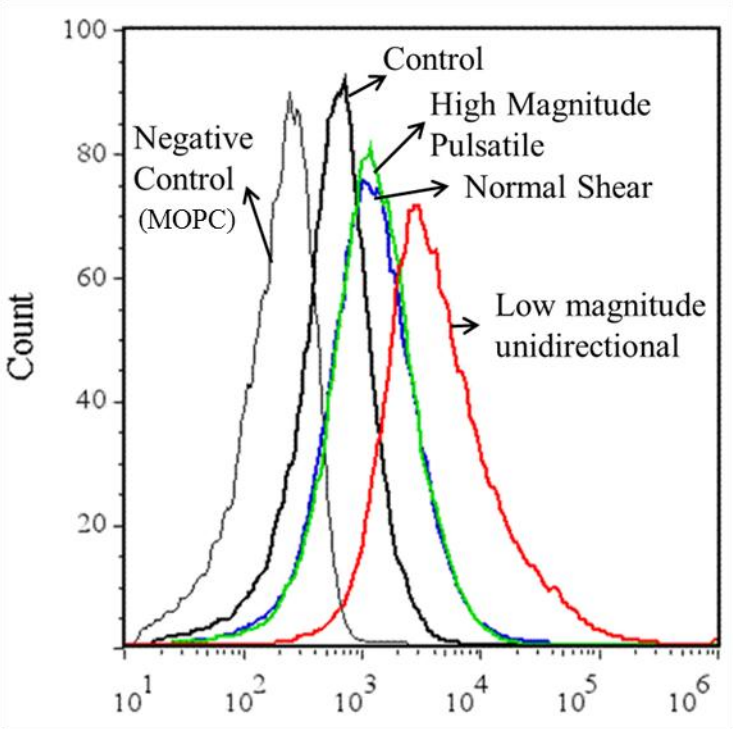

Figure 30. Representative histogram data representing changes in platelet surface C1q deposition measured using flow cytometry.

Table 3. Normalized all mean fluorescence value of platelets exposed to normal, Low magnitude unidirectional and high magnitude pulsatile shear.

		Normal	Low Magnitude Unidirectional	High Magnitude Pulsatile
C1q	**Normalized all mean fluorescence ± SD**	3.13 ± 2.12	4.45 ± 2.16	3.16 ± 2.11
	Sample size (n)	7	4	7
C4d	**Normalized all mean fluorescence ± SD**	1.066 ± 0.102	0.865 ± 0.132	0.877 ± 0.205
	Sample size (n)	5	7	4

5.3.1.2 Activation of complement inhibitors

The activation of the complement system is regulated by a set of complement inhibitors including C1-inhibitor (C1-INH) released by platelets and complement receptor 1 (CR1) present in plasma. After shearing, the amount of C1-INH released by platelets into the fluid phase was measured using a C1-INH EIA kit. The results (shown in Figure 31) revealed that the amount of C1-INH released by platelets exposed to both low unidirectional (mean ± SD: 0.95±0.12, n=6) and high pulsatile shear (1.01±0.08, n=6) was significantly higher (P<0.05) compared to those exposed to normal shear (0.87±0.10, n=6).

To investigate the role of CR1, platelets exposed to dynamic shear stress were incubated with human plasma and examined for their surface deposition of CR1 using a solid phase ELISA (Figure 32). Platelets exposed to low unidirectional shear (1.37±0.0.29, n=6) expressed an 18% increase in surface CR1 deposition compared to normal shear (1.16±0.16, n=4), while high magnitude pulsatile shear (1.42±0.43, n=8) induced a 23% increase. However, no statistical significance was detected.

In summary, low magnitude pathological shear stress induced a significant increase in classical pathway complement activation compared to normal shear. However, the activation of complement inhibitors prevented the complement activation from proceeding to completion.

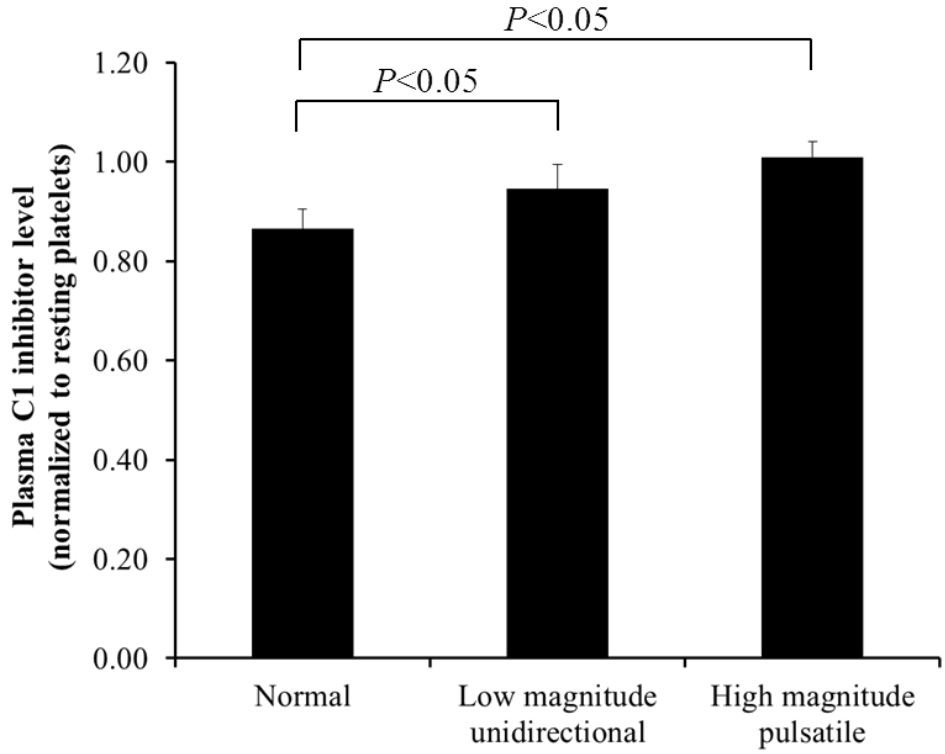

Figure 31. Amount of C1 inhibitor released by platelets when exposed to dynamic shear stress. OD values normalized to resting platelets and presented as Mean + SD.

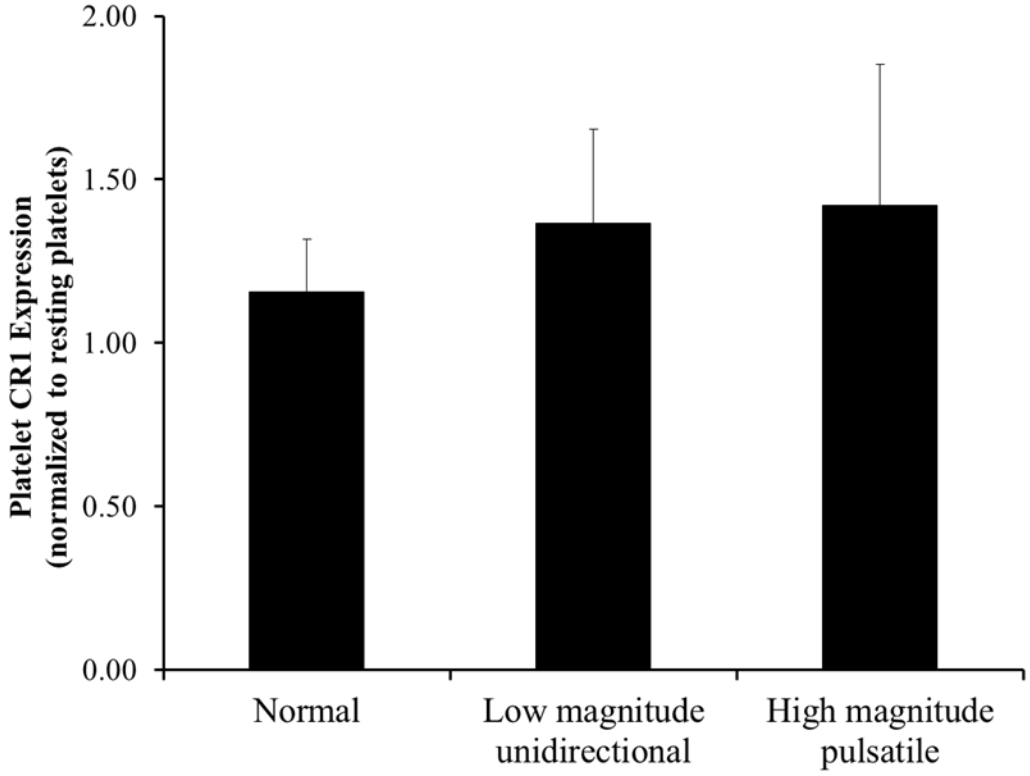

Figure 32. Platelet surface CR1 expression after exposure to dynamic shear stress measured by solid phase ELISA. OD values normalized to resting platelets and presented as Mean + SD.

5.3.2 Platelet proteomic analysis

Platelets were stimulated with both biochemical (incubated with 20μM TRAP) and mechanical stimuli steady (1 and 3Pa) and pulsatile shear (normal, low and high magnitude pulsatile shear). Platelets were then lysed and platelet proteomes were analyzed using a SELDI mass spectrometer. Protein spectral patterns obtained in the low molecular weight range (m/z range: 2-20KDa) were analyzed and multiple protein peaks were detected. The intensity of protein peaks detected under TRAP-simulated platelets was compared to that of control (resting) platelets. Fourteen statistically distinct ($P<0.05$, n = 12) protein peaks were identified. The relative changes in peak intensity and associated *P* values are listed in Table 4. Figure 33 depicts the spectral profile constructed with the protein peaks that were significantly differentiated in TRAP activated platelets compared to resting platelets. In addition to changes in magnitude of protein peaks, the shape of spectral pattern of TRAP activated platelets was also altered compared to resting platelets.

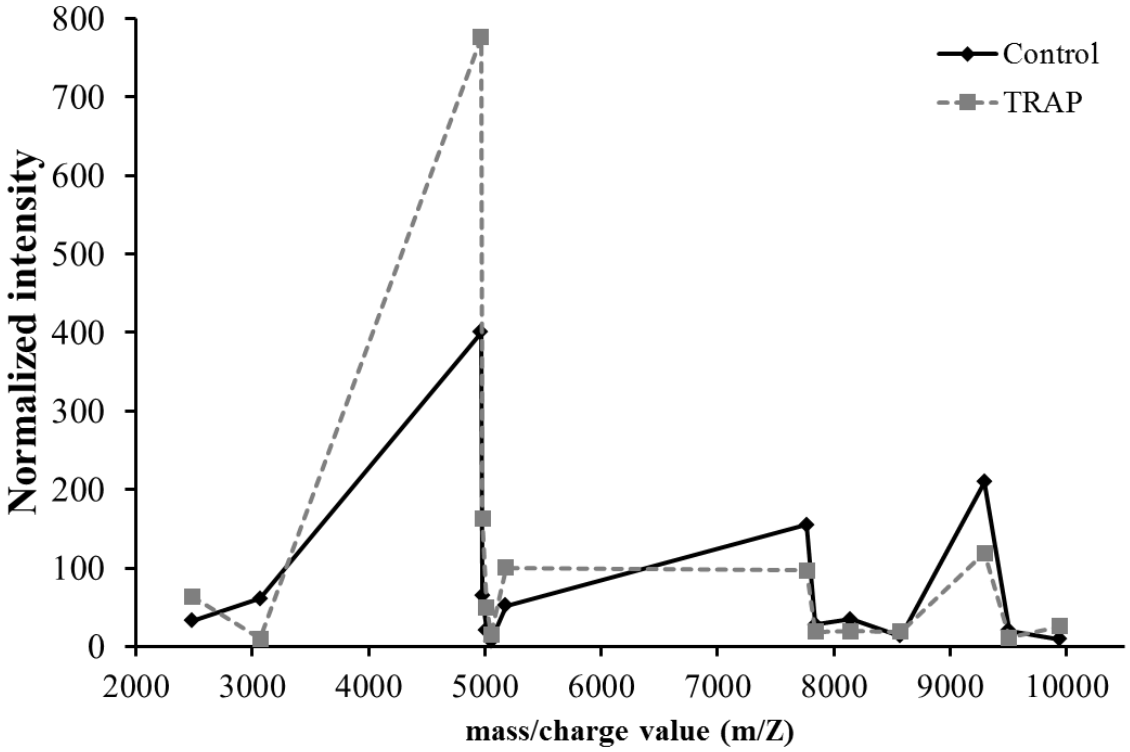

Figure 33. Peptide/Protein spectrum profile of platelets activated with TRAP compared to control (resting platelets). The markers are representative of m/Z values that are significantly different ($P<0.05$) under TRAP activation compared to control, characterized by changes in normalized intensity at every m/Z value.

Table 4. The percent change in normalized intensity compared to resting platelets along with the corresponding *P* values for each m/Z peak.

	TRAP	
m/Z ratio	**% change**	**p**
2483.61	↑ 95.59	0.0001
3067.75	↓ -83.61	0.007
4966.52	↑ 93.68	0.0001
4981.34	↑ 152.92	0.0001
5011.12	↑ 133.45	0.0001
5052.36	↑ 112.78	0.0001
5181.24	↑ 92.98	0.0001
7768.40	↓ -37.25	0.0001
7840.66	↓ -30.62	0.0001
8146.42	↓ -43.28	0.002
8574.52	↑ 37.10	0.025
9294.07	↓ -43.28	0.001
9505.18	↓ -45.63	0.0001
9945.55	↑ 179.23	0.0001

Similarly, SELDI TOF profiles of platelets exposed to both low and high constant shear stress (1 and 3Pa) were analyzed. No statistically significant difference in protein/peptide peaks was detected in platelets exposed to low constant shear (1 Pa) compared to resting platelets. However, platelets exposed to high magnitude constant shear stress (3 Pa) had three distinct protein peaks, at M/Z of 2241.04 (53% reduction), 2441.18 (59% reduction) and 4981.34 (85% increase), which were statistically significant ($P<0.05$, n=8-12) compared to resting platelets (summarized in Table 5). A spectral profile compiling the significantly differentiated protein peaks, shown in Figure 34, indicated that constant shear stress only affected the magnitude of the protein peaks but did not alter the shape of the spectral profile.

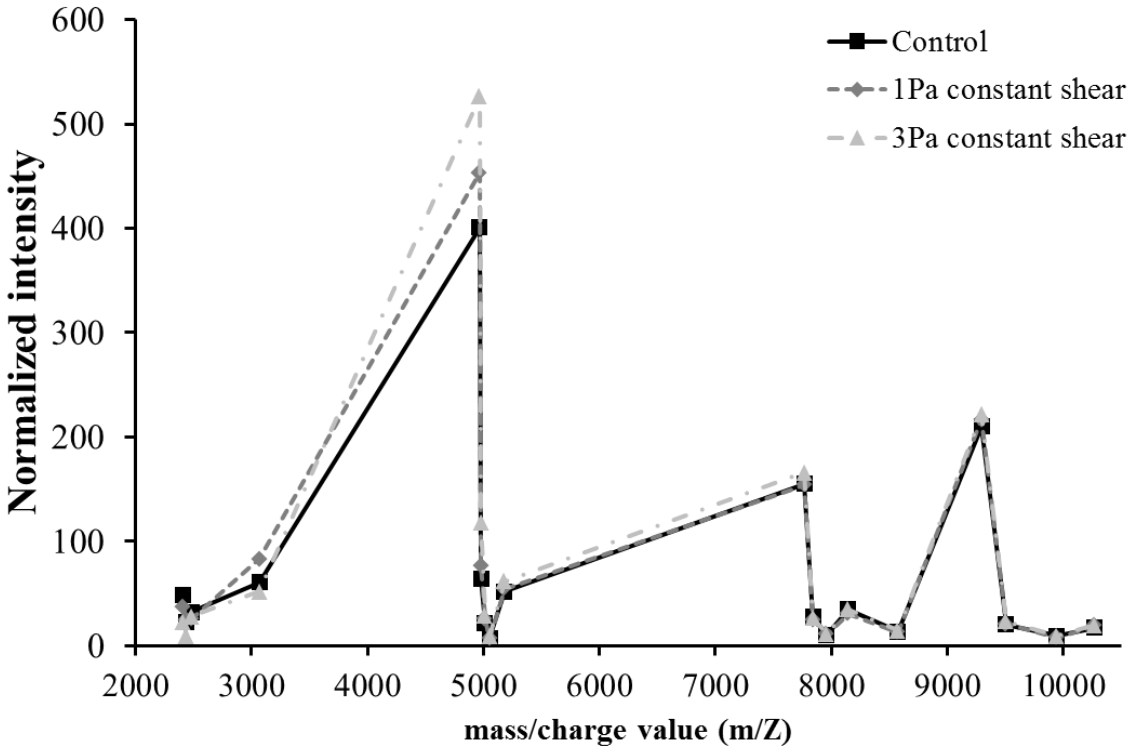

Figure 34. Peptide/Protein spectrum profile (characterized by m/Z) of platelets exposed to 3Pa and1Pa constant shear when compared to control (resting platelets, n=8-12). The three peaks (marked with *) are specific m/Z values (2411, 2441, 4981) that are significantly different constant shear of 3Pa compared to resting control platelets.

Table 5. The percent change in normalized intensity compared to resting platelets along with the corresponding *P* values for each m/Z peak.

m/Z ratio	Shear (3 Pa)	
	% change	p
2411.04	↓ -53.24	0.0001
2441.18	↓ -59.21	0.0001
4981.34	↑ 84.55	0.0001

In addition, effects of dynamic shear stress on platelet proteomes were examined. Platelets exposed to both physiological and pathological shear stress revealed different spectral patterns (composed of significantly differentiated peaks) compared to resting platelets (Figure 35). Though the shape of spectral profile was similar between pulsatile shear and resting platelets at the lower end of spectrum (m/Z<7500), changes were observed between m/Z of 7500 and 10000. High magnitude pulsatile shear induced changes in the shape of the spectral profile compared to normal shear, while no change was observed under low magnitude pulsatile shear.

In addition, at two particular m/Z, i.e., 2439.23 and 3274.88, statistically significant ($P<0.05$, $n=8$) difference was detected under pathological shear stress conditions, compared to normal shear. At m/Z = 2439, both low (49.46% reduction) and high magnitude (72.52% reduction) pulsatile shear induced a significant reduction ($P<0.05$) compared to normal shear; while at m/Z = 3274, high magnitude pulsatile shear (96.46% increase) induced a significant increase compared to normal shear. Table 6 summarizes the percent change in normalized intensity along with the *P* values of low and high magnitude pulsatile shear compared to normal shear.

In summary, spectral profiles (of significantly differentiated proteins) in the low molecular weight region clearly indicated that platelets could sense the difference in shear stress patterns.

Overall, platelet activation (i.e., CD62P expression) or thrombin generation might not be the responsive mechanisms platelets take in response to various dynamic shear

stress conditions. However, platelets could distinguish the different dynamic shear stress patterns, through complement activation, and changes in proteomic profiles.

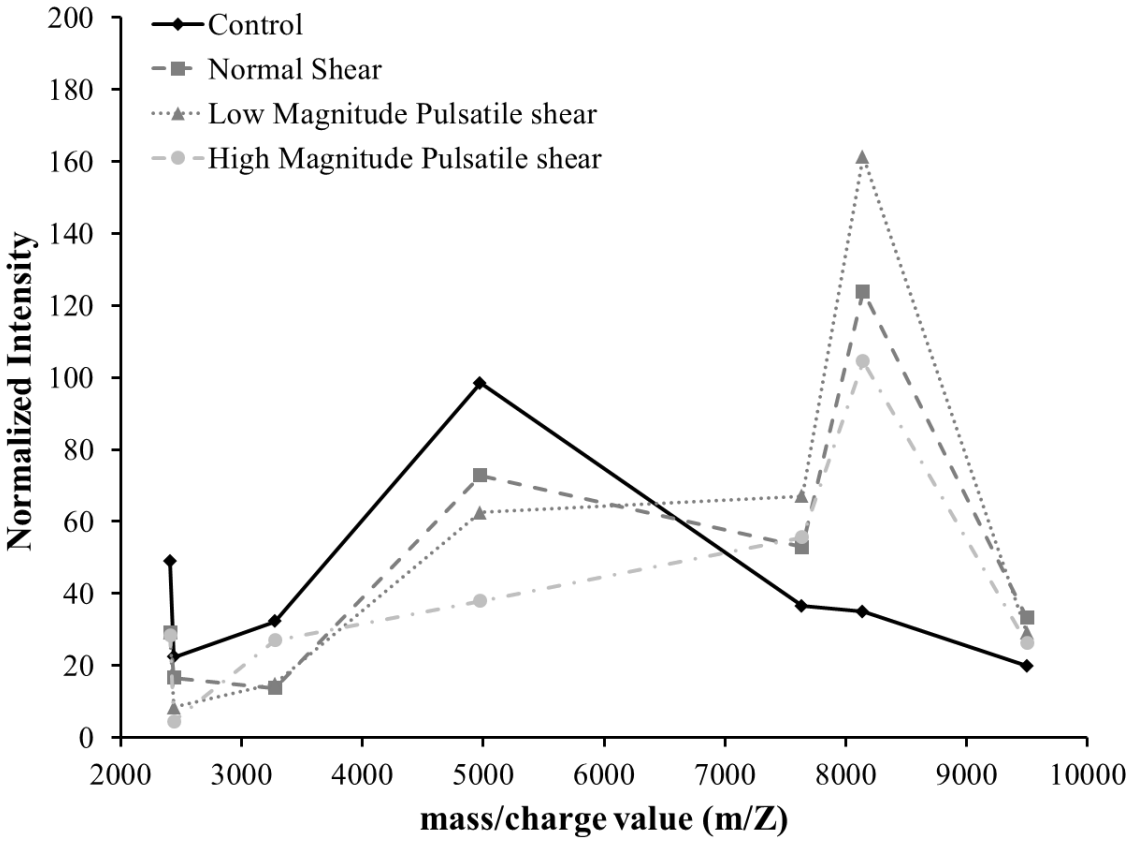

Figure 35. Protein/peptide spectrum profile of platelets exposed to normal, low and high magnitude pulsatile shear compared to resting control platelets (n=8). The two peaks (marked with *) are specific m/Z values (2439, 3274) that are significantly different under both low and high magnitude pulsatile shear compared to normal shear. The peak (marked with +) specific to m/Z value of 8139 where all three pulsatile shear conditions induced a significant increase compared to control (resting platelets).

Table 6. The percent change in normalized intensity under low and high magnitude pulsatile shear compared to platelets exposed to normal shear along with the corresponding *P* values for each m/Z peak.

m/Z ratio	Pathological shear			
	Low magnitude		High Magnitude	
	% Change	*P*	% Change	*P*
2439.23	↓ -49.46	0.0001	↓ -72.52	0.0001
3274.88	↔ 8.85	0.380	↑ 96.46	0.014

The results reported above summarized how EC and platelets responded to dynamic shear stress separately. The following section reported EC and platelet responses to dynamic shear stress when they were exposed to shear stress simultaneously. EC and platelet were exposed to only three different shear stress waveforms – normal (Figure 14), low magnitude pulsatile (Figure 14) and platelet high magnitude pulsatile shear (Figure 15). The oscillatory shear waveform was not used, because in reality platelets are not exposed to oscillatory conditions, as shear is always against them.

5.4 Effect of dynamic shear stress on EC – Platelet interaction

The effect of dynamic shear stress on EC-platelet interaction was investigated by exposing platelets to all three dynamic shear stress waveforms in the presence of HCAEC using a cone-plate shearing system, or a parallel-plate flow chamber. After EC and platelets were exposed to dynamic shear stress together for 60 min, their cellular responses, including EC activation and inflammatory responses, platelet thrombogenicity, platelet complement activation and EC-platelet adhesion were measured.

5.4.1 EC response to dynamic shear stress in the presence of platelets

Shear induced EC activation in the presence of platelets was measured by EC surface ICAM-1 and TF expression using a solid phase ELISA. The results are presented as normalized O.D. values (to that of EC incubated with platelets and not exposed to shear) in Figure 36 and 37. Compared to normal shear, both pathological dynamic shear stress did not induce any significant changes in EC surface ICAM-1 or TF expression.

However, the presence of platelets affected EC surface ICAM-1 expression, compared to when EC were exposed to shear stress alone. Under low pulsatile shear, the presence of platelets led to a significant decrease in EC surface ICAM-1 expression (n=5; $P<0.05$, from 1.38±0.44 to 0.81±0.19, normalized O.D. value). Under elevated pulsatile shear stress, EC surface ICAM-1 expression increased slightly from 0.82±0.11 (n=5) to 0.95±0.21 (n=5), but no statistical significance was detected. These results indicated that platelets could help to reduce EC activation level under pathological dynamic shear stress. Also, with the presence of platelets, EC were not able to distinguish the variation in dynamic shear stress patterns (different from when they were exposed to shear stress alone).

Similar effect from platelets was observed with EC surface TF expression: with the presence of platelets, EC were not able to respond to the changes in dynamic shear stress patterns, by varying cell surface TF expression. In a similar experiment conducted in our lab, EC surface vWF expression was examined in the presence of platelets. No significant changes (data not shown) in surface vWF expression was detected under all three dynamics shear stress conditions.

In addition, EC ICAM-1 mRNA expression was measured after 60 min coupled shearing. The relative mRNA expression measured (shown in Figure 38) revealed that both the low magnitude unidirectional and high magnitude pulsatile shear induced a significant reduction in ICAM-1 mRNA expression compared to normal shear. Compared to EC that were exposed to dynamic shear stress alone, the presence of platelets led to a significant reduction in EC ICAM-1 mRNA expression (normal: 0.99±0.05, low: 0.80±0.06, high: 0.56±0.14; n=3).

To determine the activity of EC in the presence of platelets, the cells were exposed to normal shear and the supernatant was assayed to measure the amount of nitric oxide (NO) generated using a commercially available kit (Cayman Chemicals, Ann Arbor, MI). The results indicated that EC exposed to shear stress with and without the presence of platelets produced similar levels of NO, which was higher compared to EC that was not exposed to shear stress.

In summary, the presence of platelets affected EC responses to dynamic shear stress in terms of ICAM-1 and TF expression. The effects took place in two ways: first, the presence of platelets decreased EC activation under pathological shear stress; second, with the presence of platelets, EC lost their sensitivity to different dynamic shear stresses.

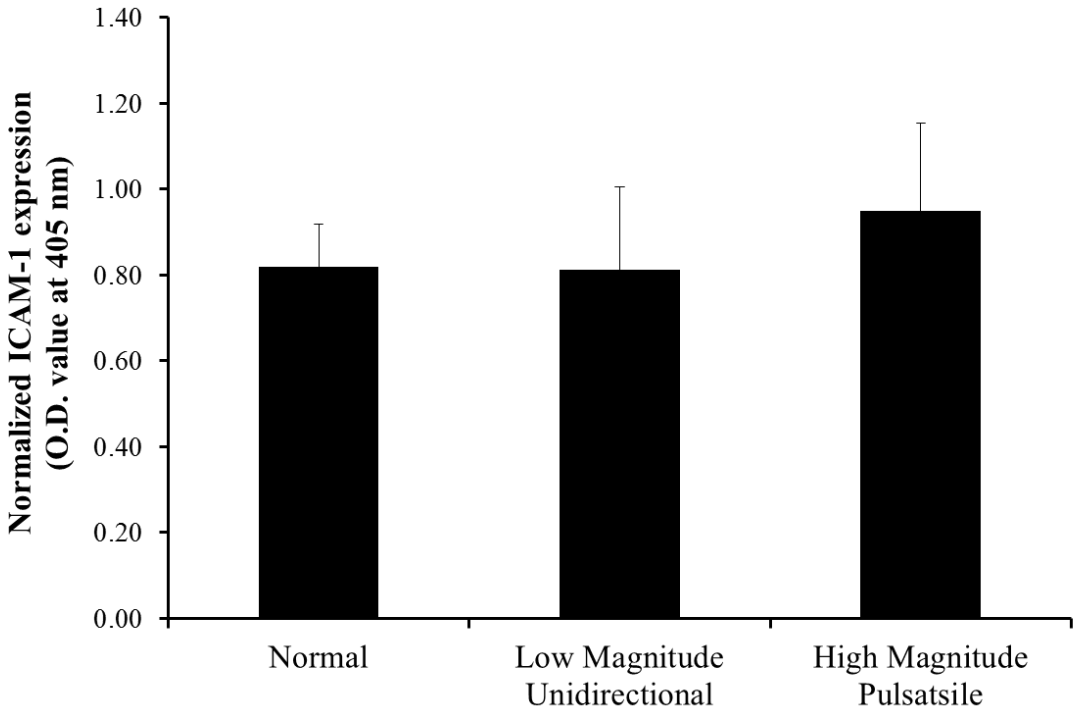

Figure 36. Normalized EC surface ICAM-1 expression after dynamic shear exposure in the presence of platelets using solid phase ELISA. No statistical significance was detected (n=5). Data presented as Mean + SD.

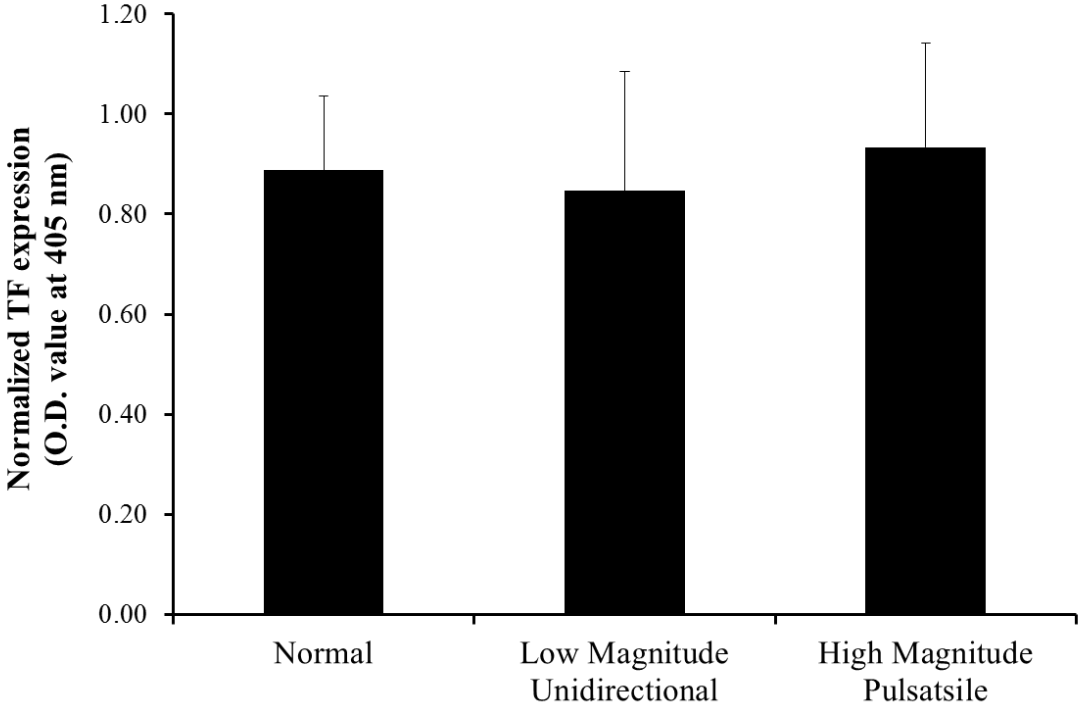

Figure 37. Normalized EC surface TF expression after dynamic shear exposure in the presence of platelets using solid phase ELISA. No statistical significance was detected (n=5). Data presented as Mean + SD.

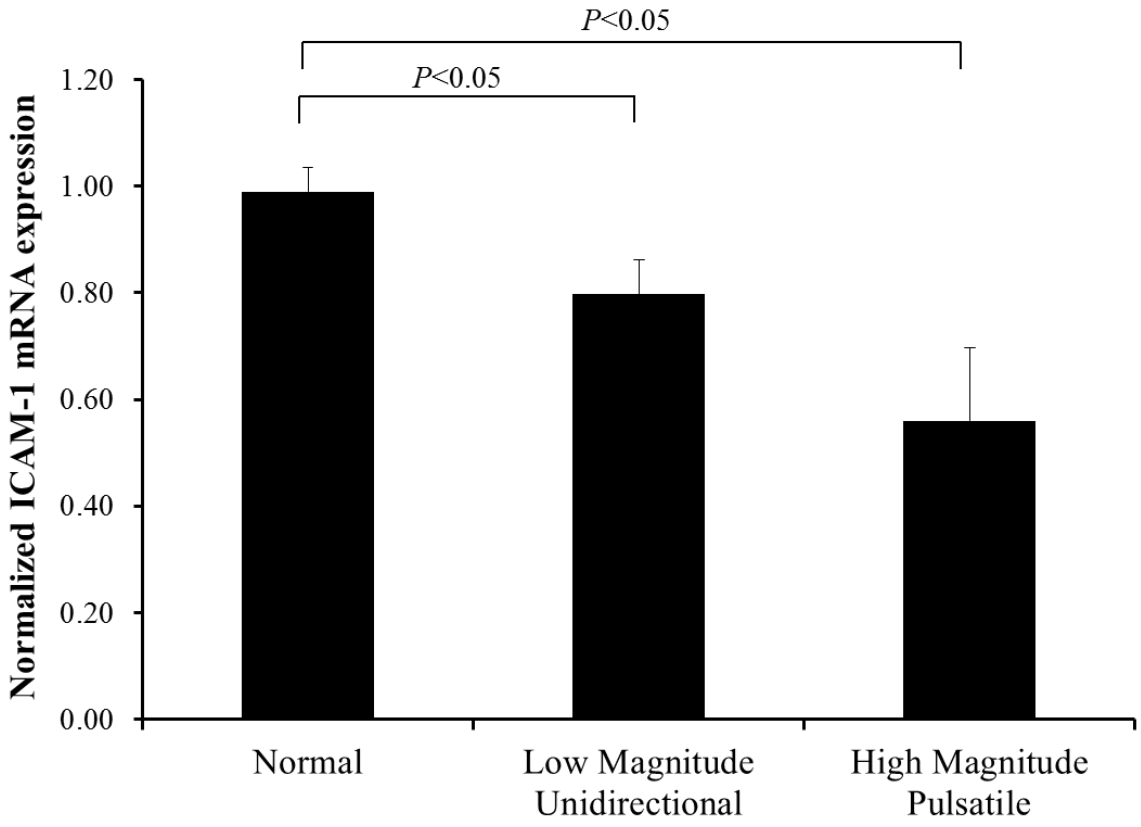

Figure 38. Normalized EC ICAM-1 mRNA expression after dynamic shear exposure in the presence of platelets using RT-PCR. Data presented as Mean + SD (n=5).

5.4.2 Platelet responses to dynamic shear stress with the presence of EC

In a study conducted in our lab, platelet activation was measured by CD62P expression when sheared in the presence of EC^{100}. The results indicated that platelet gained sensitivity to dynamic shear stress exposure, and platelet surface CD62P expression was elevated significantly under high magnitude pulsatile shear stress, compared to normal shear. After platelets were exposed to dynamic shear stress with the presence of EC, thrombin generation was measured. The results demonstrated a significant increase in thrombin generation under low magnitude and high magnitude pulsatile shear compared to normal shear (Figure 39).

In addition, to assess platelet complement activation in response to dynamic shear stress with the presence of EC, platelet surface C1q deposition was measured using flow cytometry. No significant changes in C1q deposition were detected between all three dynamic shear stress conditions. The normalized all mean fluorescence values quantifying C1q deposition is summarized in Table 6. The all mean fluorescence values are normalized to the same day resting platelets. Compared to data reported in Table 3, with the presence of EC, the low magnitude shear induced increase in C1q deposition disappeared.

In summary, EC altered platelet responses to dynamic shear stress. When platelets were exposed to dynamic shear stress alone, they did not respond to various shear stress patterns differently through cell activation or thrombin generation, but through complement activation. With the presence of EC, platelet complement activation was

completely inhibited from initiation, while platelets responded to pathological shear stress through cell activation and increased thrombin generation.

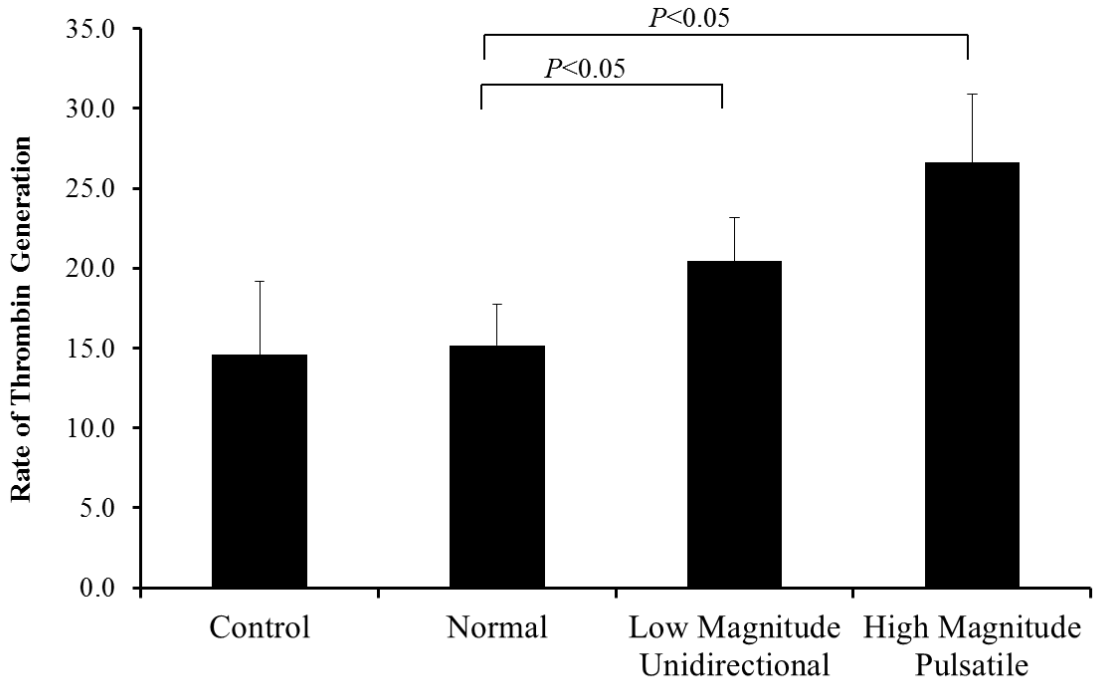

Figure 39. Platelet activation response measured as the rate of thrombin generation, at the end of 60 min exposure to various dynamic shear stress in the presence of endothelial cells. Data is presented as Mean + SD (n=6-7).

Table 7. Normalized all mean fluorescence value of platelets exposed to normal, Low magnitude unidirectional and high magnitude pulsatile shear in the presence of EC.

	Normal	Low Magnitude Unidirectional	High Magnitude Pulsatile
Normalized all mean fluorescence, Mean ± Std. Dev.	1.20 ± 0.32	1.16 ± 0.08	1.04 ± 0.25
Sample Size (n)	3	3	3

5.4.3 Platelet adhesion to EC monolayer under dynamic shear stress

After shearing simultaneously in a cone and plate shearing device, the amount of platelets or platelet microparticles adhesion to EC was measured using immunofluorescence microscopy. Actin fibers from EC and platelet cytoskeleton were detected using phalloidin (FITC/green), platelet GPIbα was detected by TRITC-conjugated mouse anti human GPIbα antibody (red), and EC nuclei were detected using DAPI (blue). Nonspecific antibody binding was detected by incubating the cells with a MOPC-FITC/TRITC antibody (Figure 40). High magnification images (100X, Figure 40A) were obtained to characterize the deposited particles, based on their size. The average size of the deposited particles was found to be 2-3μm, indicating that they were platelets. The ratio of platelet deposited area to the total image area was estimated and presented in Figure 41. Both low (Mean±SD: 17.68±3.81, n=4) and high (14.71±3.94, n=4) magnitude pulsatile shear induced a significant increase in platelet deposition compared to normal shear (9.38±4.74, n=4, $P<0.05$).

Alternatively, platelet adhesion to EC was measured using R-PE conjugated PECAM-1 antibody, FITC conjugated CD42b antibody and DAPI. Typical results are shown in Figure 42. Platelet adhesion was quantified by comparing the number of adhered platelets to the total number of EC (the ratio was calculated). Cell counting was conducted independently by two different observers. Similar to the experiments using phalloidin, both low (Mean±SD: 34.63±12.44, n=4) and high (21.4±7.01, n=5) magnitude pulsatile shear induced a significant ($P<0.05$) increase in platelet deposition compared to normal shear (10.6±3.73, n=5).

To determine if the observed platelet adhesion to EC monolayer was through GPIbα and/or GPIIb/IIIa, platelets were incubated with GPIIb and GPIbα blockers before co-shearing with EC. Representative images of platelet deposition with GPIbα and GPIIb blocked are presented in Figure 43 (A-F). The results demonstrated that blocking either GPIbα or GPIIb/IIIa did not induce any noticeable changes in platelet adhesion to EC.

As the cone-plate device did not provide a physiologically realistic EC-platelet interaction environment, similar experiments were conducted in a parallel-plate flow chamber, where platelets and EC were exposed to different dynamic shear stress at the same flow rate. Post shearing (60 min), the cells were fixed and stained with TRITC conjugated PECAM-1 (red) and DAPI (blue, EC nucleus) antibody. Figure 44 depicts the representative images of platelet adhesion to EC. In general, platelet adhesion to EC monolayer decreased compared to that observed in cone-plate shearing experiments. Platelet adhesion quantified by counting (as described above) indicated that the low pulsatile shear stress (Mean±SD: 5.33±2.65, n=4) induced a significant increase ($P<0.05$) in platelet deposition compared to normal shear (1.21±0.29, n=4), while no difference was detected under high magnitude pulsatile shear (0.89±0.16, n=4).

Since the cone and plate shearing device was a closed system, more platelet adhesion occurred, compared to the parallel plate flow chamber. Pathological shear stress (high and low) could affect platelet adhesion to EC. Particularly, low pulsatile shear stress could enhance platelet-EC adhesion. Also, platelet adhesion observed here was not primarily mediated through platelet membrane receptors GPIbα or GPIIb/IIIa.

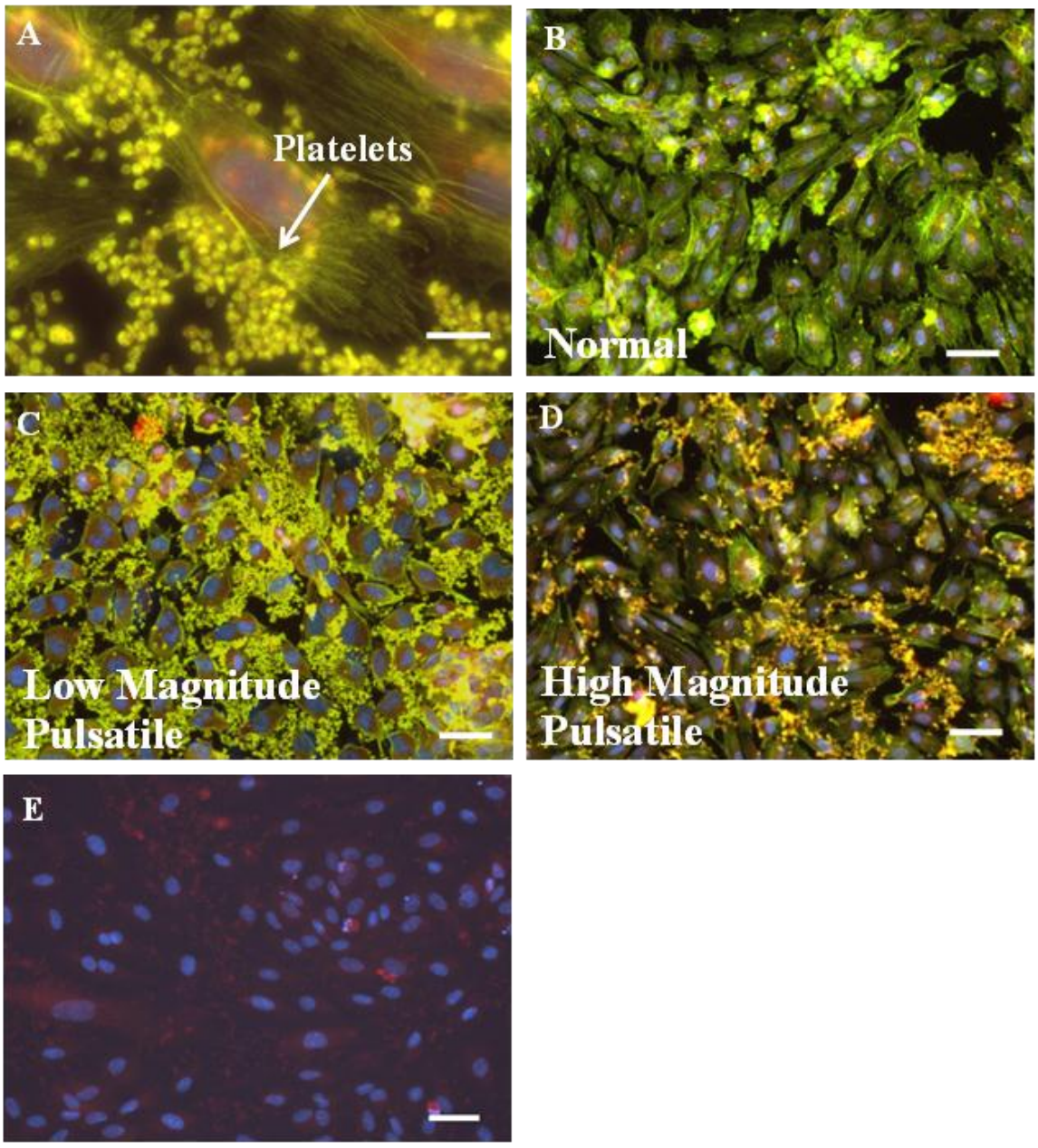

Figure 40. Representative fluorescence microscopy images indicating the amount of platelet deposition on EC after coupled shear exposure. The cells were stained for actin. (A) 100X magnification images revealing platelet adhesion, (B-D) Dynamic shear stress waveforms, (E) MOPC staining. Scale (A) 10µm, (B-E) 50µm.

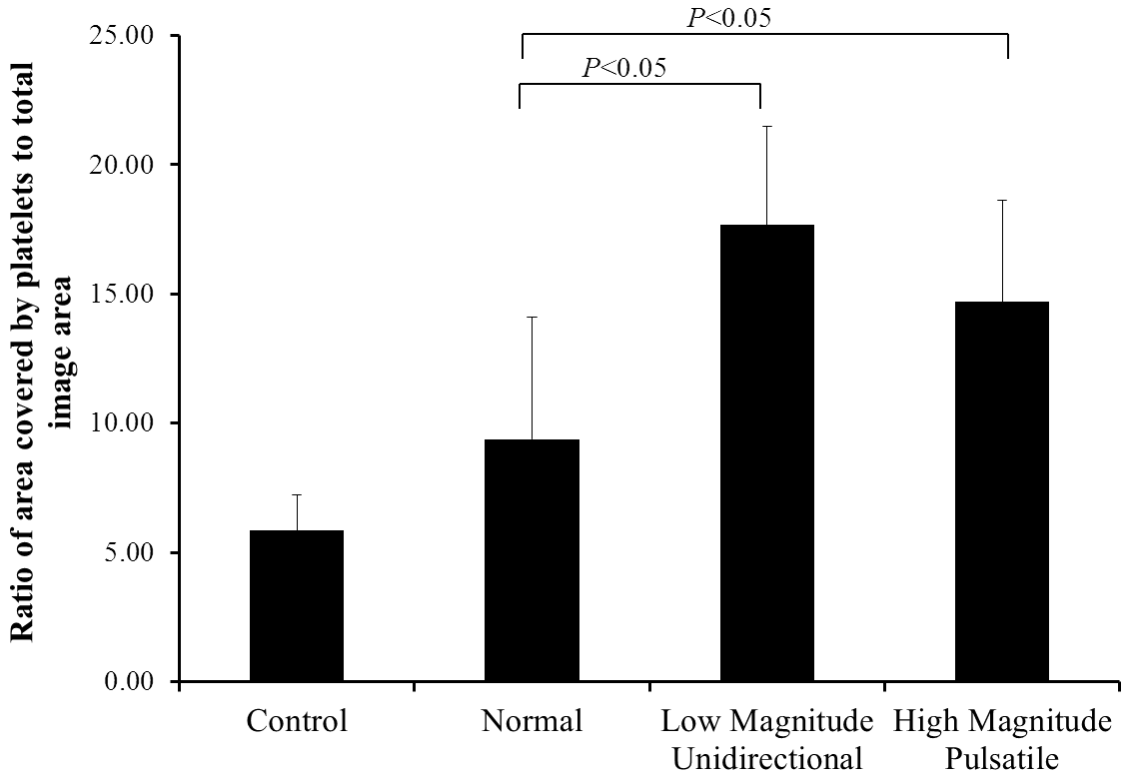

Figure 41. Area covered by platelets deposited on EC was quantified, and the ratio of platelet deposited area to the total area of the image is presented above. The bars are representative of Mean + SD (n=4).

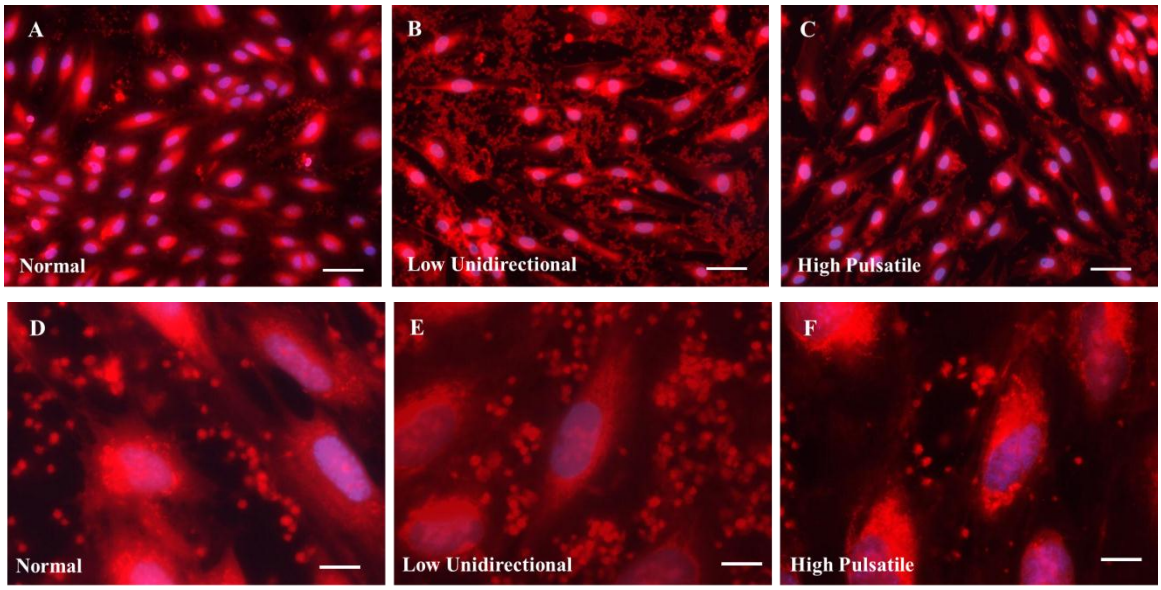

Figure 42. Representative fluorescence microscopy images (A-C 20X, D-F 100X) indicating the amount of platelet deposition on EC after coupled shear exposure by using PECAM-1 as marker protein. Scale 10 µm.

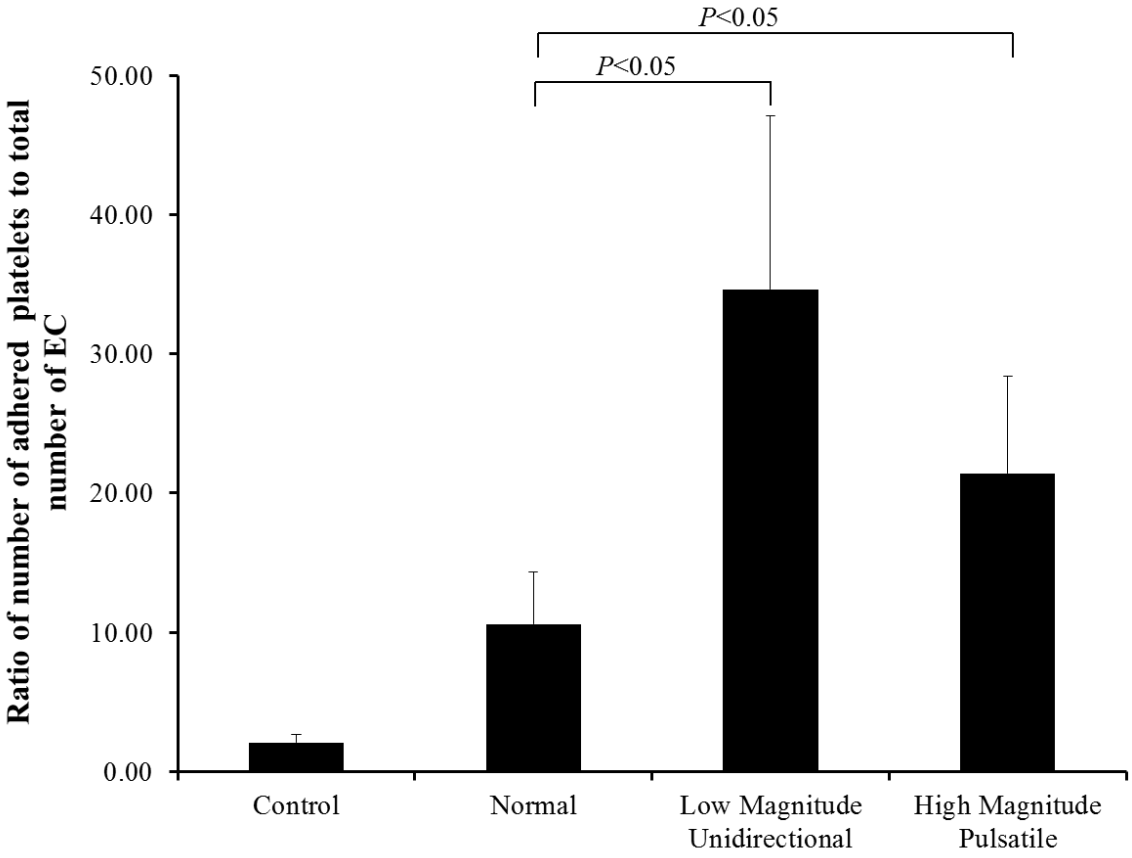

Figure 43. Ratio of total number of platelets adhered to the number of EC after exposure to pulsatile shear stress in a cone-plate shearing device. The bars of representative of Mean + SD (n=4-5).

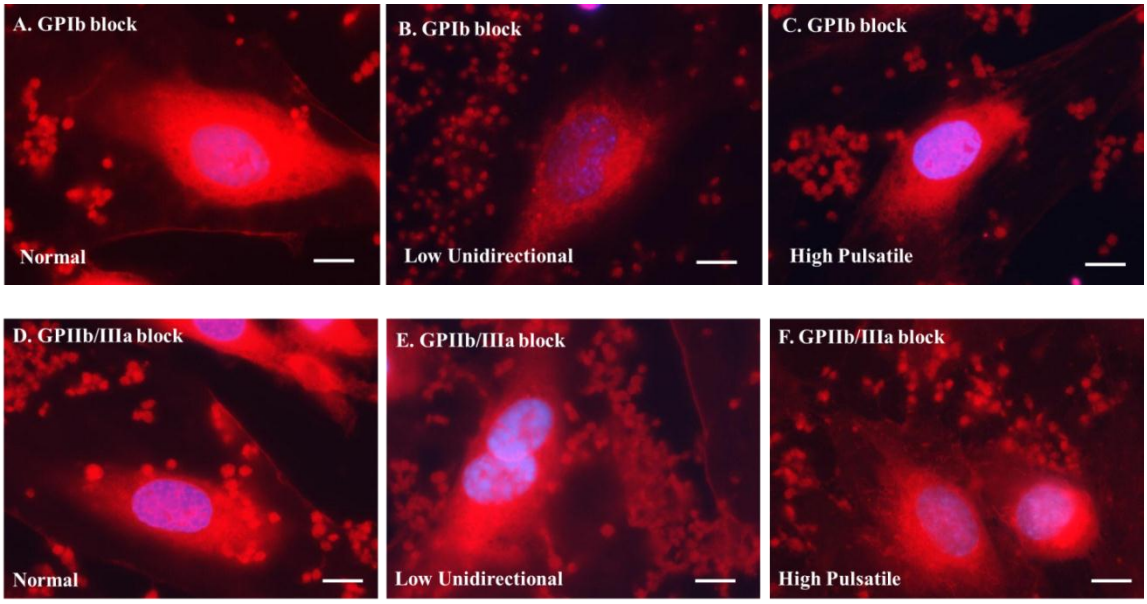

Figure 44. Platelet GPIbα (A-C) and GPIIb/IIIa (D-F) were blocked and sheared in the presence of EC. Representative fluorescence microscopy images (100X) indicating platelet deposition on EC after coupled shear exposure by using PECAM-1 as marker protein. Scale 10 µm.

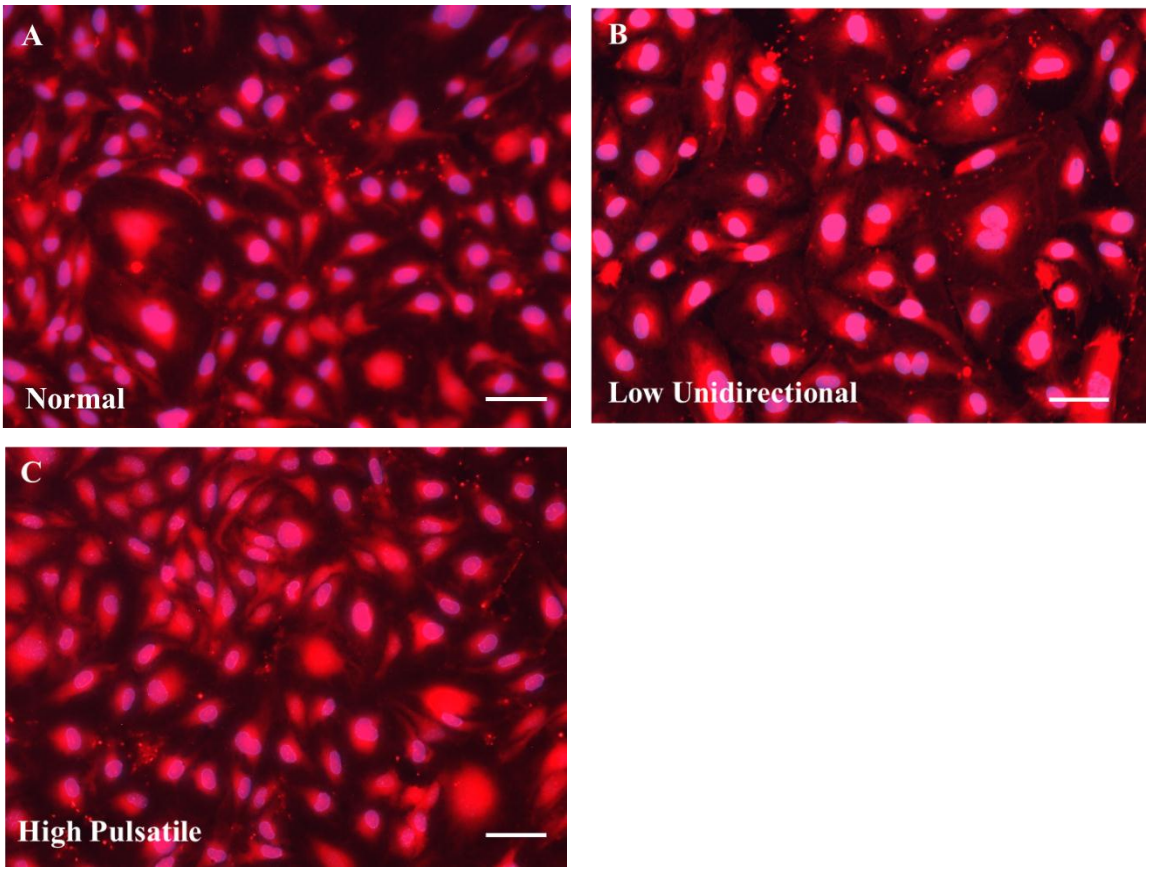

Figure 45. Representative fluorescence microscopy images (20X) indicating platelet deposition on EC after coupled shear exposure in a parallel plate flow chamber. The cells were stained for EC/Platelet PECAM-1 (red) and EC nucleus (blue). Scale 50 µm.

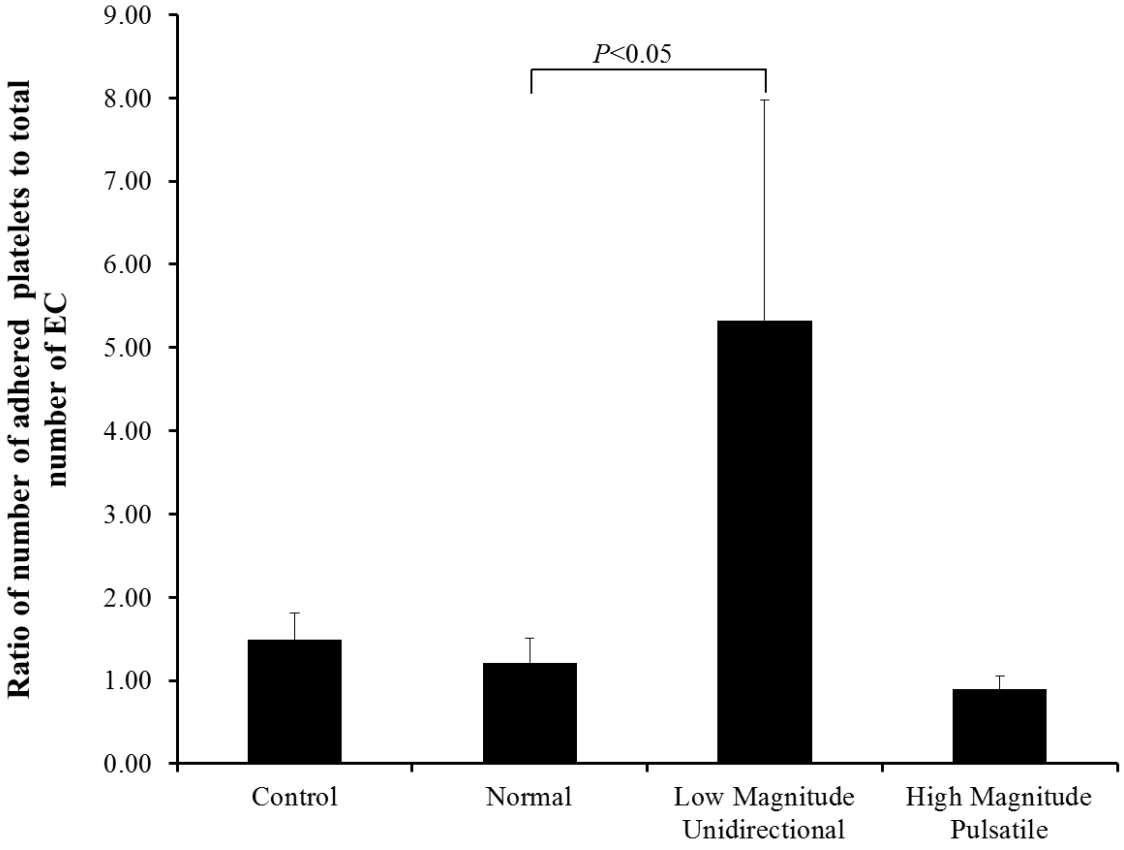

Figure 46. Ratio of total number of platelets adhered to the number of EC, after exposure to pulsatile shear stress in a flow chamber. The bars are representative of Mean + SD (n=4).

CHAPTER VI

DISCUSSION

Blood flow induced shear stress plays a critical role in the localization and pathogenesis of atherosclerosis. The anatomical location and complex geometry of coronary arteries create highly complex blood flow conditions. The characteristics of such disturbed blood flow include altered shear stress, which help the localization and growth of atherosclerotic lesions inside the coronary arteries.

Flow can affect the normal functions of vascular wall endothelial cells (EC) and circulating platelets greatly. The major focus of this study was to use numerical methods to estimate the shear environment inside the left coronary artery (LCA) under normal and disease conditions, and to investigate the effect of physiologically relevant dynamic shear stress on EC and platelet activities.

6.1 Research Design

Through four specific aims, the current study aimed to investigate how physiologically relevant dynamic shear stress affects EC and platelet activities.

The purpose of SA1 was to develop a 3D numerical model of the human left coronary artery, and utilize computational fluid dynamics tools to estimate the shear stress environment under normal and disease conditions. The estimated shear stress history on both endothelial cells (vessel wall) and platelets (particles in discrete phase) was used in the *in vitro* studies (SA2, 3 and 4) to mimic *in vivo* stress conditions. Through SA2, we wanted to investigate how physiologically relevant dynamic shear stress affects endothelial cell (EC) responses, especially those pertaining to the pathogenesis of CHD and related thrombosis. In parallel, through SA3, we aimed to investigate how physiologically relevant dynamic shear stress affects platelet activation and inflammatory responses. In SA4, a more complex coupled shearing system was developed to expose EC and platelets to dynamic shear stress simultaneously, and the role of EC-platelet interaction on cell responses to shear stress was investigated.

6.2 CFD analysis of coronary flow

6.2.1 Coronary flow geometry, model and assumptions

In this study, a physiologically realistic 3D human left coronary artery (LCA) model was reconstructed from arteriography data (Figure 8)[91;92] and fluid flow through the vessel was analyzed under normal and disease conditions (30%, 60% and 80%). A stenosis was created by adding an asymmetric flow constriction inside the LAD branch near the bifurcation. Previous studies have modeled stenosis as both asymmetric and axisymmetric constrictions[24]. Near an asymmetric stenosis, flow separates at the peak of the stenosis throat, while the core flow is skewed towards the opposite vessel wall, increasing the wall shear stress. At an axisymmetric stenosis, with a fully developed

upstream flow condition, flow separates just before the apex of the stenosis and forms symmetric recirculation zones opposite to each other. The majority of the atherosclerotic plaques found *in vivo* are asymmetric and hence our disease condition was modeled asymmetrically.

Coronary blood flow is opposite to cardiac output, with highest flow rate occurring in diastole. The pulsatile inlet flow used in this study was calculated based on cardiac output, with an average coronary inlet flow rate of 200mL/min. To avoid inlet effects, a fully developed inlet flow profile was imposed at the inlet boundary. Also, to avoid any exit effects, the outlet boundary was set at atmospheric pressure. In addition, the regions of interest (near stenosis throat) were at least 7 diameters away from the outlet. Based on an earlier work published by our lab, a laminar solver was used for normal, 30%, and 60% stenosis condition, while a low Reynolds k-ω solver was used for 80% stenosis condition with a minimal 3% turbulent intensity[99]. The CFD analysis yielded a comprehensive flow and shear stress map inside LCA.

One of the limitations of this CFD model is the assumption of a rigid non-porous vessel wall. The blood vessel wall is viscoelastic. Stretching of the vessel wall could have a major impact on the amount of cyclic circumferential/axial strain imposed on the endothelium of the vessel wall. In addition, partially embedded in the heart muscles, coronary vessels undergo continuous dynamic motion along with the myocardium. Due to the requirement of a complex fluid – structure interaction model, both the vessel wall viscoelasticity (stretching) and the bending motion of the coronary vessels was not modeled in this study.

Santamarina et al. demonstrated in their study that considering the dynamic motion of coronary vessels (cardiac base frequency of 1 Hz) induced only about 6% change in wall shear rate estimation[101]. Further, an improved coronary flow model was recently built in our lab to include the dynamic motion of the vessel. The results from this model indicated the wall motion induced a slight reduction in the magnitude of peak shear stress, but did not have any major effects on flow parameters. Hence, we expect that these two assumptions should not significantly affect our shear stress estimation.

6.2.2 EC wall shear stress distribution

According to our simulation, flow separated before the bifurcation and skewed towards the inner wall in the LAD, resulting in a high shear stress region. On the opposite side in the LAD, regions of oscillatory flow developed. Under normal conditions, the WSS varied between 0.1-1Pa (in one cardiac cycle), similar to the levels observed by Perktold et al. in their study[21].

Under stenosis, as its severity progressed, a region characterized by high fluid velocity and increased shear stress formed near the center point of the stenosis throat due to the sudden narrowing of the blood vessel. WSS peaked at about 14.21Pa with a 80% stenosis. This value was very close to that reported by Deplano et al.; in their study, the peak shear stress at the stenosis throat (75%) inside a coronary artery was found to be 12Pa, through both experimental and numerical methods[102]. A number of other previous studies that employed simplified LAD geometry (2D or 3D) estimated much higher shear stress, ranging from 125Pa to 900Pa. The huge variation in WSS estimation is due to the simplicity of geometry and flow assumptions. It was reported that endothelial cells would

be damaged at shear stress of about 40Pa and would be stripped off at 100 Pa[13], which suggested that the high WSS estimated using simplified CFD models is not physiologically accurate.

Immediately past the stenosis throat, flow separated, forming a recirculation zone characterized by low shear stress (between 0.01 to 0.5Pa in one cardiac cycle). The size of the recirculation zone was dependent on the severity of the stenosis. As stenosis severity increased, the size of the recirculation zone increased. Downstream of the stenosis, the flow reattached to the vessel wall and the shear stress returned to normal levels. The spatially and temporally localized high and low shear stress is one of the major factors contributing towards the pathogenesis of CHD. Points of interest inside the flow domain were isolated and the WSS history (over one cardiac cycle) was exported to be used in *in vitro* studies to investigate the effect of dynamic shear stress on EC and platelets.

6.2.3 Platelet shear stress distribution

Platelets are sensitive to both shear stress magnitude and the duration of shear exposure, as highlighted by recent studies[2;3]. In the present study, 1000 platelet simulating particles were released at the inlet of the left coronary artery and their trajectories were estimated using a discrete phase model (typical trajectories shown in Figure 19). Based on their trajectory, the hemodynamic shear stress history (both shear stress magnitude and shear exposure duration were considered) of each platelet as it traveled through the left coronary artery was estimated. This platelet seeding density (1000) was chosen so as to estimate maximum possible trajectories while maintaining an

optimal computational load. As the discrete phase, platelets were treated as virtual particles, which can interact with the fluid phase and affect flow parameters. The solver was able to estimate forces applied to platelets imparted by flow, including the drag force. At the end of each time step, the solver calculated the instantaneous velocity, acceleration and displacement of platelets. On the other hand, platelet induced changes in mass, momentum and energy of the fluid phase was also estimated.

In this study, platelets were modeled as solid particles. But *in vivo*, platelets are viscoelastic and they may undergo significant deformation resulting from sudden changes in shear stress, especially near a stenosis. This could potentially affect platelet biochemical responses[93]. However, to model platelet deformation in response to dynamic blood flow, a structural solver accounting for platelet membrane properties (stiffness, yield stress etc.) needs to be coupled to the fluid solver. At every time step, for each platelet, flow induced surface forces estimated by the fluid solver needs to be transported to the structural solver and used to estimate platelet deformation. Changes in platelets would need to be reported back to the fluid solver to update the flow parameters, as the fluid phase and the particle phase needed to exchange mass, momentum and energy continuously. Furthermore, the difference in length scale (mm to μm scale) between the flow domain (which is the source for deformation force) and the particulate phase (where the actual deformation happens) would present a major difficulty to the computational effort. Therefore, in the current model, platelet deformation was not considered. Also, in this model, platelets were modeled as biochemically inert particles, i.e., platelet biochemical responses to flow were not considered. In this study, three typical platelet trajectories were sampled and their corresponding shear stress history was presented in

Figure 15. The shear waveforms were estimated from trajectories that were close to the vessel wall. This is due to the fact that in larger vessels platelets tend to move close to the vessel wall rather than to the center of the flow[103]. Also, the shear gradients are greater near the vessel wall. Therefore, platelets travelling in this region have a higher chance to become activated and adhere to the vascular wall.

The normal shear waveform was chosen to represent platelets that travelled through the LAD under normal conditions, and the magnitude of shear exposure varied between 0.1-1Pa. In general, under physiological conditions, platelets traveling through a normal vessel are exposed to a shear stress range of 0.7-1.6Pa[104]. The high-magnitude pulsatile shear stress waveform was used to simulate shear stress history of platelets that travelled through the stenosis close to the vessel wall and momentarily experienced high shear. We assumed that the same platelets would pass through the same stenosis once every 90 sec. Platelets that were trapped inside the recirculation zone downstream of the stenosis experienced low magnitude shear stress. These platelets had higher collision frequency and longer residence time, which could potentially increase their activation potential[105].

6.3 Endothelial cell response under dynamic shear stress

ECs lining the innermost layer of blood vessels are directly exposed to blood flow induced shear stress and their functions are susceptible to regulation by shear stress. For this study, a cone and plate shearing device (Figure 11) was programmed with WSS history obtained from our numerical simulation. Confluent monolayers of human

coronary artery endothelial cells (HCAEC) were exposed to these shear stress waveforms and their activation/inflammation responses were monitored.

One of the major activation markers investigated in this study was intercellular adhesion molecule 1 (ICAM-1). ICAM-1 has been extensively studied as it plays a major role in binding and sub-endothelial migration of leukocytes in the initial stages of atherosclerosis. It also acts a receptor for platelet adhesion through fibrinogen. In this study, EC were exposed to four different dynamic shear stress waveforms and ICAM-1 levels were examined at surface, total protein and mRNA levels (Figure 20). Compared to normal shear, EC exposed to low magnitude unidirectional shear had a slight increase (not statistically significant) in surface ICAM-1 expression, a significant increase in ICAM-1 total protein expression, but no significant changes at mRNA level. Low oscillatory shear stress induced a significant increase in EC total ICAM-1 expression, but did not lead to any changes on the cell surface or at the mRNA level. This is similar to that observed with the low magnitude unidirectional pulsatile shear stress. The inconsistencies between surface ICAM-1 expression and total ICAM-1 expression could be potentially due to the difference in shear exposure time. In studies conducted by Morigi et al. and Nagel et al, it was observed that EC surface ICAM-1 expression increased linearly as a function of shear exposure time[38;40]. Both studies also reported significant increase in ICAM-1 mRNA expression after 2 hours of shear expsoure[38]. By increasing shear exposure time, we expect to see significant changes in ICAM-1 expression, on EC surface or at mRNA level, matching the trend we saw with the total protein expression.

In addition to EC activation, shear stress induced EC injury/inflammation was examined by measuring tissue factor (TF) and thrombomodulin (TM) expression at the surface protein, total protein and mRNA level. TF plays a major role in triggering the coagulation cascade under both physiological (maintaining hemostasis) and pathological (thrombosis) conditions. EC were sensitive to different dynamic shear stress waveforms and produced varying levels of TF. Compared to normal shear, low magnitude unidirectional shear led to an elevated (not statistically significant) surface TF expression, which could increase the coagulation potential inside the recirculation zone. However, the total protein and mRNA levels was lower compared to normal shear. In contrast, low magnitude bidirectional shear induced a slight reduction in TF protein expression (surface and total) but had an increased TF mRNA expression. It is not clear why TF expression at protein level and at mRNA level was not consistent. It could be due to the difference in shear exposure time, or some posttranscriptional regulations[106]. Elevated pulsatile shear stress did not lead to any change in TF expression at protein level (surface and total), but induced a significant reduction in mRNA expression. So, in general, pathological dynamic shear stress could reduce EC TF expression, which may indicate the activation of certain inhibitory mechanism that can prevent both EC activation and inflammation.

Thrombomodulin (TM), produced by EC, is an athero-protective protein that can inhibit thrombin. Surface ELISA and Western blot experiments revealed a significant reduction in TM expression on EC exposed to pathological shear stress. RT-PCR results indicated a downregulation in TM mRNA expression under low magnitude unidirectional

shear and high magnitude pulsatile shear compared to normal shear, though not statistically significant.

Von Willebrand Factor (vWF) provides a major binding site on EC surface (receptor) for platelet surface GPIbα (ligand), playing a key role in EC-platelet adhesion. EC produce ultra large molecular weight vWF and store them in Weibel-Pallade bodies. Compared to normal shear, both low and high magnitude pulsatile shear did not induce any changes in vWF at protein level (surface and total). This is consistent with a report by Galbusera et al., that shear stress between 0.1-1.2Pa would lead to no changes in EC vWF expression (surface protein and mRNA). Interestingly, in present study, recirculation shear led to slight upregulation in surface vWF expression along with an elevated mRNA expression measured using RT-PCR. This might indicate that the EC were able to sense low magnitude pulsatile shear and produce more vWF. An elevated vWF concentration inside the recirculation zone, along with the increased platelet population trapped inside this zone could potentially promote platelet adhesion to EC and ultimately lead to thrombus formation. However, changes from long duration shear exposure need to be investigated.

6.4 Platelet response to dynamic shear stress

Recent studies have highlighted the effect of shear stress magnitude and duration on platelet activities[2;3]. Since *in vivo* flow conditions are dynamic, it is important to investigate the role of physiologically relevant dynamic shear stress on platelet activation and other related responses. In the present study, platelets were tracked as they travelled through the left coronary artery (especially the left anterior descending artery) and their

shear stress history along their path was calculated. As mentioned above, three specific shear stress waveforms were used; they represent shear stress history of platelets that travelled through a normal artery, a 60% stenosed artery, and were trapped inside the recirculation zone downstream of the stenosis throat.

Previously, we reported that both low magnitude pulsatile shear and high magnitude pulsatile shear did not lead to platelet activation in terms of P-selectin expression[100], or induce significant changes in platelet thrombogenicity, compared to normal pulsatile shear[4]. In this study, we furthered our previous investigation by examining platelet associated complement activation and proteomic changes under dynamic shear stress.

6.4.1 Platelet complement activation

Platelets were exposed to all three different shear stress waveforms in a cone-plate shearing device, following which, the amount of complement protein deposited (C1q, C4d, iC3b and sC5b-9) was measured. The results indicated that platelets stimulated with low magnitude pulsatile shear had an elevated C1q deposition compared to normal shear (Figure 28), even though platelets were not activated. Further, high magnitude pulsatile shear did not induce any noticeable change in C1q deposition compared to normal shear. The finding matched a report by Peerschke et al.[76], that resting platelets support complement activation. However, following C1q activation, no significant changes in the subsequent complement proteins were detected. This prompted the investigation of the complement regulatory/inhibitory mechanism. C1-inhibitor could completely inhibit the progression of complement classical pathway cascade irreversibly.

Platelets exposed to both pathological shear (low and high) had a significantly increased expression of C1-inhibitor (Figure 31) compared to normal shear.

Complement receptor 1 (CR1) can inhibit complement activation by cleaving C3b and C5b. Our results showed that both pathological shear stress induced noticeable CR1 expression compared to normal shear stress, even though no statistical significance was detected (Figure 32).

These results demonstrated that even though pathological pulsatile shear stress was not able to trigger platelet activation, platelets were able to sense the difference in flow patterns. By releasing increased amount of C1-inhibitor, platelets stopped complement activation at the very first stage, preventing the production of anaphylatoxins C4a, C3a and C5a, as well as the membrane attack complex (MAC), which could potentially cause platelet activation, thrombosis and cell death. Also, platelets exposed to low pulsatile shear stress had a higher chance for C1q activation, it may suggest that the low pulsatile shear found inside recirculation zones could potentially be more atherogenic.

6.4.2 Platelet proteomics

In addition, pulsatile shear stress induced changes in the platelet proteome were examined using the SELDI-TOF technique. Yin et al. reported that platelets activated by TRAP (10 μM) or ADP (20 μM) revealed 7 distinct protein peaks that were significantly different compared to resting platelets[80]. However, platelets that were exposed to a steady shear (1.8Pa for 5min) revealed no distinct protein peaks compared to resting platelets.

These results demonstrated that SELDI-TOF might be an effective method to study platelet responses to different agonists.

In this study, platelets were activated by both constant (1 and 3 Pa) and pulsatile shear stress (normal, low magnitude unidirectional and high magnitude pulsatile shear). In addition, platelets treated with TRAP (10μM) were used as the positive control. Proteomic analysis of these samples was conducted using SELDI with a special focus on the low molecular weight range of the spectrum (M/Z 2,000 to 15,000). TRAP-treated platelet samples showed nine distinct protein peaks that were significantly different from resting platelets (Figure 33 and Table 4). Similar to the early study conducted by Yin et al., no distinct peaks were identified under low steady shear stress (1Pa); however, under high shear stress (3Pa) three distinct peaks were detected compared to resting platelets (Figure 34). Interestingly, the spectral profiles indicated that TRAP activated platelets (Figure 33) had a significantly different profile (both shape and magnitude) compared to those activated by constant shear (Figure 34). This indicates that platelets respond differently to biochemical and biomechanical stimuli; SELDI, or platelet proteomic analysis, may be useful for detection of agonist specific biomarkers. When platelets were treated with the three dynamic shear stresses, 8 new peaks were detected, which were different from the peaks detected from TRAP or constant shear stress treated platelets (Figure 35). Among the three dynamic shear stresses, both low and high pulsatile shear stress induced a significant reduction in peak intensity at M/Z of 2439.23; while high magnitude elevated pulsatile shear stress induced a significant increase in peak intensity at M/Z of 3274, compared to normal shear. Also, the differentiated protein profile (shape and magnitude) induced by high magnitude pulsatile shear stress was different from that

induced by normal shear stress. These results indicate that platelets were able to sense the difference in dynamic shear stress waveforms, by expressing different proteome patterns. In a parallel work conducted in our lab, platelets were exposed those three dynamic shear stress waveforms and platelet activation was measured by cell surface CD62P and CD41a expression using flow cytometry. No difference in CD62P and CD41a expression was detected, indicating that platelet surface CD62P and CD41 could not be used as activation markers to distinguish the difference between normal, low and elevated pulsatile shear stress[100]. Together, these results suggested platelet proteomic profiles (especially at the low molecular weight range) could be potentially used to detect subtle differences in dynamic shear stress under various flow conditions.

Among all the distinguished peaks detected by SELDI, 2 protein peaks were of special interest to us. One peak occurred at M/Z of 8,139. The peak intensity decreased significantly upon TRAP treatment (43.28% decrease) but increased significantly under dynamic shear stress activation (Normal - 255%, Low magnitude unidirectional - 362%, High magnitude pulsatile - 199%), compared to resting platelets. No significant change was detected under constant shear stress (1Pa – 11.6% decrease, 3Pa – 0.003% reduction). The other peak occurred at M/Z of 4,975. All treatment induced changes at this peak compared to resting platelets: TRAP induced a 152.92% increase, constant shear stress at 3 Pa induced a 84.55% increase, while all three dynamic shear stress waveforms (normal - 26%, Low magnitude unidirectional - 37%, high magnitude pulsatile - 61%) induced a reduction compared to resting platelets.

Platelet lysate samples were also analyzed using a liquid chromatography mass spectrometry (Orbitrap) technique, to identify platelet-associated proteins that could be

used to distinguish different stimuli. This could potentially result in the identification of particular protein biomarkers for platelet activation. Data (3 biological replicates and 4 technical replicates) obtained from Orbitrap MS/MS analysis estimated that the protein peak at M/Z of 4,975 could possibly be Thymosin Beta - 4 (5kDa), an actin monomer sequestering protein; and the protein peak occurring at M/Z of 8,139 could possibly be Platelet Factor 4 (7.8kDa). Thymosin beta-4 has recently been implicated in regulating EC functions[107], especially in proliferation and angiogenesis regulation[108], while Platelet Factor 4 is involved in angiogenic responses during tumor metastasis conditions[109]. Since Orbitrap MS/MS was not able to provide very accurate information on protein ID at low molecular weight (<10,000 Da), no more differentiated proteins were detected by both SELDI and Orbitrap techniques. Further experiments are required to confirm the protein identification and to verify their role in shear induced platelet activation.

6.5 Endothelial cell – platelet interaction

Under *in vivo* conditions, EC are constantly exposed to dynamic shear stress in the presence of platelets. The complex interaction between EC and platelets play a central role in hemostasis, thrombosis and atherosclerosis. In order to investigate how EC-platelet interaction would affect EC and platelet cellular responses to dynamic shear stress, a coupled shearing system (washed platelets placed on confluent monolayer of EC and exposed to shear stress) was employed.

Our results showed that with the presence of platelets, pathological shear stress (low and high) failed to induce any changes in EC surface ICAM-1 expression, which was different from what was observed when EC were exposed to dynamic shear stress

alone. Further, similar amount of NO generation by EC was observed when the platelets were present indicating that the EC activity was intact. This result strongly suggested an inhibitory role of platelets on EC activation. This inhibitory effect from platelets was further investigated at mRNA level. RT-PCR demonstrated that with the presence of platelets, there was a significant reduction in ICAM-1 mRNA expression under pathological shear stress, compared to normal shear. In addition, when sheared alone, low magnitude pulsatile shear stress induced a slight increase (not significant) in EC TF expression. However, with the presence of platelets, no changes in EC surface TF expression was detected under both low and high pathological shear stress conditions. Further, in a parallel experiment conducted in our lab, no significant change in EC surface vWF was detected. Hence, in the presence of platelets, EC lost their sensitivity to dynamic shear stress waveforms, and failed to express any changes in ICAM-1, TF and vWF expression.

The protective interaction between platelets and EC could take place in two ways: 1) through soluble factors released by platelets, such as substances from platelet α granules, dense bodies and platelet microparticles; 2) through direct physical contact between platelets and EC, such as surface adhesion molecules or receptors; or 3) a combination of both mechanisms.

The major biochemical factors released by platelets include ADP, thrombin, platelet derived growth factor (PDGF) and fibrinogen. Studies conducted in the past indicated that most of these factors induce EC activation[110]. In a study conducted by Hess et al., ADP was found to modulate eNOS (endothelial nitric oxide synthase) expression and cell migration in EC[111]. The presence of fibrinogen was found to synergistically

enhance interleukin-8 induced NO (nitric oxide) production[112], and PDGF was found to modulate endothelial proliferation and angiogenesis[113]. In addition, platelet microparticles released by shear stress were found to promote EC activation (cytokine production and adhesion molecule expression)[114]. Based on the above literature evidence, it is highly unlikely that one of the platelet releasate was responsible for inhibition of EC activation. On the other hand, direct interaction of platelets with EC could potentially be responsible for inhibition of EC activation.

Platelet adhesion to EC was measured using immunofluorescence microscopy. The results indicated that more platelets deposited on EC monolayer under pathological shear stress (high and low) conditions. By analyzing higher magnification images, the deposited particles were found to be 2-3μm in diameter, indicating it was not platelet microparticles, but platelets, adhered to EC monolayer. Further, control experiments were conducted to test the effect of washing on platelet adhesion. The results indicated that there was no change in amount of platelet adhesion between washing and not washing the cells after shearing. The key platelet membrane receptors that are responsible for platelet adhesion to EC are GPIbα and GPIIb/IIIa. vWF, expressed on EC surface, acts as a key ligand for these receptors. EC surface vWF was abundant[115]. Results obtained from this study demonstrated that EC surface vWF expression was not affected by dynamic shear stress. However, free vWF in the fluid phase (released by EC and platelets) increased after EC and platelets were simultaneously exposed to low magnitude pulsatile shear stress.

When platelets were exposed to dynamic shear stress alone, cell surface GPIbα and GPIIb/IIIa expression was not affected by shear stress patterns. While in the coupled

shearing experiments, with the presence of EC, the low magnitude pathological shear stress resulted in an increase in platelet surface GPIbα expression, while no change in GPIIb/IIIa expression was noticed[100]. Increased soluble vWF and GPIbα indicated an increased potential in platelet adhesion to EC. To determine if these receptors (GPIbα, GPIIb/IIIa and vWF) were responsible for platelet-EC adhesion we observed in the co-shearing studies, GPIb was blocked by anti-human GPIbα blocking antibody, and GPIIb was blocked by tirofiban. The results showed that blocking both GPIbα and GPIIb/IIIa did not cause any change in platelet adhesion to EC monolayer. However, the efficiency of both the blocking agents (against GPIbα and GPIIb/IIIa) on platelets was not verified in this study. This suggested platelet adhesion to EC under dynamic shear stress conditions was through other proteins. Some of the other potential target EC surface adhesion molecules that support platelet binding includes PECAM-1, P-selectin[116] and ICAM-1[83]. Further studies are needed to evaluate their expression and adhesion potential under dynamic shear stress conditions.

The major limitation to the coupled shearing study was the use of the cone and plate shearing device. The flow pattern in the cone and plate device did not provide a physiologically realistic shear environment for EC and platelets (it was a closed system). Therefore, a parallel plate flow chamber was used alternatively. The adhesion experiments indicated a slight increase in platelet adhesion to EC monolayer under both low and high pulsatile shear stress, compared to normal shear stress, which was similar to that found using a cone and plate device.

In general, under all three dynamic shear stress conditions, the overall platelet binding was lower in the parallel plate flow chamber, compared to that observed with the

cone and plate shearing device. This is primarily due to the fact that the cone and plate shearing device was a closed system, where platelets were continuously exposed to EC. Platelet-EC interaction time in the cone and plate shearing device was much longer than that in the flow chamber. The other major limitation in using the cone and plate shearing device for EC-platelet interaction was that substances released by both EC and platelets were accumulated within the same environment over time, which could possibly lead us to overestimate the effect from shear stress.

6.6 Proposed Models

6.6.1 Thrombus formation mechanism

Based on these observations and findings, a possible mechanism for platelet activation and thrombus formation is presented in Figure 47. EC in the recirculation zone are exposed to pathological low shear stress, which could enhance EC surface ICAM-1 and vWF expression. Platelets (quiescent or activated) could be trapped inside a recirculation zone. GPIbα is always available on platelet surface, which would assist platelets adhere to the blood vessel wall (or EC). In addition, platelets also have abundant GPIIb/IIIa on their cell surface, which can assist firm adhesion to endothelium after the initial binding through GPIbα and vWF. GPIIb/IIIa binding to the endothelium can occur through either, (1) GPIIb/IIIa – fibrinogen – ICAM-1 (more probable adhesion binding under low shear) or (2) GPIIb/IIIa – vWF (more probable under high shear) binding. Platelet binding to EC is also facilitated by the low shear stress presented in this region, which produces less bond breakage force and longer rolling time.

After the initial binding between GPIbα and vWF, through intercellular signaling cascades, platelet membrane GPIIb/IIIa molecules become activated. Through fibrinogen, activated platelets can start aggregation. The activation and aggregation potential is higher inside the recirculation zone due to longer retention time for platelets trapped inside and elevated local concentration of agonists released by platelets upon activation. These would lead to thrombus formation in the recirculation zone.

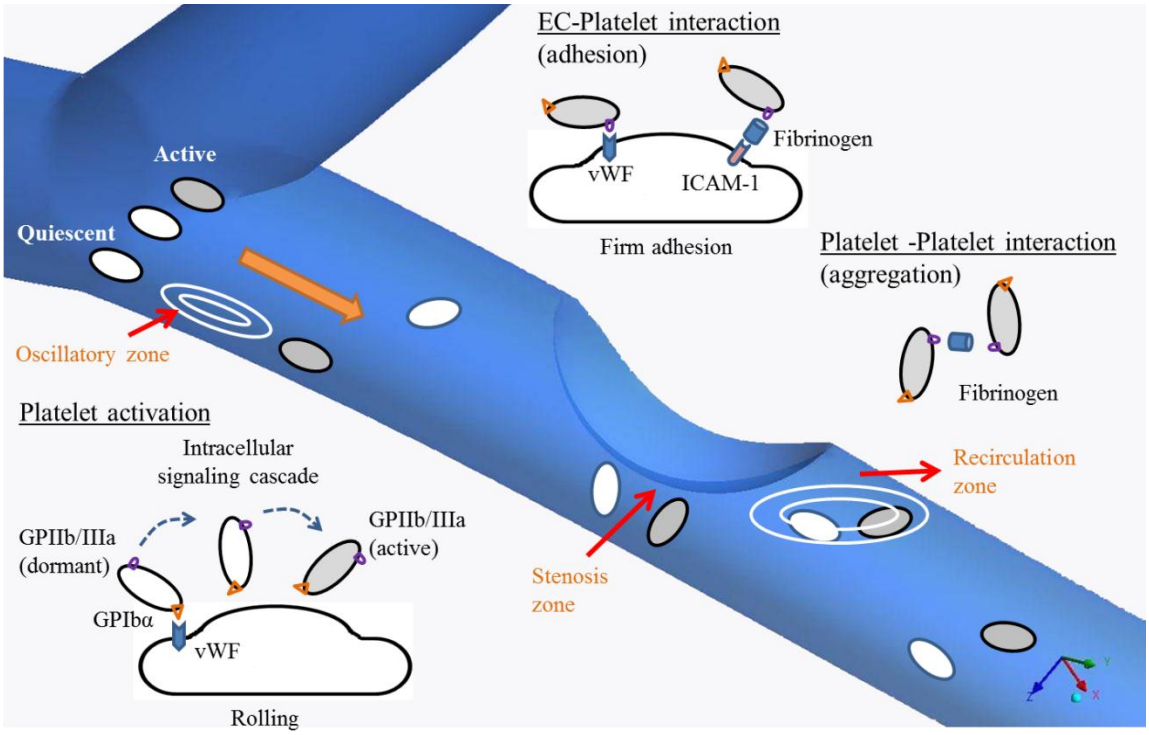

Figure 47. Proposed thrombus formation mechanism. Quiescent platelets rolling inside oscillatory zone gets activated. Quiescent/activated platelets get trapped inside the recirculation zone with active EC and promote thrombus formation.

6.6.2 Regulatory Mechanism

The EC-platelet interaction studies revealed a protective effect of platelets on EC under pathological shear stress. Here we propose two hypotheses for this protective mechanism.

First, the protective mechanism could take place through certain substances released by activated platelets, inhibiting EC activation under pathological shear stress. The continuous convective mass transfer of biochemical factors, especially in medium to large sized blood vessels (such as the left coronary artery), would prevent the accumulation of such substances and reduce their local concentration. The only possible locations for EC-activation-inhibiting substance to accumulate are the recirculation zones. Further, most substances like ADP, thrombin and PDGF released by platelets are known to induce EC activation. The only substance known to be released by platelets that could potentially inhibit EC activation is plasminogen activator inhibitor – 1 (PAI-1)[117]. PAI-1 has been shown to play a major role in angiogenesis and cancer metastasis, but the effect of dynamic shear stress on PAI-1 is yet to be known.

The second possible explanation is that this protective mechanism occurs through the direct physical contact between platelets and EC. Both EC (ICAM-1, vWF, PSGL-1 and PECAM-1) and platelets (GPIbα, GPIIb/IIIa, P-selectin and PECAM-1) have a few surface proteins that are involved in anchoring of platelets to EC. On EC, though ICAM-1, vWF and PSGL-1 enable platelet adhesion, they are not known to trigger any downstream signaling cascades. PECAM-1 is the only adhesion molecule that is known to form a mechanosensory complex along with VE-cadherin and VEGFR2[98]. This

junctional protein complex plays a key role in sensing flow. The cytoplasmic tail of PECAM-1 has been shown to be phosphorylated in response to shear stress[118]. Downstream, PECAM-1 activation triggers AKT/PI3K pathways[98], which are involved in major shear induced responses including generation of ICAM-1. Also, on platelets, PECAM-1 has been recently shown to inhibit the GPIbα triggered activation of GPIIb/IIIa leading to firm adhesion or aggregation (Figure 48)[119;120]. Hence, PECAM-1 is a potential target that could be responsible for EC losing their sensitivity to shear stress and platelets gaining their sensitivity. Future experiments focused on assessing the activation and function of PECAM-1 on both EC and platelets might uncover a mechanosensing mechanism under pathological dynamic shear stress and reveal a potential therapeutic target.

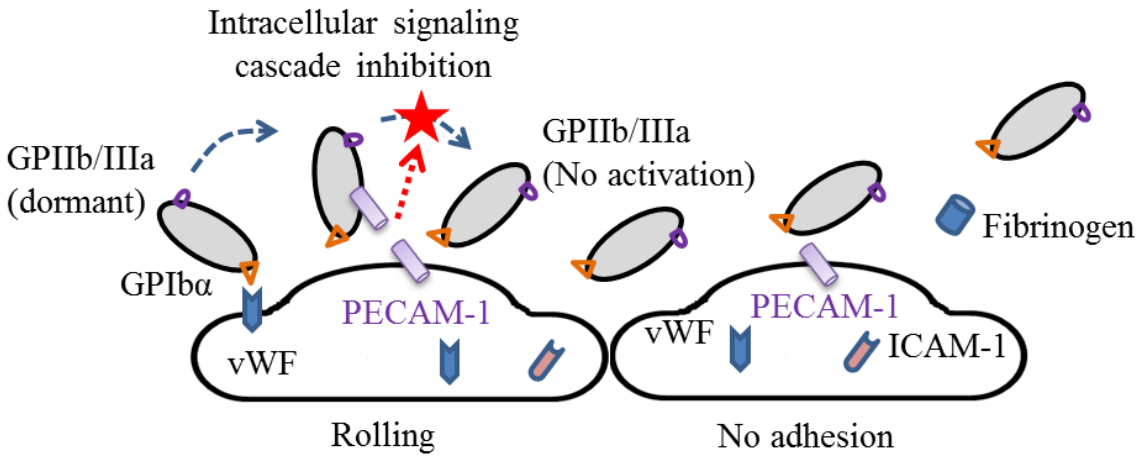

Figure 48. Proposed regulatory mechanism mediated through PECAM-1. EC and platelet surface PECAM-1 regulate internal functions of both the cell types and prevent firm adhesion, platelet activation and EC activation.

CHAPTER VII

CONCLUSION AND FUTURE DIRECTIONS

7.1 Summary

The key observations from this study are summarized below:

Under normal conditions, low magnitude bidirectional oscillatory shear zone formed near the LM bifurcation. Under stenosis conditions (30%, 60% and 80%), flow separated near the stenosis with elevated shear stress developing at the stenosis throat. Zones with low magnitude unidirectional or oscillatory shear stress develop downstream of the stenosis. Endothelial cells could therefore experience low unidirectional pulsatile shear stress downstream of the stenosis, and these cells had a higher chance to get activated by flow. The inconsistence in surface protein expression, total protein expression and mRNA changes for factors tested in this study indicated that long duration shear exposure experiments are needed to investigate EC response to dynamic shear and their functional/physiological significance. On the other hand, EC present at the stenosis throat and exposed to high magnitude shear were not activated compared to those exposed to physiological levels of shear stress. This might indicate a potential inhibitory mechanism triggered by high magnitude shear stress.

As platelets travelled through the left anterior descending artery, they could be exposed to various shear stress conditions: physiological, low or elevated pulsatile shear stress. Platelet sensitivity to dynamic shear stress was not detected in terms of certain surface protein expression (data not shown in this study). However, proteomics analysis demonstrated that platelets expressed different proteomic patterns under various dynamic shear stress conditions. Platelets were also sensitive to differences in dynamic shear stress patterns in terms of complement activation. Platelets that were exposed to low magnitude unidirectional shear could initiate classical pathway complement activation (elevated C1q deposition). However, this activation could not proceed to completion due to the triggering of complement inhibitors.

When platelets and EC were exposed to shear stress simultaneously, their cellular responses to dynamic shear stress changed. EC could not sense the difference between different dynamic shear stress patterns in the presence of platelets, at least in terms of cell activation, at both protein level and mRNA level. On the other hand, platelet sensitivity to various dynamic shear stress patterns increased. With the presence of EC, platelets exposed to pathological levels of shear stress (high and low) had an elevated activation level evidenced by their increased thrombin generation potential. These sensitized platelets when trapped inside the recirculation zone, due to the increased retention time, revealed an increased potential to adhere to injured endothelial cells or the blood vessel wall. It suggests that thrombosis and atherosclerotic lesion has a potential to grow towards the downstream region of an existing stenosis.

The major goal of this study was to estimate physiological levels of shear stress in human left coronary artery and to examine the behavior of EC and platelets when

exposed to such forces. The novel approach of utilizing numerical simulations to guide *in vitro* experiments enabled us to understand the activation and inflammatory response of EC and platelets under physiologically realistic shear environments. In general, the findings from this study indicate that both EC and platelet responses are altered under disturbed shear stress conditions, especially their interaction. In addition, the low magnitude pulsatile shear stress was found to be more potent for EC and platelet activation, as well as their interaction, compared to the high magnitude pulsatile shear.

7.2 Future Studies

In the future, the numerical model could potentially be extended to incorporate biological responses like platelet-platelet interaction and platelet-vessel wall interaction. Biochemical responses like changes in protein concentration or increase in activation/adhesion potential could be modeled by incorporating the empirical results back into the CFD model. However, the major hurdle to realize such a model is the involvement of multiple length and time scales.

As reported in the literature, EC ICAM-1 generation is controlled by a key mechanotransduction pathway – the MAP-Kinase pathway. Investigation of the effect of low magnitude pulsatile shear on this pathway could lead to a better understanding of EC activation and corresponding ICAM-1 generation. The discrepancies in the changes observed in endothelial cell mRNA and protein level indicate the need for further investigation under longer shearing durations.

Further, the proteomic analysis of platelets has revealed two potential protein targets (thymosin β4, Platelet Factor-4) which need to be further investigated. This may

lead to detection of potential platelet agonist specific biomarkers, which could have greater clinical implications.

In addition, as reported in this study, in the presence of platelets EC lost their sensitivity to pulsatile shear stress. PECAM-1 is one of the major mechanosensory complex on EC, and has the ability to bind to PECAM-1 on platelet surface[118]. The cross talk between PECAM-1 molecules could potentially have led to EC losing sensitivity to pulsatile shear while platelets gained sensitivity. Hence, it will be interesting to investigate the effect of physiological and pathological levels of shear stress on PECAM-1 expression and function.

.

REFERENCES

1. Roger VL, Go AS, Lloyd-Jones DM et al. Heart Disease and Stroke Statistics--2012 Update: A Report From the American Heart Association. Circulation 2012;125:e2-e220.
2. Rubenstein DA, Yin W. Quantifying the effects of shear stress and shear exposure duration regulation on flow induced platelet activation and aggregation. J.Thromb.Thrombolysis. 2010;30:36-45.
3. Yin W, Rubenstein D. Dose Effect of Shear Stress in Platelet Complement Activation in a Cone and Plate Shearing Device. Cellular and Molecular Bioengineering 2009;2:274-280.
4. Yin W, Shanmugavelayudam SK, Rubenstein DA. The effect of physiologically relevant dynamic shear stress on platelet and endothelial cell activation. Thromb.Res. 2011;127:235-241.
5. Lusis AJ. Atherosclerosis. Nature 2000;407:233-241.
6. Ross R. Atherosclerosis--an inflammatory disease. N.Engl.J.Med. 1999;340:115-126.
7. Van Thienen JV, Fledderus JO, Dekker RJ et al. Shear stress sustains atheroprotective endothelial KLF2 expression more potently than statins through mRNA stabilization. Cardiovasc.Res. 2006;72:231-240. .

8. Yoshizumi M, Abe J, Tsuchiya K, Berk BC, Tamaki T. Stress and vascular responses: atheroprotective effect of laminar fluid shear stress in endothelial cells: possible role of mitogen-activated protein kinases. J.Pharmacol.Sci. 2003;91:172-176.
9. DeBakey ME, Lawrie GM, Glaeser DH. Patterns of atherosclerosis and their surgical significance. Ann.Surg. 1985;201:115-131.
10. Chandran KB, Yoganathan AP, Rittgers SE. Biofluid Mechanics. Boca Raton: CRC Press; 2007.
11. Asakura T, Karino T. Flow patterns and spatial distribution of atherosclerotic lesions in human coronary arteries. Circ.Res. 1990;66:1045-1066.
12. Ahmed SA, Giddens DP. Pulsatile poststenotic flow studies with laser Doppler anemometry. J.Biomech. 1984;17:695-705.
13. Fry DL. Acute vascular endothelial changes associated with increased blood velocity gradients. Circ.Res. 1968;22:165-197.
14. Hellum JD. Biorheology in thrombosis research. Ann.Biomed.Eng 94 A.D.;22:445-455.
15. Martini FH, Nath JL. Fundamentals of Anatomy and Physiology. San Frisco: Pearson Benjamin Cummings; 2009.
16. He X, Ku DN. Pulsatile flow in the human left coronary artery bifurcation: average conditions. J.Biomech.Eng 1996;118:74-82.
17. Iwami T, Fujii T, Miura T et al. Importance of left anterior descending coronary artery curvature in determining cross-sectional plaque distribution assessed by intravascular ultrasound. Am.J.Cardiol. 1998;82:381-384.

18. Stokholm R, Oyre S, Ringgaard S et al. Determination of wall shear rate in the human carotid artery by magnetic resonance techniques. Eur.J.Vasc.Endovasc.Surg. 2000;20:427-433.
19. Brands PJ, Hoeks AP, Hofstra L, Reneman RS. A noninvasive method to estimate wall shear rate using ultrasound. Ultrasound Med.Biol. 1995;21:171-185.
20. Carvalho JL, Nielsen JF, Nayak KS. Feasibility of in vivo measurement of carotid wall shear rate using spiral Fourier velocity encoded MRI. Magn Reson.Med. 2010;63:1537-1547.
21. Perktold K, Hofer M, Rappitsch G et al. Validated computation of physiologic flow in a realistic coronary artery branch. J.Biomech. 1998;31:217-228.
22. Varghese SS, Frankel SH. Numerical modeling of pulsatile turbulent flow in stenotic vessels. J.Biomech.Eng 2003;125:445-460.
23. Yao H, Ang KC, Yeo JH, Sim EK. Computational modelling of blood flow through curved stenosed arteries. J.Med.Eng Technol. 2000;24:163-168.
24. Nosovitsky VA, Ilegbusi OJ, Jiang J, Stone PH, Feldman CL. Effects of curvature and stenosis-like narrowing on wall shear stress in a coronary artery model with phasic flow. Comput.Biomed.Res. 1997;30:61-82.
25. Pober JS, Sessa WC. Evolving functions of endothelial cells in inflammation. Nat.Rev.Immunol. 2007;7:803-815.
26. Kaiser D, Freyberg MA, Friedl P. Lack of hemodynamic forces triggers apoptosis in vascular endothelial cells. Biochem.Biophys.Res.Commun. 1997;231:586-590.
27. Dewey CF, Jr., Bussolari SR, Gimbrone MA, Jr., Davies PF. The dynamic response of vascular endothelial cells to fluid shear stress. J.Biomech.Eng

1981;103:177-185.

28. Partridge J, Carlsen H, Enesa K et al. Laminar shear stress acts as a switch to regulate divergent functions of NF-kappaB in endothelial cells. FASEB J. 2007;21:3553-3561.
29. Davies PF, Remuzzi A, Gordon EJ, Dewey CF, Jr., Gimbrone MA, Jr. Turbulent fluid shear stress induces vascular endothelial cell turnover in vitro. Proc.Natl.Acad.Sci.U.S.A 1986;83:2114-2117.
30. Ku DN, Giddens DP, Zarins CK, Glagov S. Pulsatile flow and atherosclerosis in the human carotid bifurcation. Positive correlation between plaque location and low oscillating shear stress. Arteriosclerosis 1985;5:293-302.
31. Gibson CM, Diaz L, Kandarpa K et al. Relation of vessel wall shear stress to atherosclerosis progression in human coronary arteries. Arterioscler.Thromb. 1993;13:310-315.
32. Hunt BJ, Jurd KM. Endothelial cell activation. A central pathophysiological process. BMJ 1998;316:1328-1329.
33. Esmon NL, Carroll RC, Esmon CT. Thrombomodulin blocks the ability of thrombin to activate platelets. J.Biol.Chem. 1983;258:12238-12242.
34. Wilcox JN, Smith KM, Schwartz SM, Gordon D. Localization of tissue factor in the normal vessel wall and in the atherosclerotic plaque. Proc.Natl.Acad.Sci.U.S.A 1989;86:2839-2843.
35. Ruggeri ZM. The role of von Willebrand factor in thrombus formation. Thromb.Res. 2007;120 Suppl 1:S5-S9.
36. Yang L, Froio RM, Sciuto TE et al. ICAM-1 regulates neutrophil adhesion and

transcellular migration of TNF-alpha-activated vascular endothelium under flow. Blood 2005;106:584-592.

37. Davies MJ, Gordon JL, Gearing AJ et al. The expression of the adhesion molecules ICAM-1, VCAM-1, PECAM, and E-selectin in human atherosclerosis. J.Pathol. 1993;171:223-229.
38. Nagel T, Resnick N, Atkinson WJ, Dewey CF, Jr., Gimbrone MA, Jr. Shear stress selectively upregulates intercellular adhesion molecule-1 expression in cultured human vascular endothelial cells. J.Clin.Invest 1994;94:885-891.
39. Chappell DC, Varner SE, Nerem RM, Medford RM, Alexander RW. Oscillatory shear stress stimulates adhesion molecule expression in cultured human endothelium. Circ.Res. 1998;82:532-539.
40. Morigi M, Zoja C, Figliuzzi M et al. Fluid shear stress modulates surface expression of adhesion molecules by endothelial cells. Blood 1995;85:1696-1703.
41. Tsuboi H, Ando J, Korenaga R, Takada Y, Kamiya A. Flow stimulates ICAM-1 expression time and shear stress dependently in cultured human endothelial cells. Biochem.Biophys.Res.Commun. 1995;206:988-996.
42. Nakashima Y, Raines EW, Plump AS, Breslow JL, Ross R. Upregulation of VCAM-1 and ICAM-1 at atherosclerosis-prone sites on the endothelium in the ApoE-deficient mouse. Arterioscler.Thromb.Vasc.Biol. 1998;18:842-851.
43. Osterud B, Rapaport SI. Activation of factor IX by the reaction product of tissue factor and factor VII: additional pathway for initiating blood coagulation. Proc.Natl.Acad.Sci.U.S.A 1977;74:5260-5264.
44. Grabowski EF, Reininger AJ, Petteruti PG, Tsukurov O, Orkin RW. Shear stress

decreases endothelial cell tissue factor activity by augmenting secretion of tissue factor pathway inhibitor. Arterioscler.Thromb.Vasc.Biol. 2001;21:157-162.

45. Wilcox JN, Smith KM, Schwartz SM, Gordon D. Localization of tissue factor in the normal vessel wall and in the atherosclerotic plaque. Proc.Natl.Acad.Sci.U.S.A 1989;86:2839-2843.
46. Houston P, Dickson MC, Ludbrook V et al. Fluid shear stress induction of the tissue factor promoter in vitro and in vivo is mediated by Egr-1. Arterioscler.Thromb.Vasc.Biol. 1999;19:281-289.
47. Lo SK, Cheung A, Zheng Q, Silverstein RL. Induction of tissue factor on monocytes by adhesion to endothelial cells. J.Immunol. 1995;154:4768-4777.
48. Lin MC, Almus-Jacobs F, Chen HH et al. Shear stress induction of the tissue factor gene. J.Clin.Invest 1997;99:737-744.
49. Esmon CT, Esmon NL, Harris KW. Complex formation between thrombin and thrombomodulin inhibits both thrombin-catalyzed fibrin formation and factor V activation. J.Biol.Chem. 1982;257:7944-7947.
50. Gomi K, Zushi M, Honda G et al. Antithrombotic effect of recombinant human thrombomodulin on thrombin-induced thromboembolism in mice. Blood 1990;75:1396-1399.
51. Malek AM, Jackman R, Rosenberg RD, Izumo S. Endothelial expression of thrombomodulin is reversibly regulated by fluid shear stress. Circ.Res. 1994;74:852-860.
52. Takada Y, Shinkai F, Kondo S et al. Fluid shear stress increases the expression of thrombomodulin by cultured human endothelial cells.

Biochem.Biophys.Res.Commun. 1994;205:1345-1352.

53. Wagner DD. The Weibel-Palade body: the storage granule for von Willebrand factor and P-selectin. Thromb.Haemost. 1993;70:105-110.

54. Sporn LA, Marder VJ, Wagner DD. Inducible secretion of large, biologically potent von Willebrand factor multimers. Cell 1986;46:185-190.

55. Hattori R, Hamilton KK, McEver RP, Sims PJ. Complement proteins C5b-9 induce secretion of high molecular weight multimers of endothelial von Willebrand factor and translocation of granule membrane protein GMP-140 to the cell surface. J.Biol.Chem. 1989;264:9053-9060.

56. Reidy MA, Chopek M, Chao S, McDonald T, Schwartz SM. Injury induces increase of von Willebrand factor in rat endothelial cells. Am.J.Pathol. 1989;134:857-864.

57. Siedlecki CA, Lestini BJ, Kottke-Marchant KK et al. Shear-dependent changes in the three-dimensional structure of human von Willebrand factor. Blood 1996;88:2939-2950.

58. Ruggeri ZM. Platelet and von Willebrand factor interactions at the vessel wall. Hamostaseologie. 2004;24:1-11.

59. Brown CH, III, Leverett LB, Lewis CW, Alfrey CP, Jr., Hellums JD. Morphological, biochemical, and functional changes in human platelets subjected to shear stress. J.Lab Clin.Med. 1975;86:462-471.

60. Anderson GH, Hellums JD, Moake JL, Alfrey CP, Jr. Platelet lysis and aggregation in shear fields. Blood Cells 1978;4:499-511.

61. Wagner CT, Kroll MH, Chow TW, Hellums JD, Schafer AI. Epinephrine and

shear stress synergistically induce platelet aggregation via a mechanism that partially bypasses VWF-GP IB interactions. Biorheology 1996;33:209-229.

62. Sakariassen KS, Bolhuis PA, Sixma JJ. Human blood platelet adhesion to artery subendothelium is mediated by factor VIII-Von Willebrand factor bound to the subendothelium. Nature 1979;279:636-638.

63. Savage B, Almus-Jacobs F, Ruggeri ZM. Specific synergy of multiple substrate-receptor interactions in platelet thrombus formation under flow. Cell 1998;94:657-666.

64. Chow TW, Hellums JD, Moake JL, Kroll MH. Shear stress-induced von Willebrand factor binding to platelet glycoprotein Ib initiates calcium influx associated with aggregation. Blood 1992;80:113-120.

65. Iijima K, Murata M, Nakamura K et al. High shear stress attenuates agonist-induced, glycoprotein IIb/IIIa-mediated platelet aggregation when von Willebrand factor binding to glycoprotein Ib/IX is blocked. Biochem.Biophys.Res.Commun. 1997;233:796-800.

66. Zhang JN, Bergeron AL, Yu Q et al. Duration of exposure to high fluid shear stress is critical in shear-induced platelet activation-aggregation. Thromb.Haemost. 2003;90:672-678.

67. Libby P, Ridker PM, Hansson GK. Progress and challenges in translating the biology of atherosclerosis. Nature 2011;473:317-325.

68. Oki T, Kitaura J, Eto K et al. Integrin alphaIIbbeta3 induces the adhesion and activation of mast cells through interaction with fibrinogen. J.Immunol. 2006;176:52-60.

69. Rutkowski MJ, Sughrue ME, Kane AJ, Mills SA, Parsa AT. Cancer and the complement cascade. Mol.Cancer Res. 2010;8:1453-1465.

70. Krych-Goldberg M, Hauhart RE, Subramanian VB et al. Decay accelerating activity of complement receptor type 1 (CD35). Two active sites are required for dissociating C5 convertases. J.Biol.Chem. 1999;274:31160-31168.

71. Hourcade DE, Mitchell L, Kuttner-Kondo LA, Atkinson JP, Medof ME. Decay-accelerating factor (DAF), complement receptor 1 (CR1), and factor H dissociate the complement AP C3 convertase (C3bBb) via sites on the type A domain of Bb. J.Biol.Chem. 2002;277:1107-1112.

72. Rus HG, Niculescu F, Constantinescu E, Cristea A, Vlaicu R. Immunoelectron-microscopic localization of the terminal C5b-9 complement complex in human atherosclerotic fibrous plaque. Atherosclerosis 1986;61:35-42.

73. Vlaicu R, Rus HG, Niculescu F, Cristea A. Quantitative determinations of immunoglobulins and complement components in human aortic atherosclerotic wall. Med.Interne 1985;23:29-35.

74. Vlaicu R, Niculescu F, Rus HG, Cristea A. Immunohistochemical localization of the terminal C5b-9 complement complex in human aortic fibrous plaque. Atherosclerosis 1985;57:163-177.

75. Oksjoki R, Laine P, Helske S et al. Receptors for the anaphylatoxins C3a and C5a are expressed in human atherosclerotic coronary plaques. Atherosclerosis 2007;195:90-99.

76. Peerschke EI, Yin W, Grigg SE, Ghebrehiwet B. Blood platelets activate the classical pathway of human complement. J Thromb.Haemost. 2006;4:2035-2042.

77. Huber-Lang M, Sarma JV, Zetoune FS et al. Generation of C5a in the absence of C3: a new complement activation pathway. Nat.Med. 2006;12:682-687.

78. Wiedmer T, Sims PJ. Effect of complement proteins C5b-9 on blood platelets. Evidence for reversible depolarization of membrane potential. J Biol Chem. 1985;260:8014-8019.

79. Wiedmer T, Esmon CT, Sims PJ. Complement proteins C5b-9 stimulate procoagulant activity through platelet prothrombinase. Blood 1986;68:875-880.

80. Yin W, Czuchlewski D, Peerschke EI. Development of proteomic signatures of platelet activation using surface-enhanced laser desorption/ionization technology in a clinical setting. Am.J.Clin.Pathol. 2008;129:862-869.

81. Issaq HJ, Conrads TP, Prieto DA, Tirumalai R, Veenstra TD. SELDI-TOF MS for diagnostic proteomics. Anal.Chem. 2003;75:148A-155A.

82. Frenette PS, Johnson RC, Hynes RO, Wagner DD. Platelets roll on stimulated endothelium in vivo: an interaction mediated by endothelial P-selectin. Proc.Natl.Acad.Sci.U.S.A 1995;92:7450-7454.

83. Bombeli T, Schwartz BR, Harlan JM. Adhesion of activated platelets to endothelial cells: evidence for a GPIIbIIIa-dependent bridging mechanism and novel roles for endothelial intercellular adhesion molecule 1 (ICAM-1), alphavbeta3 integrin, and GPIbalpha. J.Exp.Med. 1998;187:329-339.

84. Massberg S, Enders G, Leiderer R et al. Platelet-endothelial cell interactions during ischemia/reperfusion: the role of P-selectin. Blood 1998;92:507-515.

85. Macey MG, Wolf SI, Lawson C. Microparticle formation after exposure of blood to activated endothelium under flow. Cytometry A 2010;77:761-768.

86. Coppinger JA, Cagney G, Toomey S et al. Characterization of the proteins released from activated platelets leads to localization of novel platelet proteins in human atherosclerotic lesions. Blood 2004;103:2096-2104.

87. Dickfeld T, Lengyel E, May AE et al. Transient interaction of activated platelets with endothelial cells induces expression of monocyte-chemoattractant protein-1 via a p38 mitogen-activated protein kinase mediated pathway. Implications for atherogenesis. Cardiovasc.Res. 2001;49:189-199.

88. Gawaz M, Neumann FJ, Dickfeld T et al. Activated platelets induce monocyte chemotactic protein-1 secretion and surface expression of intercellular adhesion molecule-1 on endothelial cells. Circulation 1998;98:1164-1171.

89. Burger PC, Wagner DD. Platelet P-selectin facilitates atherosclerotic lesion development. Blood 2003;101:2661-2666.

90. von HP, Weber C. Platelets as immune cells: bridging inflammation and cardiovascular disease. Circ.Res. 2007;100:27-40.

91. Dodge JT, Jr., Brown BG, Bolson EL, Dodge HT. Intrathoracic spatial location of specified coronary segments on the normal human heart. Applications in quantitative arteriography, assessment of regional risk and contraction, and anatomic display. Circulation 1988;78:1167-1180.

92. Dodge JT, Jr., Brown BG, Bolson EL, Dodge HT. Lumen diameter of normal human coronary arteries. Influence of age, sex, anatomic variation, and left ventricular hypertrophy or dilation. Circulation 1992;86:232-246.

93. Bluestein D, Li YM, Krukenkamp IB. Free emboli formation in the wake of bi-leaflet mechanical heart valves and the effects of implantation techniques.

J.Biomech. 2002;35:1533-1540.

94. Blackman BR, Barbee KA, Thibault LE. In vitro cell shearing device to investigate the dynamic response of cells in a controlled hydrodynamic environment. Ann.Biomed.Eng 2000;28:363-372.
95. Buschmann MH, Dieterich P, Adams NA, Schnittler HJ. Analysis of flow in a cone-and-plate apparatus with respect to spatial and temporal effects on endothelial cells. Biotechnol.Bioeng. 2005;89:493-502.
96. Schmaier AH, Amenta S, Xiong T, Heda GD, Gewirtz AM. Expression of platelet C1 inhibitor. Blood 1993;82:465-474.
97. Jesty J, Bluestein D. Acetylated prothrombin as a substrate in the measurement of the procoagulant activity of platelets: elimination of the feedback activation of platelets by thrombin. Anal.Biochem. 1999;272:64-70.
98. Tzima E, Irani-Tehrani M, Kiosses WB et al. A mechanosensory complex that mediates the endothelial cell response to fluid shear stress. Nature 2005;437:426-431.
99. Shanmugavelayudam SK, Rubenstein DA, Yin W. Effect of geometrical assumptions on numerical modeling of coronary blood flow under normal and disease conditions. J.Biomech.Eng 2010;132:061004.
100. Rouf, F. The effects of physiologically relevant shear stress and platelet-endothelial cell interaction on platelet activation and platelet microparticle generation. 2008. Stillwater, OK, Oklahoma State University.

    Ref Type: Thesis/Dissertation
101. Santamarina A, Weydahl E, Siegel JM, Jr., Moore JE, Jr. Computational analysis

of flow in a curved tube model of the coronary arteries: effects of time-varying curvature. Ann.Biomed.Eng 1998;26:944-954.

102. Deplano V, Siouffi M. Experimental and numerical study of pulsatile flows through stenosis: wall shear stress analysis. J.Biomech. 1999;32:1081-1090.

103. Aarts PA, van den Broek SA, Prins GW et al. Blood platelets are concentrated near the wall and red blood cells, in the center in flowing blood. Arteriosclerosis 1988;8:819-824.

104. Wootton DM, Ku DN. Fluid mechanics of vascular systems, diseases, and thrombosis. Annu.Rev.Biomed.Eng 1999;1:299-329.

105. Bluestein D, Niu L, Schoephoerster RT, Dewanjee MK. Fluid mechanics of arterial stenosis: relationship to the development of mural thrombus. Ann.Biomed.Eng 1997;25:344-356.

106. Crossman DC, Carr DP, Tuddenham EG, Pearson JD, McVey JH. The regulation of tissue factor mRNA in human endothelial cells in response to endotoxin or phorbol ester. J.Biol.Chem. 1990;265:9782-9787.

107. Grant DS, Rose W, Yaen C et al. Thymosin beta4 enhances endothelial cell differentiation and angiogenesis. Angiogenesis. 1999;3:125-135.

108. Philp D, Huff T, Gho YS, Hannappel E, Kleinman HK. The actin binding site on thymosin beta4 promotes angiogenesis. FASEB J. 2003;17:2103-2105.

109. Bikfalvi A, Gimenez-Gallego G. The control of angiogenesis and tumor invasion by platelet factor-4 and platelet factor-4-derived molecules. Semin.Thromb.Hemost. 2004;30:137-144.

110. Siegel-Axel DI, Gawaz M. Platelets and endothelial cells. Semin.Thromb.Hemost.

2007;33:128-135.

111. Hess CN, Kou R, Johnson RP, Li GK, Michel T. ADP signaling in vascular endothelial cells: ADP-dependent activation of the endothelial isoform of nitric-oxide synthase requires the expression but not the kinase activity of AMP-activated protein kinase. J.Biol.Chem. 2009;284:32209-32224.

112. Sahni A, Sahni SK, Francis CW. Endothelial cell activation by IL-1beta in the presence of fibrinogen requires alphavbeta3. Arterioscler.Thromb.Vasc.Biol. 2005;25:2222-2227.

113. Battegay EJ, Rupp J, Iruela-Arispe L, Sage EH, Pech M. PDGF-BB modulates endothelial proliferation and angiogenesis in vitro via PDGF beta-receptors. J.Cell Biol. 1994;125:917-928.

114. VanWijk MJ, VanBavel E, Sturk A, Nieuwland R. Microparticles in cardiovascular diseases. Cardiovasc.Res. 2003;59:277-287.

115. Giblin JP, Hewlett LJ, Hannah MJ. Basal secretion of von Willebrand factor from human endothelial cells. Blood 2008;112:957-964.

116. Blann AD, Nadar SK, Lip GY. The adhesion molecule P-selectin and cardiovascular disease. Eur.Heart J. 2003;24:2166-2179.

117. Chen SC, Henry DO, Reczek PR, Wong MK. Plasminogen activator inhibitor-1 inhibits prostate tumor growth through endothelial apoptosis. Mol.Cancer Ther. 2008;7:1227-1236.

118. Fujiwara K. Platelet endothelial cell adhesion molecule-1 and mechanotransduction in vascular endothelial cells. J.Intern.Med. 2006;259:373-380.

119. Cicmil M, Thomas JM, Leduc M, Bon C, Gibbins JM. Platelet endothelial cell adhesion molecule-1 signaling inhibits the activation of human platelets. Blood 2002;99:137-144.

120. Rathore V, Stapleton MA, Hillery CA et al. PECAM-1 negatively regulates GPIb/V/IX signaling in murine platelets. Blood 2003;102:3658-3664.

VITA

Saravan Kumar Shanmugavelayudam

Candidate for the Degree of

Doctor of Philosophy

Thesis: EFFECT OF DYNAMIC SHEAR STRESS ON ENDOTHELIAL CELLS, PLATELETS, AND THEIR INTERACTION

Major Field: Mechanical Engineering

Biographical:

Education:

Completed the requirements for the Doctor of Philosophy in Mechanical Engineering specializing in Biofluids and Biomechanics at Oklahoma State University, Stillwater, Oklahoma in May, 2013.

Completed the requirements for the Master of Science in Mechanical Engineering specializing in Biofluids and Biomechanics at Oklahoma State University, Stillwater, Oklahoma in May, 2009.

Completed the requirements for the Bachelor of Engineering in Mechanical engineering at Anna University, Chennai, TamilNadu, India in May 2007.

Experience:

Research Associate, Biomedical engineering lab, Oklahoma State University, Stillwater, Oklahoma between Jun 2009 – Jan 2013
Research Assistant, Biomedical engineering lab, Oklahoma State University, Stillwater, Oklahoma between Jan 2008 – May 2009
Teaching Assistant, Department of Mechanical and Aerospace Engineering, Oklahoma State University, Stillwater, Oklahoma between Aug 2007 – Dec 2007

Professional Memberships:

Biomedical Engineering Society
American Heart Association
The Microcirculatory Society